PREDICTION OF TEMPERATURE RISE IN CONCRETE DUE TO HEAT OF HYDRATION OF CEMENT

Anura I.G.K. Mataraarachchi

(09/8103)

Degree of Master of Philosophy

Department of Civil Engineering

University of Moratuwa

Sri Lanka

March 2016

PREDICTION OF TEMPERATURE RISE IN CONCRETE DUE TO HEAT OF HYDRATION OF CEMENT

Anura I.G.K. Mataraarachchi

(09/8103)

Thesis submitted in fulfillment of the requirements for the degree Master of Philosophy in Civil Engineering

Department of Civil Engineering

University of Moratuwa

Sri Lanka

March 2016

Declaration

I declare that this is my own work and this thesis does not incorporate without acknowledgement any material previously submitted for a Degree or Diploma in any other University or institute of higher learning and to the best of my knowledge and belief it does not contain any material previously published or written by another person except where the acknowledgement is made in the text.

Also, I hereby grant to University of Moratuwa the non-exclusive right to reproduce and distribute my thesis, in whole or in part in print, electronic or other medium. I retain the right to use this content in whole or part in future works (such as articles or books).

Signature Date

The above candidate has carried out research for the MPhil thesis under our supervision.

Name of the supervisor

Signature of the supervisor Date

Name of the co supervisor

Signature of the co supervisor Date

Abstract

Temperature rise due to heat of hydration in concrete depends on many factors such as geometry of the concrete element, chemical, physical and thermal properties of concrete materials, mix proportion, initial temperature during concrete batching, and thermal boundary conditions during concrete hardening etc. The multicomponent cement hydration model developed by Maekawa et al., predicts the heat generation due to cement hydration based on cement contents, water contents, reference heat generation rate of main mineral components in cement, i.e. alite (C_3S), belite (C_2S), aluminate (C_3A), ferrite (C_4AF), and gypsum (CS_2H), mineral of cement, fineness of cement, thermal activity and interdependences of mineral components, and effects of consumption of free water during the hydration process etc. This cement hydration model was incorporated in the transient heat conduction analysis. The transient heat conduction analysis was carried out with ANSYS, finite element analysis software using Advance Parametric Design Language (APDL) computer programming to predict the temperature ruse due to heat of hydration of cement in concrete element for a given thermal boundary conditions.

Since the heat of hydration of cement is highly temperature dependent, variation of thermal properties of concrete at early ages is essential to predict the temperature response due to heat of hydration of cement in concrete. Experimental investigations were carried out to develop a model to estimate the variation of thermal conductivity of concrete from fresh to hardened state. The specific heat capacity of concrete (c) was estimated based on the specific heat capacities of cement powder and hydration products using Dulong – Petit Rule (DPR), Neumann – Kopp Rule (NKR), and mixing theory. Thermal conductivity of concrete (λ) was determined by fitting temperature rise curve at center of cube with temperature rise curve predicted by transient heat conduction analysis. Estimated specific heat capacity of concrete was applied in

transient heat conduction analysis program, to predict temperature rise curve from 1hrs to 1day for several mix proportions.

A mathematical model was developed to predict the variation of thermal conductivity based on experimentally investigated thermal conductivity data, mix proportions, thermal conductivity of concrete material found in literature, cement and water contents, formation, shapes, and saturation of gel and capillary pores of cement paste , degrees of hydration, surface saturation of aggregates by applying into general and effective medium theories used in estimation of effective thermal conductivity of a multicomponent material. The developed model was calibrated and verified with experimental data of concrete cube samples for several mix proportions. A computer program was developed using APDL coding of ANSYS software to predict the thermal properties of concrete once mix proportion, chemical, physical and thermal properties of concrete materials are known. This model was coupled with the multicomponent heat of hydration model to improve the program's ability to predict temperature rise with effects of variation of thermal properties with degree of hydration of cement.

The developed multicomponent heat of hydration model was calibrated and verified with temperature rise data detained from several field tests which were carried out in several construction projects in Sri Lanka. Measured and predicted temperature response are in good agreement, and therefore the proposed model can be used to predict temperature rise when chemical composition, mix proportions, and thermal boundary conditions are known.

Furthermore, the developed hydration model was used to obtain appropriate values for T1 (i.e. temperature drop between hydration peak and ambient temperature under local conditions which are required in design of water retaining structures.

Keywords: heat of hydration, thermal conductivity, specific heat capacity, early age concrete, transient heat conduction analysis.

This thesis is dedicated

To my Parents, Loving Wife and Son

Without whom none of my success would be possible

Acknowledgement

First, I would like to thank my main supervisor, Prof. S.M.A. Nanayakkara, and co-supervisor, Prof. Shingo Asamoto, who have guided me these last six years. I sincerely appreciate their continuous support, generosity and advice in both academic and personal way throughout my MPhil study. Under their guidance, I successfully overcame many difficulties and learned a lot. This achievement in my life would not have been possible without their guidance, support and encouragement.

Also, I would like to thank the faculty of engineering specifically those in the Department of Civil Engineering who have contributed to my education or aided me in my research. I am especially grateful to Dr. Mrs. Premini Hettiarachchi for the initial encouragement to start this research degree, once I successfully completed my post graduate diploma in Structural Engineering Designs.

I greatly appreciate for the assistance that I received from the staff of the Materials Testing Laboratory. Without their support and technical knowledge, I would not able to complete experimental investigation works of my research.

Specially, I greatly acknowledge HOLCIM Lanka about their financial assistance to carry out experimental investigations to initial verifications, and calibrations of the research outcomes.

Last, but certainly not least, I would like to thank my family for the love and support they showed me along this journey. This includes my father, mother, and wife, who pushed me the most and always encouraged me to work harder when it got tough. I do not consider this achievement to be my sole accomplishment but instead one that I share with them.

Table of Content

List of Figures

List of Tables

List of Symbols

Latin Symbols

OPC	Ordinary Portland Cement
APDL	Advance Parametric Design Language
THW	Transient Hot Wire
TLS	Transient Line Source
THS	Transient Hot Strip
TPS	Transient Plane Source
C	Carbon
Mg	Magnesium
Al	Aluminum
Fe	Ferrous
Si	Silicon
Ca	Calcium
C_3S	$3CaO.SiO_2$ - Alite
C_2S	$2CaO.SiO_2$ - Belite
C_3A	$3CaO.Al_2O_3$ - Aluminate
C_4AF	$4CaO.Al_2O_3.Fe_2O_3$ - Ferrite
CSH	Calcium Silicate Hydrates
$C\dot{S}2H$	Gypsum
AEt & FEt	Ettringite
CH	Calcium Hydroxide
LH	Low Heat
SR	Sulfate Resistant
DPR	Dulong-Petit Rule
NKR	Neumann - Kopp Rule
HS	Hashin-Strikman Bound Theorem
MM	Maxwell Model
MEL	Maxwell – Eucken Limits
EMT	Effective Medium Theory
DoH	Degrees of Hydration
T_0	Temperature at 0 K
T_{100}	Temperature at 100 K
Q_R	Volumetric Heat Generation Rate
K	Thermal Conductivity
K_0	Thermal Conductivity of Concrete at 0 K
K_{100}	Thermal Conductivity of Concrete at 100 K
M	Fractional Mass
X	Molar Fraction

P	Pressure
V	Volume
W	Weight
A	Area
Q	Heat Flow
T_s	Surface Temperature
T_a	Ambient Temperature
NLS	Number of Time Intervals
H_c	Specific Heat Generation Rate for Cement Powder
p	Fractional Mass of Cement Minerals
Q_i	Accumulated Heat
R	Gas Constant
E/R	Thermal Activity
T	Temperature
s_i	Fineness of Cement Powder
S_i	Blaine Value of Cement Minerals
S_{io}	Reference Blaine Value of Cement Minerals
WC	Unite Weight of Cement
P3A	Weight Percentage of Aluminate
P3S	Weight Percentage of Alite
P4AF	Weight Percentage of Ferrite
P2S	Weight Percentage of Belite
PPCS2H	Weight Percentage of Gypsum
PPC	Weight Percentage of OPC
BLN	Blaine Value of OPC
PSG	Weight Percentage of Slab
BLNSG	Blaine Value of Slag
SGCS2H	Weight Percentage of Sulfate in Slag
PFA	Weight Percentage of Fly Ash
BLNFA	Blaine Value of Fly Ash
FACS2H	Weight Percentage of Sulfate in Fly Ash
PLS	Weight Percentage of Superplasticizer
BLNLS	Blaine Value of Superplasticizer
WP	Water to Powder Ratio
QSP	Constant for the Effects of Superplasticizer Dosage
QSPAD	Constant for the Effects of Superplasticizer Dosage
CHARSP	Constant for the Effects of Superplasticizer Dosage
QSGMX	Final Accumulated Heat Generated by Slag
RSGW1	Weight Percentage of Consumed Water of by Slab
RSGCA	Weight Percentage of Consumed Calcium

	Hydroxide when reacts with Slag
QFAMX	Final Accumulated Heat Generated by Fly Ash
RFAW1	Weight Percentage of Consumed Water by Fly Ash
RFACA	Weight Percentage of Consumed Calcium Hydroxide when reacts with Fly Ash
RH3AMN	Factor for Mono-sulfate Conversion
w	Velocity of Wind
h	Convection Coefficient
E_N	Solar Radiation on Horizontal Surface
E_V	Solar Radiation on Vertical Surface
L_a	Latitude
L_o	Longitude
LST	Local Standard Time
LSM	Local Standard Time Meridian
q	Heat Flux
T_{dp}	Dew Point

Greek Symbols

c	Specific Heat Capacity of Concrete
ρ	Density of Concrete
γ	Retarding effects of fly ash and admixture
β	Free water content
μ	Effects of weight percentage of clinker minerals
λ	Effects of calcium hydroxide production on reaction of fly and slag
ø	Porosity
δ	Solar Declination Angle
σ	Stefan – Boltzmann Constant
ε	Emissivity
α	Thermal Diffusivity

Subscript

i, j, k	Counters
t	Time
x, y, z	Directions

1 Introduction

1.1 Background

BS 8007:1987, Code of Practice for Design of Concrete Structures for Retaining Aqueous Liquids, gives guidelines and recommendations to obtain appropriate values for temperature rise due to heat of hydration to use in structural designing to control thermal cracks in immature concrete assuming thermal boundary conditions which are not relevant to local conditions in Sri Lanka. However, Eurocode 2 (EC2): BS EN 1992-3:2006, Design of Concrete Structures for Liquid Retaining and Containment Structures, recommends that the heat evaluation and temperature response due to cement hydration process should generally be obtained from experimental investigations, and the actual heat evaluation should be determined taking into account the expected conditions during early life of concrete member. This is mainly due to the fact that maximum temperature rises and it's time to reach, highly depend on chemical composition of cement, mix proportions, nature of formworks and thermal boundary condition and many more factors. Therefore, predicting the maximum temperature of concrete with respect to local conditions is always being the main concern of structural engineers and builders both in mass scale and high strength class concrete construction industry as the large scale experimental investigations are not economically sustainable.

Earliest efforts to predict the maximum temperature rise in concrete due to cement hydration were started in late 20's and early 30's [1]. Various studies were reported later on developing methods based on experimental data to predict the maximum temperature rise in concrete. One of the most popular methods to predict the temperature rise is using adiabatic temperature rise curves with nonlinear regression analysis. American Concrete Institute (ACI) has published adiabatic temperature rise curves that are widely used, for example ACI 207.1R-96 [2]. These curves were

developed a few decades ago by laboratory experiments for concrete mixes made with different cement and aggregate types, and placing temperatures etc.

Microstructural models that were developed with finite element modelling technique were based on several multicomponent hydration models. Microstructural models that are of interest in this respect are the CEMHYD3D model with molecular level simulation by Bentz et al. [3], and DUCOM system with mineral component level simulation launched by Meakawa et al. [4]. These models are usually used to describe the microstructure evolution during hydration process of cement. The CEMHYD3D model requires highly sophisticated super computer tools which is capable of simulating millions of cement and aggregate particles to simulate heat conduction to get the thermal responses as the program deals with molecular level microstructural simulation. The heat of hydration model used in DUCOM system deals with mineral component level simulation that can be easily installed into a general multi physics finite element computer program to simulate the temperature rise using a desktop computer.

As the cement hydration is highly depend on temperature, thermal and physical properties of constitutional materials of concrete and their variations during hardening of concrete is significantly important in order to simulate the thermal behavior of concrete with transient heat conduction analysis. Essential thermal and physical input parameters to solve a transient heat conduction analysis are thermal conductivity (K), specific heat capacity (c), and density (ρ) of concrete. Results reported in literature on experimental investigations of thermal conductivity and specific heat capacity of fresh concrete are highly scattered with contradictory results [5, 6, 7, 8, 9, 10]. This is mainly due to the conventional steady state methods used to estimate thermal conductivity of fresh concrete produce large errors as the parameters used in estimation are very sensitive [6].

According to the new design guidelines, given in EC2, it is a requirement to analyse the temperature rise due to heat of hydration considering the thermal and material conditions expected during the service life of the structure. This may be by a temperature monitoring test at site or laboratory maintaining real exposure conditions before starting structural designs. These experiments will result in unnecessary financial burden for clients as well as contractors in the construction industry. A simulation of temperature variation due to heat of hydration of cement using FEM program will be a cost-effective solution for this problem. Therefore, a research is needed to investigate temperature rise due to cement hydration using finite element program coupled with a model to simulate variation of thermal properties and thermal boundary conditions.

1.2 Objectives

Cement hydration is an exothermic reaction. Temperature rise due to heat of hydration of cement within a concrete mass with higher cement content or large in geometry can be quite high. As a consequence, significant tensile strains may develop against change in volume with respect to gradient in temperature from surface to core of concrete mass. These tensile strains can cause to form surface and internal cracks which mainly affects durability, and structural integrity of the structure. It is, therefore, necessary to predict the temperature rise for a given concrete mix to take necessary measures to prevent cracking due to thermal behavior during cement hydration.

Thermal response due to heat of hydration for a given concrete mass is analyzed with transient heat conduction analysis based on Furrier low and Laplacian theory in three-dimensional Cartesian coordinate system. Thermal properties of material are utmost important to predict the thermal response as per the fundamental theories behind heat conduction analysis. Thermal properties of concrete are highly depending on microstructural formation, mass and volumetric fractions of material components, and shape of fine and coarse aggregates etc. Therefore, it is necessary to investigate

behaviors of thermal properties during hydration process in order to predict the temperature response accurately.

The main objective of this research is to predict temperature rise of a concrete structure due to heat of hydration of cement incorporating variation of thermal properties of concrete during the hydration process.

In order to achieve the above objective, the following tasks were considered.

1. Development of a method to estimate specific heat capacity of concrete if the mix proportion is known.
2. Development of a method to estimate thermal conductivity of concrete from fresh to hardened state.
3. Prediction of early age temperature rise of a concrete structure using an existing cement hydration model incorporating variation of thermal properties of concrete with hydration process.

In order to predict early age temperature rise, heat conduction analysis was carried out using finite element method of analysis. The general purpose FEM software ANSYS was used for this purpose.

1.3 Outline of Thesis

Chapter 2 presents a literature review of the followings;

a. Modelling of Heat of Hydration of Cement covering OPC Cement types.
b. Computer Programming using Advance Parametric Design Language (APDL) to carry out transient heat conduction analysis with ANSYS software.
c. Thermal and physical properties of constituents in concrete.
d. Thermal and physical properties of concrete relevant to heat conduction analysis, microstructural formations and variations with the degrees of hydration, and theories and effective parameters to simulate thermal properties and their variations.

e. Experimental methods to investigate the thermal properties of concrete.
f. Thermal boundary conditions and ambient temperature variations.
g. Experimental methods to investigate temperature rise due to heat of hydration of concrete under semi adiabatic and natural conditions.

Chapter 3 describes the heat of hydration model proposed by Maekawa et al. [4] and developed a macro program using APDL coding to simulate the heat generation due to cement hydration. This macro program is coupled with ANSYS software to carry out transient heat conduction analysis to simulate thermal response for any given concrete member, once chemical composition and mix proportions are known. This program was improved to model thermal response with the effects of formwork material type, and variation of thermal boundary conditions. Furthermore, a model was developed to predict the thermal properties and their variations in fresh concrete with degrees of hydration for a given mix.

A comprehensive detail of concrete mixes used in investigation of thermal properties, initial calibration & verification using experimental data, and data from different construction projects was compiled, and briefed in Chapter 4 with regard to verification of temperature predictions by the heat of hydration simulation program.

Chapter 5 describes the development of a model to predict thermal properties of concrete and its variations with time.

Chapter 6 presents the experimental investigations carried out to obtain the temperature rise under controlled boundary conditions. Furthermore, comprehensive set of temperature rise data were collected from different projects and previous studies which were conducted with different exposure conditions to use in further verification of predictions by the proposed model.

Chapter 7 presents initial calibrations, verifications of temperature predictions by the developed heat of hydration model incorporating the model to estimate thermal properties of concrete.

Chapter 8 describes the application of the calibrated and verified simulation model incorporating thermal properties and thermal boundary conditions to predict temperature rise in different structural members based on chemical composition of cement, mix proportions, type of formwork under different thermal boundary conditions.

Chapter 9 presents the main findings of this research and finally Chapter 10 presents suggestions for future works.

2 Literature Review

2.1 Introduction

A literature review was carried out mainly focusing the followings;

a. Cement hydration, performances of concrete, constituent material, microstructural formations during cement hydration process, chemical reactions involves in cement hydration.
b. Principles of heat transfer through heterogeneous mediums.
c. How APDL can be used to communicate with ANSYS software to perform transient heat conduction analysis.
d. Experimental methodologies and experimental data on thermal properties of concrete and temperature rise in concrete due to heat of hydration of cement.
e. Modeling of thermal properties of concrete.
f. Thermal simulation techniques in terms of predicting the thermal responses due to cement hydration in concrete.

2.2 Ordinary Portland Cement

Cement clinker is manufactured with limestone, clay, quartzite, and small number of additives by burning at 1400 ^{o}C. Portland cement is manufactured by grinding clinker into finer particles termed as pulverization, burning, and intergriding with gypsum. Cement clinker consists of four major minerals known as alite (C_3S), belite (C_2S), aluminate (C_3A), and ferrite (C_4AF). Generally, alite and belite are calcium silicates which occupy more than 85% of cement clinker, and aluminate and ferrite fill the interstitial spaces surround the calcium silicates [4, 11].

Figure 2-1 shows microstructure of alite and belite with different crystal arrangement. Alite is early crystalized tiny crystal, and substituting basic elements are magnesium (Mg), aluminum (Al), and ferrous (Fe). Belite are usually in the form of polymorph with twin and crossed twin lamellae mainly consists of with Al, and Fe. Aluminate

are polymorphs include cubic fine grained or orthorhombic substituents elements with Mg, Al, Fe, and silicon (Si). Ferrite includes mainly Fe, Si, and Mg.

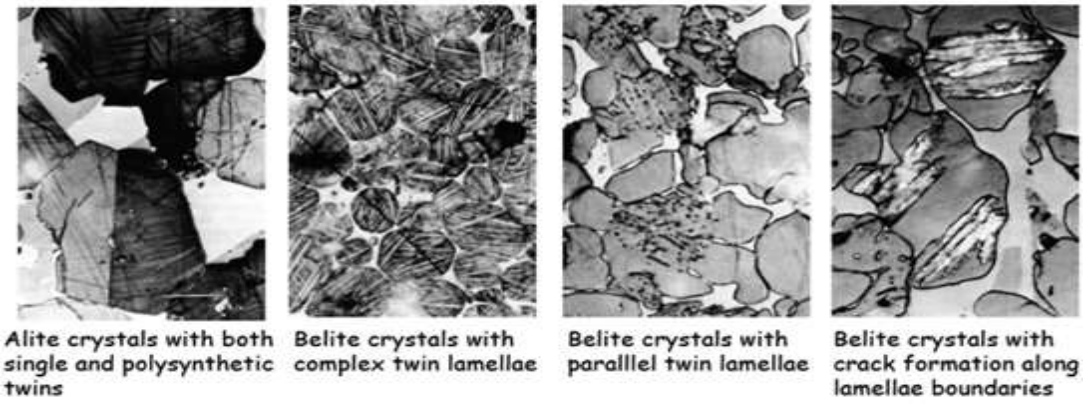

Figure 2-1: Microstructure of different clinker polymorphs

Source: Presentation on Portland cement by Groberty B. [12]

Usually, gypsum or anhydrite are added to cement clinker to achieve the desired setting qualities in the finished product by grinding to form fine cement powder. The grinding process is controlled to obtain a powder with a broad particle size range, in which typically 15% by mass consists of particles below 5 μm diameter, and 5% of particles above 45 μm. The measure of fineness usually used is the "specific surface area", which is the total particle surface area of a unit mass of cement. The rate of initial reaction of the cement on addition of water is directly proportional to the specific surface area. Typical values are 3200–3800 cm^2/kg for general purpose cements, and 4500–6500 cm^2/kg for "rapid hardening" cements [11].

It is required to limit the formation of tri-calcium aluminate ($3CaO.Al_2O_3$) for special cements, such as Low Heat (LH) and Sulfate Resistant (SR) types. To achieve this, limestone ($CaCO_3$), which is the major raw material in production of clinker are usually mixed with a second material containing clay as source of alumina-silicate. Normally, an impure limestone which contains clay or SiO_2 with less than 80% of $CaCO_3$ is also an alternative option. Secondary raw material which depends on the

purity of the limestone are normally clay, shale, sand, iron ore, bauxite, fly ash, and slag. The fired coal ash is also use as a secondary row material in these cement types.

Mineral composition of OPC are generally determined either by direct analysis or chemical analysis. Here direct analysis method is complex and require sophisticated equipment with special skill [13]. Therefore, chemical analysis results are preferred to use to estimate mineral composition of cements. Oxide compositions of OPC are first examined using a technique such as X-ray Fluorescence Spectroscopy or chemical analysis, and then converted to obtain mineral compositions with Bouge analysis [14] as recommended in ASTM C150 [15]. Table 2-1 indicates Oxides with notations.

Table 2-1: Oxides in Ordinary Portland cement

Oxide	Chemical Notation	Standard Notation
Lime	CaO	C
Silica	SiO_2	S
Alumina	Al_2O_3	A
Ferric oxide	Fe_2O_3	F
Magnesia	MgO	M
Potassium alkalis	K_2O	K
Sodium alkalis	Na_2O	N
Sulfur trioxide	SO_3	$\overline{S}$
Chlorine	Cl^-	-
Water	H_2O	H

Bouge analysis [14] suggest the following formulae which categorized into two phenomena based on alumina: ferric Oxides ratio (A/F) to convert the oxide composition into mineral compositions. Greater A/F ratio more than 0.64 produces all mineral compositions alite (C_3S), belite (C_2S), aluminite (C_3A) and ferrite (C_4AF). Otherwise, no belite component is available in cement. Therefore, oxide percentages given by chemical analysis of particular type of cement, can be used to estimate the weight percentages of mineral components for a given cement using the suggested formulae given in Table 2-2 below.

Table 2-2: Bouge Equations to Convert Oxide Composition into Mineral Composition in OPC

A/F Ratio	Formulae
≥ 0.64	$C_3S = 4.071C - 7.6S - 6.781A - 1.43F - 2.852\overline{S}$ $C_2S = 2.867S - 0.7544C_3S$ $C_3A = 2.65A - 1.692F$ $C_4AF = 3.043F$
< 0.64	$C_3S = 4.071C - 7.6S - 4.479A - 2.852\overline{S}$ $C_3A = 0$ $C_4AF + C_2F = 2.1A + 1.702F$

Specifying the mineral composition in cement standards in many countries shows some clauses relating to the chemical compositions of cement. Some limitations are often placed by controlling the excess lime content restricting the formation of acidic oxides in terms of maintaining soundness properties. ASTM C150 defines Portland cement as "hydraulic cement which has hardened and water resistive characteristics.

Usually Portland cements contain one or more forms of calcium sulfate uses the definition given in Table 2-3 below as per ASTM standards. Further, this provides certain limitations for maximum and minimum weight percentages of oxides as well as mineral components of cements considering different type of applications.

Table 2-3: ASTM C150 Standard Requirements for OPC and Blended Cements

Category	SiO_2 min [%]	Al_2O_3 max [%]	Fe_2O_3 max [%]	SO_3 C3A<8 [%]	SO_3 C3A>8 [%]	C_3S max [%]	C_2S min [%]	C_3A max [%]
Type I	-	-	-	3.0	3.5	-	-	-
Type II	20	6.0	6.0	3.0	-	-	-	8
Type III	-	-	-	3.5	4.5	-	-	15
Type IV	-	-	6.5	2.3	-	35	40	7
Type V	-	-	-	2.3	-	-	-	5

European Standard states that Portland cement clinker is to be made by sintering a precisely specified mixture of raw materials (raw meal, paste or slurry) containing elements, usually expressed as oxides, CaO, SiO_2, Al_2O_3, Fe_2O_3 and small quantities of other materials. Portland cement clinker is a hydraulic material which shall consist of at least two-thirds by mass of calcium silicates ($3CaO.SiO_2$ and $2CaO.SiO_2$), the remainder consisting of aluminum and iron containing clinker phases and other compounds. The ratio by mass $(CaO)/(SiO_2)$ shall be not less than 2, and content of magnesium oxide (MgO) shall not exceed 5% by mass. According to European and British standards, type of cement specifies as shown in Table 2-4 considering different industrial applications.

Table 2-4: EN197-1 and BS8500 Standards for OPC & Blended Cements

Type	Notations as per Standard		Clinker [%]	Fly Ash [%]	GGBS [%]
	EN197-1	BS8500			
Portland	CEM I	-	95-100	-	-
Portland fly ash	CEM II/A-V	CIIA-V	80-94	6-20	-
	CEM II/B-V	CIIB-V	65-79	21-35	-
Portland slag	CEM II/A-S	CII-S	80-96	-	6-20
	CEM II/B-S		65-79	-	21-35
Blast-furnace	CEM III/A	CIIIA	35-74	-	36-65
	CEM III/B	CIIIB	20-34	-	66-80

2.3 History of Studies on Heat Generation Associated with Cement Hydration

Hydration of cement is an exothermic chemical reaction releasing a large amount of heat. The importance of thermal effects in early age concrete was first identified and studied by Tetmayer [16] in 1883. This study was based on early temperature measurements and exploring the effects on temperature rise with a view to minimize cracking in mass concrete structures. Further, studies were reported in period of 1930 to 1970 during construction of few dams in USA [1]. These studies were to determine the effects of composition and fineness of cement, placing and curing temperature, aggregate sizes, etc. Later on, researchers understood the concept of degrees of hydration, influence of temperature rise and effects on curing temperature on the rate of reaction of cement hydration, probably after the studies by Rastrup [17] and efforts

were undertaken to determine the temperature rise relying on experimental temperature rise data.

Various prediction methods were developed based on temperature rise curves developed with data from adiabatic or semi adiabatic tests. For examples, experimental investigations carried out at University of Dundee [18, 19] were used to develop linear regression model reported in CIRIA C660 report. The CIRIA R916 [20] which was developed later as CIRIA C660 by Bamforth [21], is the classical empirical model runs with linear regression analysis to predict the temperature rise due to hydration of cement. This was used to predict temperature rise for different cements types [22, 23, 24] such as OPC, blended cements and combinations. However, these models were not capable to predict the effects on variation of chemical composition of cements, variation of thermal boundary conditions, and mutual interaction of cement minerals, etc.

Van Breugel [25] was the first researcher who started to develop a model to predict strength and degree of hydration from quantitative microstructure development model due to cement hydration in 1991. In the same time, a model to predict the rate of heat liberated by cement using Arrhenius's law of chemical reaction was developed by Suzuki at el. [26] in parallel to Bruegel, enabling to predict the corresponding temperature rises based on rate of penetration of reaction in cement particles, resistance to mass transport, thermal activity, etc. Overall rate of hydration is estimated as summation of rate of hydration of individual mineral components, i.e. Alite, Belite, Aluminite, Ferrite, and Gypsum.

Bentze et al. [3] developed a computer model simulating molecular level chemical reactions which enables to predict heat generation, moisture transport mechanisms, and microstructural development etc. However, highly sophisticated computer tools are required in this type of simulations which is questionable in implementing for field applications.

It is essential to know the thermal properties of concrete to understand any heat transfer phenomena. These properties are specific heat, conductivity and diffusivity of particular material. Lu et al. [27] reported that changes in aggregate types, mix proportions, and concrete age do not affect significantly on the specific heat of ordinary concrete at normal temperature. Boulder Canyon Project report [28] in 1940 was the earliest effort in finding thermal conductivity of concrete. Here, an empirical method was proposed for prediction of thermal conductivity and heat capacity of concrete with the basis of mix proportions, and composition of the aggregate. Campbell at al. [29] suggested a theoretical model to predict the thermal conductivity of concrete using principle of Ohm's law. Here volume fractions and the thermal conductivities of the coarse aggregate and mortar are the main input parameters for the model. Harmathy [30], considered porosity of concrete, conductivity of equivalent solid and moisture content as factors on which conductivity of concrete is dependent. A model in this form is more realistic in natures of heat transfer in concrete [31].

In last decays, several researchers developed methods in measuring thermal properties of concrete known as the transient hot wire [32, 33], transient line source [34], transient hot strip and transient plane source techniques [35, 36]. These methods estimate the thermal properties of isotropic and homogeneous materials with a reasonable accuracy. Transient hot wire (THW) and transient line source (TLS) techniques use a heating wire or cylindrical heating element and a temperature sensor for monitoring the temperature rise. The thermal conductivity and the thermal diffusivity of the material under investigation are then calculated from the mathematical solution of heat conduction equation, the known heat liberation and the temperature history of the wire or the probe [37]. The transient hot strip (THS) technique was developed and has applied for measurements of thermal properties of insulating solids and fluids [35]. In these measurements, a metal strip is used as a heat source as well as a temperature sensor. However, measurements of thermal properties

of cement materials as heterogeneous, wet and porous materials using conventional line source or strip techniques produce large errors as the estimation process deals with highly sensitive formulae [6]. Bouguerra et al. [37] describes accuracy of using transient plane source (TPS) technique to use in measuring thermal conductivity, and diffusivity of porous material with reasonably higher accuracy. This method involves recording the temperature increase at the center of the plane source which sandwiched between two identical samples. A two-phase theoretical model to estimate the thermal diffusivity is developed. However, this method can be used to predict thermal properties of concrete in dry state only.

2.4 Thermal Cracking

Thermal behavior is a leading characteristic of concrete that differentiates its behavior from that of structural concrete. Generally, temperature rise is significantly low in structural members having relatively thin sections with larger exposure surface area. In contrast, structures having thick members with limited surface reports higher temperature rises and thermal gradient from section core to outer face. The main reason behind this phenomenon is the low rate of liberated heat dissipation to the surroundings as the thermal conductivity is comparatively low in concrete. In some cases, semi adiabatic or adiabatic conditions may be developed in the core of concrete member. This phenomenon causes to make volumetric changes within concrete member resulting tensile strains and stresses in surface [2, 4]. These thermal stresses may create cracking when tensile stress exceeds its capacity to withstand. These surface cracking eventually affect durability and structural integrity of the structure as these cracks are irreversible surface opening that expose reinforcement to start deterioration.

2.5 Microstructure of Concrete

Concrete consists three basic components referred as; a. Matrix of hardened cement paste, b. Interfacial zone and capillary paths in between aggregate and cement paste

matrixes, and c. Aggregates [4, 38]. These three basic components are schematically represented in Figure 2-2 below.

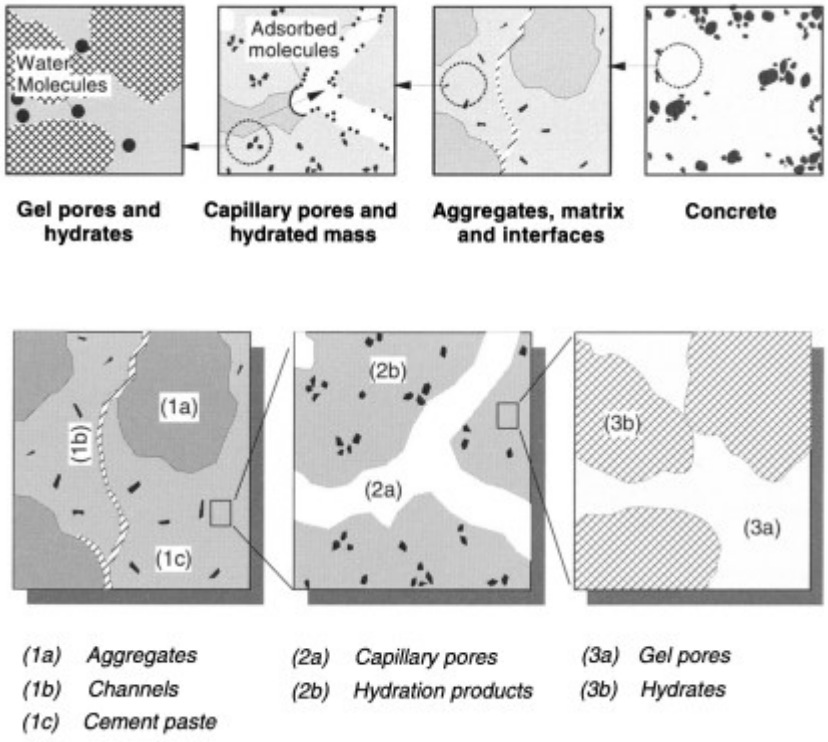

Figure 2-2: Component of concrete

Source: Modelling of Concrete Performance by Maekawa et al. [4]

Matrix of cement paste constitutes un-hydrated cement grains, cement hydration products, capillary pores, and gel pores [4, 38]. Un-hydrated cement particles start to react with water forming various hydration products known as cement gel. Bleeding paths which developed in between hydration products termed as capillary pores. Cement gel can be, further divided into gel pores and the solids which comprised calcium silicate hydrate, and interlayer spaces. Capillary and gel pores are initially filled with free water which encroached by vaporized air with the consumption of free water by the cement hydration reaction. Fractional volume of each constitutes vary with the degrees of hydration without overall volume changes in cement paste. Capillary pores are comparatively larger than gel pores having complex shapes and

random interconnections. Generally capillary pores are in the range from 10 μm - 50 nm in size. Gel pores range in size from 2.5 - 10 nm. Thus, the amount of free water available in capillary pores are relatively higher compared to water in gel pores.

Interfacial zone in between aggregate matrix and cement paste includes large pores or bleeding paths which might form as a result of insufficient compaction or higher water contents. Amount of free water available in this zone, is relatively higher primarily with the cause of wall effect [38, 39]. Wall effect for fine aggregate is negligible with respect to coarse aggregates. The thickness of interfacial zone is reported in the range of 15 - 50 μm.

Aggregates are usually dispersed in the matrix of cement paste. Direct interconnected interfacial pathways are significantly extraordinary, when fine and coarse aggregate contents are increased. When water to cement, ratio is increased, microstructure of cement paste become coarse, and interfacial zones or capillary paths continuous enhancing moisture movements within the matrix of cement paste [4].

A model illustrating the microstructural behaviors of cement paste was developed by Powers et al. [40]. This study was on the hypothesis of water vapor adsorption isotherms of the cement paste, BET theory [41], and capillary condensation theory. Hansen developed set of equations further to Power's model to simulate the effects of composition of different cement types, and amount of total hydration products. Later models, such as the one proposed by Jennings [42], predict the volume fractions of the various hydration products. In conclusion, these microstructural development models clearly indicate that the structural variations during the cement hydration process that concrete element can undergo, and can be used in thermal analysis to simulate thermal responses due to heat transferring phenomena.

2.6 Cement Hydration

Cement hydration is an exothermic chemical reaction determined by the nature of reactions, and the state of the system for a particular instance [4]. As reported by Jeffrey et al. [11], these chemical processes involve molecular dissolution, diffusion, growth, nucleation, complexation, and adsorption. Maekawa et al. [4] and many researchers [11, 43, 44, 45, 46, 47, 48, 49, 50, 51] describe the entire cement hydration process of Ordinary Portland cement (OPC) categorizing into five different stages such that; (1). Initial stage, (2). Dormant period, (3). Acceleration period, (4). Deceleration period, and (5). Later stage as shown in Figure 2-3.

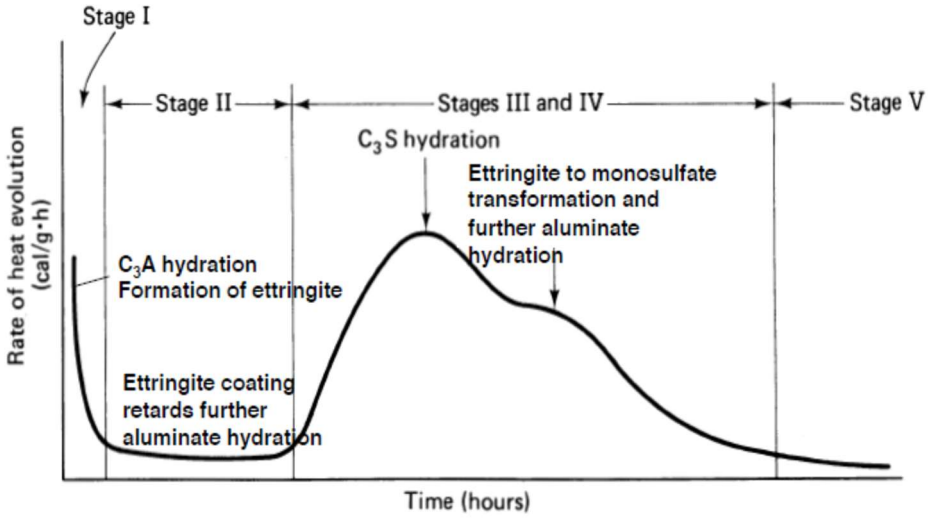

Figure 2-3: General stages of exothermic hydration process in OPC

Source: Presentation on Portland cement by Groberty B. [12]

Rapid reaction which shows the highest rate of heat generation occurs due to wetting of cement particle, and dissolution of ions in water during *initial stage*, resulting formation of semi stable calcium silicate hydrate (CSH), ettringite (AEt & FEt), and calcium hydroxide (CH) [4, 11]. These hydration products precipitate on the outer surface of cement grain as an interstitial layer in between liquid medium and cement particles [4]. Jeffrey et al. [43] proved that the main mineral component which actively involves in formation of semi stable hydrates is C_3S as a result of its rapid dissolving

characteristics in water. Garrault et al. [52], describe concentration of silicate increases in water with dissolution of C_3S within the first minute after wetting, and later nucleation of CSH consumes these silicate ions resulting a sharp decrease in rate of hydration initially. Maekawa et al. [4] reports that formation of ettringite as a result of reaction of C_3A & C_4AF with gypsum and water. As reported by many researchers [4, 11], C_2S hydration occurs very slowly contributing less heat generation relative to C_3A and C_3S initially. At the beginning of cement hydration, ettringite forms, and chemical reactions are as described in equations 2-1 to 2-4 below.

$$C_3A + 3C\bar{S}H_2 + 26H \rightarrow C_3A.3C\bar{S}.H_{32} \quad 2\text{-}1$$

$$C_3A + 3C\bar{S}H_2 + 26H \rightarrow C_3A.3C\bar{S}.H_{32} \quad 2\text{-}2$$

$$C_3A + 3C\bar{S}H_2 + 26H \rightarrow C_3A.3C\bar{S}.H_{32} \quad 2\text{-}3$$

$$C_4AF + 3C\bar{S}H_2 + 27H \rightarrow C_3AF.3C\bar{S}.H_{32} + CH \quad 2\text{-}4$$

An illustration of chemical process during initial stage can be interpreted as shown in Figure 2-4.

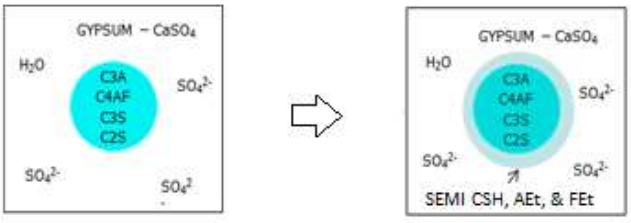

Figure 2-4: Chemical reactions during initial stage of cement hydration [53]

During the *dormant period*, the rate of cement hydration is significantly small [4, 11, 43]. Jeffrey et al. [43] describes that the hydration reactions of C_3S drastically decelerate as semi stable CSH precipitates cover the C_3S surfaces with the high saturation of solved ions in water. This phenomenon reduces the overall dissolution rate of C_3S resulting stagnant in nucleation of CSH delaying crystallization of CSH. Maekawa et al. [4] suggest that the nucleation of C_3A idle with the formation of

ettringite layer covering the C_3A & C_4AF grains, behaves as a barrier to ion movements. Minard et al. [52] describes that reduction in hydration of C_3A is due to a change in dissolution rate with the increase saturation of sulfate ions in liquid, not due to a barrier layer. However, these two-different nucleation and growth mechanisms describe the same phenomena i.e. if the amount of sulfate ions are high in the liquid, the spaces available to pass the calcium silicate ions through the layer is limited, thus, ettringite layer with the presence of high sulfate ions is virtually strong, and behave as a barrier. However, Jeffrey et al. [43] argue that this is merely reduction in sulfate ions saturation in liquid explaining formation of diffusion barrier around C_3A and other phases, and absorption of solved spices by dissolved calcium sulfate. Figure 2-5 shows a photograph taken from electronic microscope about precipitation of ettringite hexagonal rods surrounding C_3A grains.

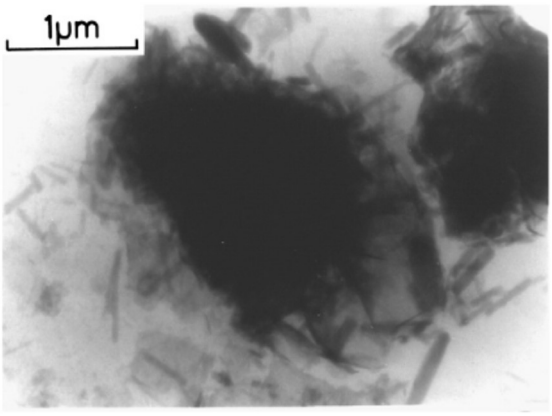

Figure 2-5: C_3A Grain after 10min Hydration with the Presence of Calcium Sulfate

Source: The Development of microstructure during hydration of Portland cement [54]

Hydration process is significantly active during *acceleration period* increasing the rate of heat generation following termination of dormant period. Maekawa et al. [4] suggest that reason behind this is due to increase in permeability of the protective layer formed during the dormant period. Crystallization of CSH starts after reacting C_3S & C_2S with water and presents as shown in Figure 2-7.

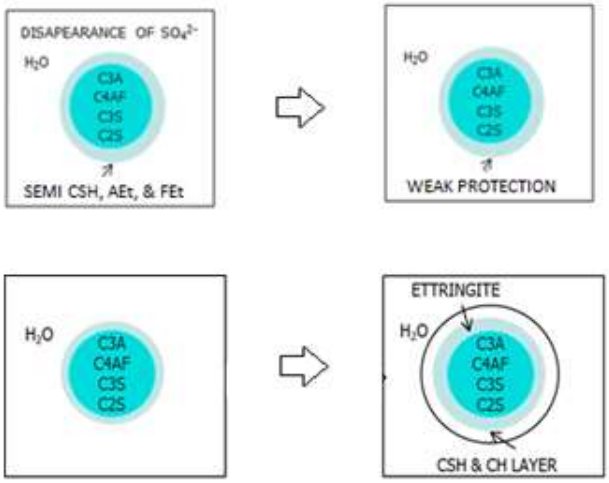

Figure 2-6: Increasing the permeability of semi stable CSH, and ettringite layer at termination of dormant period [53]

Formation of calcium silicate hydrate is given by the chemical formulae given with equations 2-5 to 2-6 below.

$$2C_3S + 6H \rightarrow C_3S_2H_3 + 3CH \qquad 2\text{-}5$$

$$2C_2S + 4H \rightarrow C_3S_2H_3 + 3CH \qquad 2\text{-}6$$

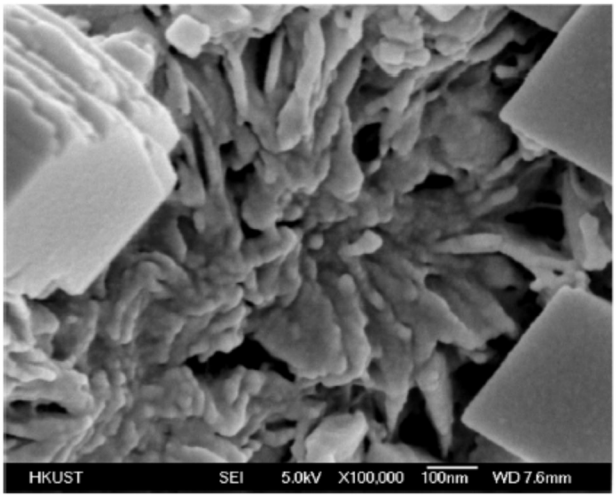

Figure 2-7: SEM Photograph of C-S-H

Source: Study on hydration process of early-age concrete using embedded active acoustic and non-contact complex resistivity methods by Youyuan Lu et al. [55]

Then the ettringite starts to react with free C_3A and C_4AF in cement particle and converts to monosulfate during *decelleration period* as shown Figure 2-8.

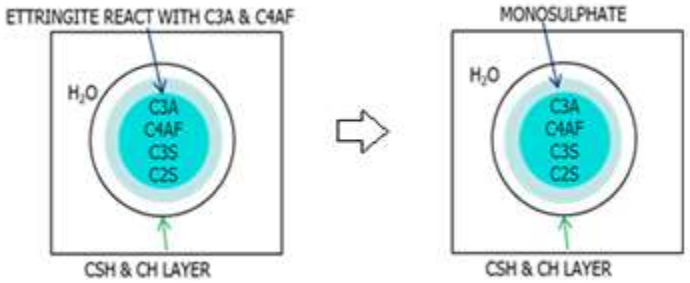

Figure 2-8: Chemical reaction process during acceleration and deceleration periods of cement hydration process

Formation by converting the formed ettringite into mono-sulfate is described by the following chemical reactions.

$$2C_3A + C_3A.3C\overline{S}.H_{32} + 4H \rightarrow 3\left[C_3A.3C\overline{S}.H_{32}\right] \quad 2\text{-}7$$

$$2C_4AF + C_3AF.3C\overline{S}.H_{32} + 6H \rightarrow 3\left[C_3AF.3C\overline{S}.H_{32}\right] + 2CH \quad 2\text{-}8$$

During later stage, the rate of hydration process retards remarkebly as the thick layer of hydrates deposited prevent contactions of cement particles with dissloved ions, and these decellaration and later stages are called as diffusion control phases during cement hydration process [4].

2.7 Parameters Influence the Cement Hydration

Many factors such as chemical composition of cement, fineness, dependency on tempearature, water to cement ratio, interdependence among mineral components of cement, effects of admixtures, initial temperature, and supplementary cementitious

material content influence the cement hydration [4, 13]. However, in this study effects of admixture and effects of supplimentary blended material are not studied.

2.7.1 Mineral Composition

Heat generation rates in different cement types are reported by Mindess et al. [56] as illustrated in Figure 2-9. As per ASTM C150 standard [15], cement type I to IV include different mineral compositions, and Type III cement reports the maximum adiabatic temperature rise in mass concrete. This is mainly due to the fact that it consists the highest weight percentage of C_3A which eventually prpduce the highest total liberated heat during cement hydration.

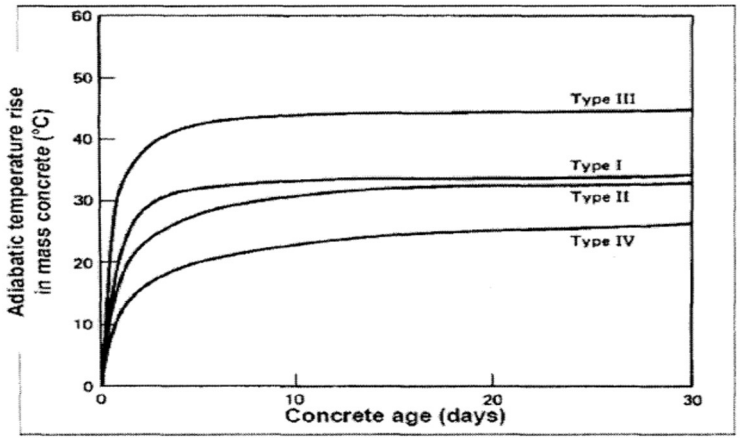

Figure 2-9: Adiabatic Temperature Rise in Mass Concrete for Different Cement Types

Source: Text Book on Concrete by Mindess et al [56]

The hydration characteristics such rate of hydration, and total liberated heat of C_3S, C_2S, C_3A, and C_4AF are reported by Zhi Be [13] as moderate, slow, high, and moderate respectively. A study which carried by Lerch et al. [57] reports that total liberated heat almost doubles when C_3A content is increased by 20% in OPC. Therefore, mineral composition of cement affects the cement hydration rate, and it should be included in hydration model.

2.7.2 Sulfate Contents

Sulfate is introduced by adding gypsum in addition to clinker in OPC, and it controls the early reaction of C_3A. A study by Lerch [58] reveals that heat generation by C_3A during time duration of 30 minute, reduces with increase of sulfate contents despite the C_3A content as shown in Figure 2-10. This is mainly due to the fact that C_3A is less soluble in a medium with rich sulfate [59], and eventually hydration reaction of C_3A delays.

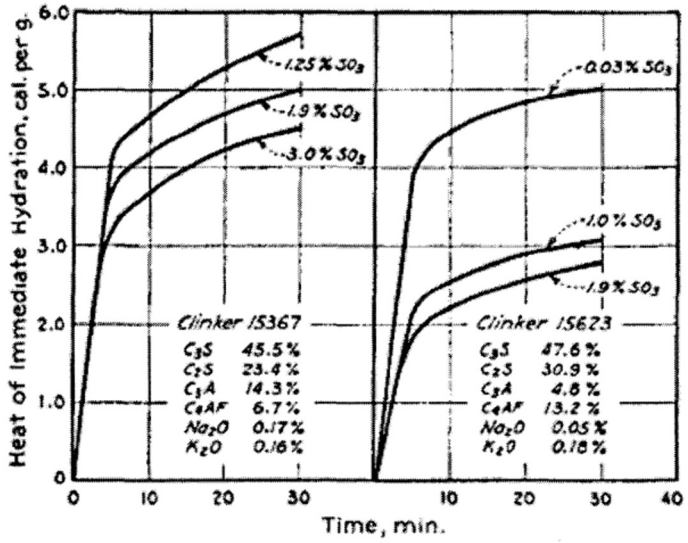

Figure 2-10: Variation of Instant Heat of Hydration Rate against Sulfate Content

Source: The Influence of Gypsum on the Hydration and Properties of Portland cement paste by Lerch W. [58]

2.7.3 Powder Fineness

Fineness of cement powder reveals the exposed surface area of cement particle available to contact with water to start hydration reactions. If the exposed surface area is higher, that contributes to increase the rate of hydration reactions. Generally, fineness of cements is in the range of 3,000 cm^2/g to 5,000 cm^2/g [13]. Report on Thermal and Volume Change Effects on Cracking of Mass Concrete published by American Concrete Institute (ACI), ACI 207.2R – 07 [60], describes effectiveness of

powder fineness of cement to the hydration process regardless of mineral composition of cements as shown in Figure 2-11. Further, a study by Shuhua et al. [61] reveals that hydration heat generated can be gradually increased by increasing fineness of cement.

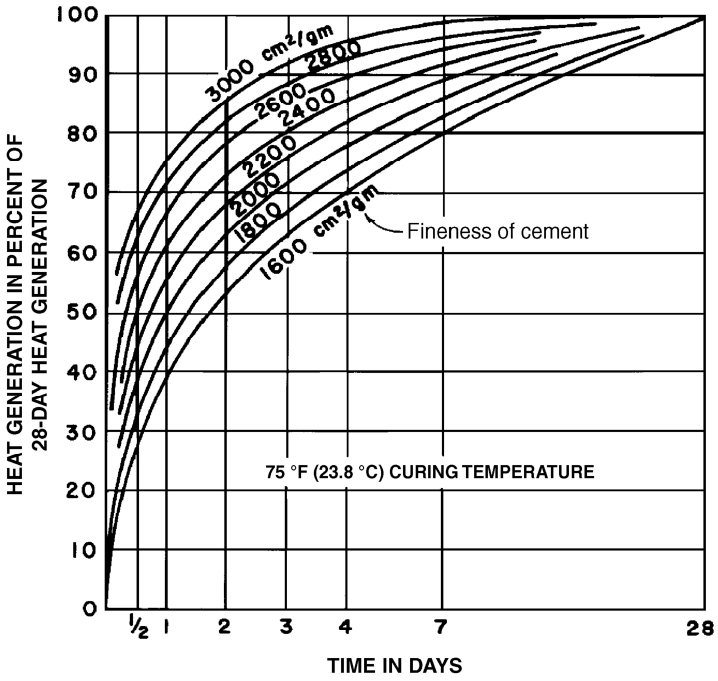

Figure 2-11: Rate of heat generation as affected by Wagner fineness of cement (ASTM C 115) for cement paste cured at 75 °F (23.8 °C)

Source: Report on Thermal and Volume Change Effects on Cracking of Mass Concrete published by American Concrete Institute (ACI), ACI 207.2R – 07 [60]

2.7.4 Water Content

Hydration reaction starts instantaneously with contact of cement particles and water. Presence of free water is essential to continue hydration reaction, and it provides space to precipitates cement hydrates surrounds cement grains [4]. Van Bruegel [25] states that minimum required w/c ratio is about 0.4 for the completion of cement hydration. Cement hydration reaction terminates with the lack of free water available to form CSH [4]. High w/c ratio results higher degrees of hydration due to availability of microstructural space. As shown in Figure 2-12, the rate of hydration reaction is not

significantly affected by the w/c during initial stages, however during later ages, the hydration rate decreases with reduced w/c [62].

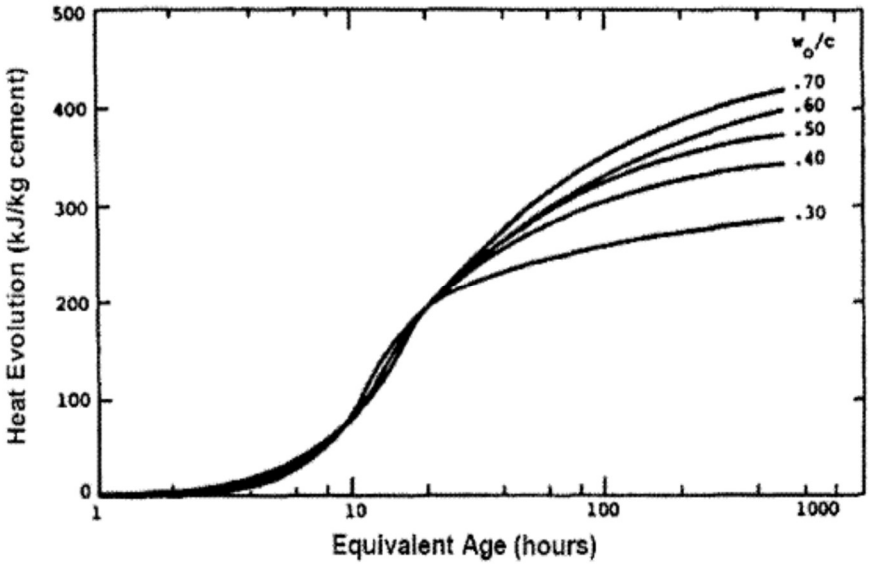

Figure 2-12: Effects w/c ration on Heat of Hydration Rate in cement

Source: Properties of set concrete at early ages by RILEM 42-CEA [62]

2.7.5 Initial and Curing Temperature

Escalante et al. [63] reports that curing temperature effectively affect the heat generation rate. Cement hydration accelerates with elevated ambient temperatures [13], however, due to formation of barrier on the cement particle, it gets decelerated during later stages as presented in Figure 2-13. Similarly, higher initial temperature increases the hydration rate during initial stages.

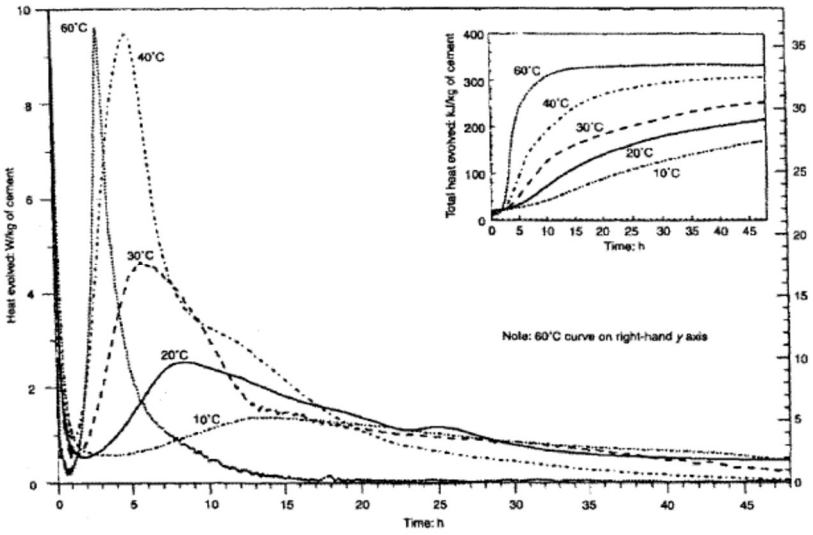

Figure 2-13: Effects of Curing Temperature on cement Hydration [63]

Source: The effects of temperature on the early hydration of Portland cement and blended cements by Escalante et al.

2.8 Modelling of Heat of Hydration of cement

Over the past few decades several efforts have been made to model cement hydration in order to understand and predict the cement hydration kinetics and microstructural development of cement-based materials. Many of these studies are based on experimental data extracted through adiabatic of semi adiabatic test, and prediction are based on regression analysis. However, few efforts were made with micro scale kinetic models dealing initially with individual cement grain nucleation and growth mechanisms, and later it was expanded to random distribution of cement grain nucleation and growth focusing atomic level simulation [3]. Apart from these two techniques, multicomponent level simulation based on hydration kinetic at mineral component level are reported [4].

One of the popular early effort was to predict the temperature rise by processing adiabatic temperature rise data extracted from experimental investigations with nonlinear regression analysis. Adiabatic temperature rises curves, published by American Concrete Institute (ACI), ACI 207.1R-96 [2] are widely used in this method.

These curves were developed a few decades ago by laboratory experiments for concrete mixes made with different cement and aggregate types, and placing temperatures etc. under adiabatic or semi adiabatic conditions. However, applicability of these method is limited as it does not represent certain variations of mineral composition of cements, thermal boundary conditions, etc.

The hydration kinetic model developed on assumption of concentric layered growth of hydrates proposed by Kondo et al. [64] in 1968, was the initial effort with regard to hydration kinetic modelling. Later on, in 1979 and 1982, Clifton and Fronhnsdoff [65, 66] further developed the model proposed by Kondo et al. [64] by integrating reaction diffusion with microstructural development model developed by Williamson [67] for cement hydration. This model effectively describes cement hydration reaction with time dependent diffusion and water transport through CSH layers in spherical coordinates system. General shortfall with these single-particle models are, it does not prevail interaction in between particles, difference in size of grain, and space filling in between particles [68].

Nucleation and growth models such as CEMHYD3D, and HYMOSTRUC are effectively account the above shortfall exists in single particle models as explained above. These nucleation growth model effectively simulate phase transformation from one to another. Here whole kinetics of nucleation and growth are described mathematically based on simple Power law [69]. Later on, early and JMAK nucleation and growth phenomena are applied to address more complex behaviors once the stable nucleus completes its initiations [70]. However, these simulations require sophisticated computer tools with advanced computing power which is a little obstacle to implement in general purpose computers with regards to predict behaviors in concrete hydration.

Maekawa et al. [4], developed a multicomponent model to simulate hydration of Portland cement relying on individual mineral component's hydration reactions with

and their liberated total heat. Furthermore, it is capable to simulate the effects of other influencing parameters as described in section 3.3. This model was selected to use in this study as it can be easily implement with general computer tools to predict cement hydration behavior that can be used in industrial applications.

2.9 Thermal Properties of Concrete

Thermal properties of concrete are essential parameters in heat conduction analysis with regard to cement hydration simulations. These simulations with transient heat conduction analysis are used to predict temperature rise and distribution in early age concrete under exothermic cement hydration with various thermal boundary conditions.

Essential thermal and physical input parameters to solve a transient heat conduction analysis are specific heat capacity (c), thermal conductivity (λ, k), density (ρ) of concrete, and thermal characteristics exists at boundaries of structural member. The specific heat capacity of a material is defined as the total amount of energy required to increase temperature by unit degree. The amount of heat transfer per unit temperature gradient during a unit time is termed as thermal conductivity, and this represents heat transferring rate through a medium within a time interval.

Lu et al. [27], reports that the specific heat capacity for various types of concrete are within the range from 0.22 to 0.25 kcal/kg/K, and variation is mainly due to changes in aggregate types, and mixture proportions only. Furthermore, it is reported that the specific heat capacity of concrete remains unchanged with age of concrete under 100 ^{0}C, as concrete mass contains mostly with aggregates which has thermal stability.

Specific heat capacity of mineral components of cement powder can be estimated based on Dulong-Petit Rule (DPR) and Neumann-Kopp Rule (NKR), and the results are accurate at room temperature [71]. Jindrich et al. [72] reports that many researchers use the estimated specific heat data from DPR & NKR with 3.3% mean

deviation to the absolute data. Many authors [73, 74] reported that the specific heat capacity of OPC powder as 0.167 kcal/kg/K which is approximately equal with DPR & NKR estimation.

The thermal conductivity is significantly influence by fractional volumes of each material components, shape of aggregates, and thermal conductivity characteristics of individual material components of a specific concrete [38]. Thermal conductivity of concrete with limestone aggregates is reported as 61.924 kcal/day/m/K [7, 8] and concrete with siliceous aggregates such as quartz with higher thermal conductivity is reported in the range of 103 ~ 165 kcal/day/m/K [7, 9, 10]. Results reported in literature on Experimental investigations of thermal conductivity of fresh concrete are highly scattered with contradictory results [5, 6, 7, 8, 9, 10]. This is mainly due to conventional steady state methods to estimate thermal conductivity of fresh concrete, which is a heterogeneous, saturated porous material, produce large errors as the parameters used in estimation are very sensitive [6]. Transient measurement methods reducing moisture movements are desirable to estimate thermal properties of fresh concrete [7].

Steady state, transient and flash methods are popular in most researches in terms of investigating the thermal conductivity of concrete. Conventional methodology adopted in steady state techniques is to maintain steady thermal boundary conditions for a specimen with given material, and measure the heat flux to estimate thermal conductivity [38]. Many researchers prefer to adopt this method as this can be applied to measure heat flux with most of liquid and solid phases while maintaining steady thermal boundary conditions. Specific disadvantage of this technique is inability to use to investigate thermal conductivity of material having higher heat capacity as it takes long time to reach steady state conditions with slow rate of temperature rise. However, this can be omitted by making the size of sample smaller with reduced mass. Further, to control steady thermal boundary conditions, temperature controlling

should be maintained with highly sensitive tools in order to maintain constant thermal boundary conditions. ASTM recommends to deploy apparatus with guarded hot plate, heat flow meter, thin heater, and guarded longitudinal heat flow technique in these regards [75, 76, 77, 78].

Specimens are applied instant heat flux to increase temperature either heating specific boundary, or line heat source in transient technique to obtain thermal conductivity of a given material sample. Transient line source technique, and hot wire technique are recommended by ASTM to investigate thermal conductivity [79, 80]. In this technique, a line heater coupled with thermocouple or a platinum wire is used as the heat source to increase temperature inside the sample instantly, and measure the increased temperature at the heating source and the time taken to reach. As the power input to the heat source known with supplied power, thermal conductivity of the specimen is derived using these parameters [38]. The main advantage of this method is comparatively short measuring time. However, the parameter involves in derivation of thermal conductivity are highly sensitive where parameters should be measured with highly sensitive tools in order to get accurate results.

Parker et al. [81] introduced the flash technique to calculate thermal diffusivity firstly for given material specimen. Once the specific heat capacity and the density of material known, thermal conductivity is estimated. Here thermal diffusivity of material is computed by measuring energy absorbed by the front face of specimen and measuring the temperature rise at the rear face due to heat conduction through the specimen. The main disadvantage of this method is the heat loss due to radiation effect from the sample surfaces include error in estimations. This can be overcome by addition correction factor as described by Daniel P.H. [38].

Analysis of heat conduction in heterogenic materials such as composite material similar to concrete, is mathematically analogous to theories of electrical conductivity, permittivity and magnetic permeability of such materials. Study of these topics dates

back to early works of Maxwell and Lord Rayleigh [82]. Since the late 19th century, many models allowing the prediction of effective thermal conductivity of various types of composite materials were proposed, for example, Winner upper and lower bounds theory, Hashin-Shtrikman Bounds theorem (HS), Maxwell Model (MM), Maxwell-Eucken Limits (MEL) theory, and Effective Medium Theory (EMT) [38].

MM and MEL models have been developed assuming heterogeneous material is made out with two basic isotropic and microscopically homogenous material, and the discontinuous phase is dispersed in continuous phase, and no consideration is given for the shape of dispersed material. However, Landauer [82] explored firstly the EMT by applying to a composite medium with two phases with regard to compute electrical resistance, and thermal conductivity. Here it is assumed that each different phase is distributed in a random dispersed distribution throughout the composite medium.

In the majority of these models, the interfacial thermal resistance (ITR) between matrix and filler is not taken into account. However, later studies show that this type of thermal resistance may have a relatively large influence on the value of effective thermal conductivity [82]. First expressions for effective thermal conductivity of composite materials, which included the influence of ITR, were derived by Hasselman and Johnson [83] in the 1980s by modifying the original Maxwell model.

3 Methodology

3.1 Introduction

This chapter describe the methodologies which are adopted to achieve the scopes of this study. A heat conduction analysis is required in order to predict thermal responses and sensitivity with respect to various conditions that can be anticipated during service life of a concrete structure. As the main objective is to predict temperature rise in concrete due to heat of hydration of cement under various initial and thermal boundary conditions, a dynamic thermal analysis is required to carry out for a given concrete mix, chemical composition of cement, geometric size of concrete member, type of formwork used in concrete casting, initial temperature during concrete batching, ambient temperature variations anticipated during hardening of concrete, effective thermal properties and their variations, etc. To evaluate all these effects at each time steps, a main heat conduction analysis program is used linking with several subroutines to simulate, heat generation due to heat of hydration of cement, variation of thermal property of concrete, and thermal boundary conditions. In section 3.2, procedures of the main transient heat conduction analysis program are briefly described.

A multicomponent subroutine which computes heat generation inputs is described in section 3.3. Heat generations due to heat of hydration of cement at each time steps for a particular element is estimated based on; updated element's temperature, mineral compositions of cement, reference heat generation rates of mineral components, fineness of cement powder, thermal activity of mineral components, etc. Section 3.4 describes about the subroutine which predicts thermal properties and their variations with respect to age of concrete. Prediction is based on chemical compositions of cements, mix proportions, degrees of hydration, etc. Specific heat capacity of concrete is predicted with application of DPR, NKR, and mixing theory. Thermal conductivity model, which describes in section 3.5, is computed based on factional volume changes

of constituents in cement paste with respect to degree of hydration of cement, and applying Winner upper & lower bound theory, and effective medium theory as described in section 2.9. Model to apply ambient temperature variations with respect to time of a day as thermal boundary conditions is described in section 3.6.

Experimental investigation program with predetermined concrete mixes were implemented in order to calibrate, and verify the subroutines used to predict thermal properties and temperature rise due to heat of hydration under known thermal boundary conditions. Concrete mixes were defined covering strength classes of concrete and cement types defined as per ASTM, British, and European design guidelines as stated in sections 5.5 and 6.3. Initial calibration and verification of model to predict thermal properties were achieved following the method stated in section 5. Model to predict temperature rise due to heat of hydration were initially calibrated and verified with experimental data as described in section 6. Further verifications were undertaken with temperature rise data available in previous experimental investigations conducted in the field.

3.2 Transient Heat Conduction Analysis

Transient heat conduction analysis, supported by ANSYS Multiphysics, determines temperatures, thermal gradients, heat flow rates, and heat fluxes in an object that are caused by thermal loads which are time dependent. Such thermal loads include, convections, radiation, heat flow, heat fluxes, heat generation rates, variable temperature boundaries. Subroutine programs are used to specify time-dependent loads defining an equation or function describing the curve and then apply the function as a boundary condition, or divide the load-versus-time curve into load steps. Here, thermal analysis is nonlinear, with constant material properties; or nonlinear, with material properties that depend on temperature, time or another parameter.

Analysis are conducted using below defined unit system which deviated slightly to suite with the output from heat generation model described in section 3.3. User defined unit systems are as shown in Table 3-1.

Table 3-1: User defined system of units uses in thermal analysis

Measurement	Unit	Symbol
Distance	Meters	m
Weight	Kilograms	kg
Time	Day	d
Energy	Kilocalorie	kcal
Temperature	Kelvin	K

Material index numbers are first defined for concrete and formwork. These numbers are eventually used by the cement hydration subroutine to identify only concrete element to which heat generation is to be assigned. Concrete member and form geometry is initially created with volumes defined based on key nodes. Meshing of volume with pre-determined sizes are then carried out assigning material index numbers for concrete and formwork. Element type uses in meshing of all volumes is SOLID70 which is 3-D thermal solid element having 8 nodes and degrees of freedom of temperature.

A flow chart illustrating procedure of the main heat conduction analysis program is shown in Figure 3-1.

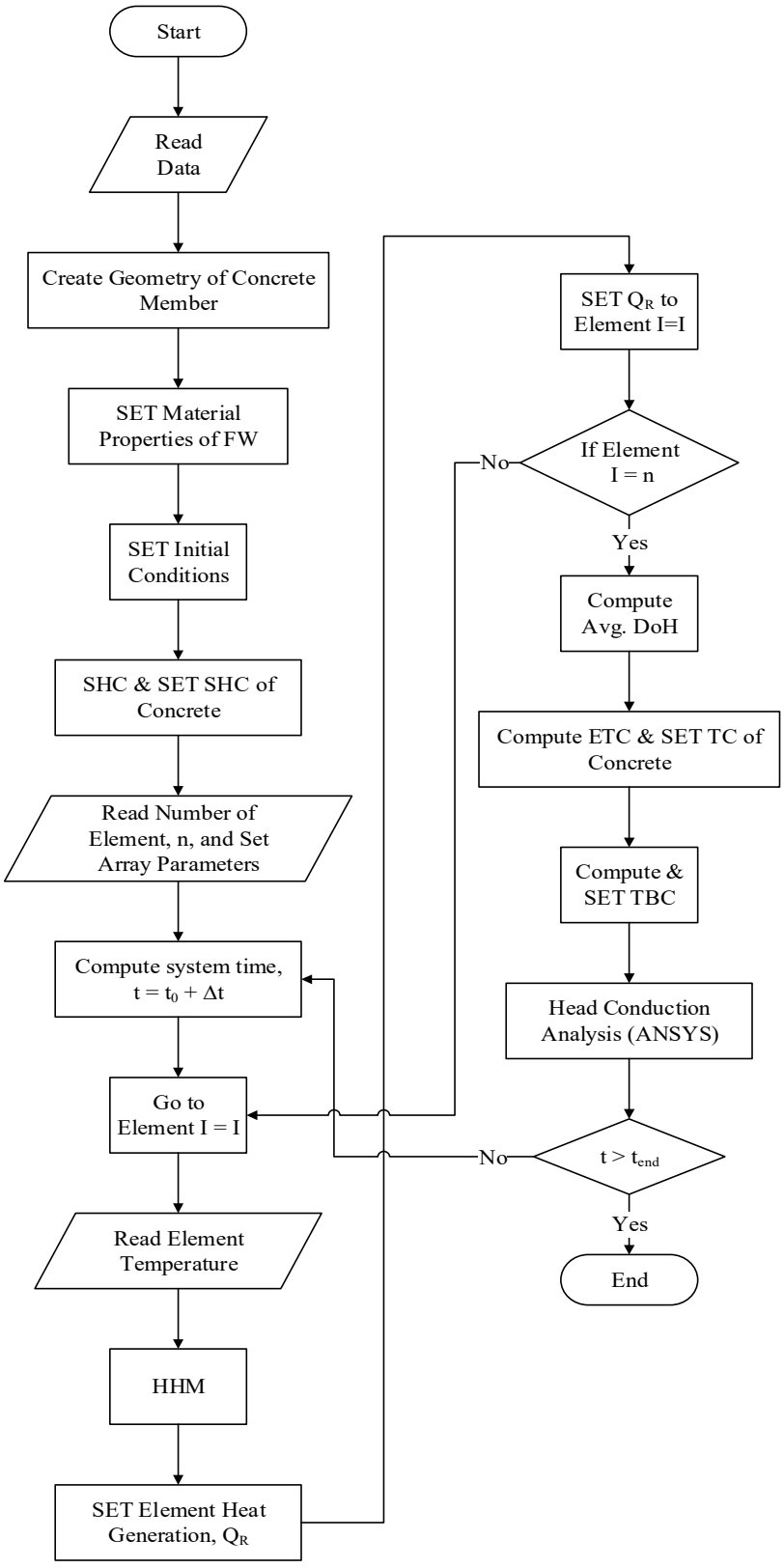

Figure 3-1: Flow Chart for Heat Conduction Analysis

Array parameters are defined to store and retrieve data during heat conduction analysis process. Further, these arrays are used to pass data in between different subroutines as local parameters uses in temporary memory are erased once returned from subroutine. These arrays extend up to third dimension (Dim) depending on scope as described in Table 3-2.

Table 3-2: List of arrays used to store and retrieve data during thermal analysis

Name	Dim	Scope	Remarks
PARADEF(I_1)	1D	Uses to store data of concrete mix, chemical composition of cement, thermal and physical properties of concrete material, time and etc. 66 numbers of parameters are initially defined using user inputs.	I_1 denotes number of elements, where; I_1 = 1, 2, ….,66
TNOD(K_2,I_2,J_2)	3D	Nodal temperatures of each elements are stored. Elements in this array are specified in terms of number of nodes of an element (8), element number (ET), and number of load steps to be solved (NLS).	K2, I2, and J2 denote index number of node, index number of element, and number of load steps, where; K_2 =1, 2, …., 8 I_2 = 1, 2, …., ET , and J_2 = 1, 2, …, NLS

ND(K_3,I_3,J_3)	3D	Parameters such as average temperature of elements, heat generation rate, accumulated heat, free water, and etc. computed during cement hydration process are stored for each element. Array elements are defined with respect to 169 parameters with adjustment to the size of the array based on number elements (ET) and load steps (NLS) to be carried out for the heat conduction analysis.	K_3, I_3, and J_3 denote parameter index number, element number and number of load steps where; K_3 = 1, 2, …, 169 I_3 = 1, 2, …, ET , and J_3 = 1, 2, …, NLS
MI(I_4)	1D	Material index numbers defined during meshing of each volumes are stored relevant to element number (ET). Size of the array is determined with the number of elements available after meshing.	I_4 denotes number of elements, where; I_4 = 1, 2, …, ET
ET(I_5)	1D	Uses to store index numbers of 8 nodes associated with a single solid element. This is temporary array uses to estimate average temperature before starting estimation cement hydration rate for each element.	I_5 denotes number of nodes associated in 8 node solid element, where; I_5 = 1, 2, ……., 8

Thermal and physical properties such as specific heat capacity, thermal conductivity, and density are defined for material, as given in Table 3-3, to carry out heat conduction analysis.

Table 3-3: Physical and thermal properties of material uses in thermal analysis

Material	Physical Properties	Thermal Properties		
	Density, ρ [kg/m^3]	Specific Heat Capacity, C [kcal/kg/K]	Thermal Conductivity, K [kcal/day/m/K]	Coefficient of Thermal Convection, H [kcal/day/m^2/K]
Concrete	Estimates with respect to mix proportions as described in sections 3.4 and 3.5			108
Fly wood	530	0.30	8.00	95
Steel	7850	0.11	2.62	308
Soil	1800	0.26	1.00	115

Initial system time is then set following 24-hour time to use in calculation the time at the end of each load steps, once material properties which remains as constant during hydration of cement in concrete are defined. Initial condition is then set to concrete elements, before starting computation of heat of hydration of cement. Such initial condition is defined as temperature at concrete batching.

Before initiation of heat computations for the first load step, specific heat capacity and possible upper and lower boundaries of thermal conductivity in concrete are estimated with user input data on concrete mix. Such data are mix proportions, chemical composition of cement, and thermal properties of constituent material. Specific heat capacity is set as a constant material property as described in section 3.4. Thermal conductivity is defined varies with continuation of cement hydration. Therefore, reference temperature boundaries (T_0 & T_{100}) are assigned to compute thermal conductivity with degrees of hydration (DoH).

Nodal temperatures of associated nodes of an element is read before initiate computations of heat of hydration of cement, and stored into array TNOD. Then nodal temperature data are processed to estimate the average element temperature, and stored them into array ND. Eventually, computation of heat generation due to cement hydration process is started and estimate the volumetric heat generation rate (Q_R), and DoH for each concrete element. The estimated Q_R is assigned to relevant concrete solid element as a self-generated heat body load. Approach for computation of cement hydration is explained in section 3.3.

Once DoH is known for each concrete element, thermal conductivity of concrete is assessed during each load steps using, average DoH, thermal conductivity at 0% and 100% DoH, and associated temperatures T_0 & T_{100}. In contrast, say that thermal conductivity of concrete at 0% and 100% DoH are K_0 & K_{100}, and respective associated temperatures originally defined are T_0 & T_{100}. Then back calculate the associated temperatures T_{0R} & T_{100R} to be set to obtain the estimated thermal conductivity K_1 as described in section 3.5, in conjunction with average DoH, and elemental temperature. Before starting solving the load step, updated T_{0R} and T_{100R} are set, so that ANSYS linearly interpolate and use appropriate thermal conductivity K_1 to solve heat conduction analysis phenomena for the load step.

After setting elemental heat generation loads for each concrete element, and thermal conductivity of concrete, compute the boundary temperature using ambient temperature with respect to time of day, and set thermal boundary condition accordingly. Methodology of subroutine to compute the ambient temperature is describe in section 3.6. Then solution of load step is started and update resulting temperatures at each node. This process repeats until the numbers of load steps reaches to NLS, and terminates the heat conduction analysis. During termination of program all the data in array ND writes to Text file so that it can be used for further analysis to investigate maximum temperature rise, temperature gradient etc.

APDL coding of main heat conduction analysis program is given in APPENDIX C.

3.3 Modelling of Heat of Hydration of Cement

This section outlines basic methodology of the heat of hydration model developed by Maekawa et al. [4] that is implemented in program subroutine to compute heat generation rate due to cement hydration process in terms of predicting the thermal responses in concrete. This section mainly focuses on methodology of heat evaluation model. Chemical reactions relate to cement hydration process are described in section 2.6 above. This model compute heat generation rate based on chemical and physical properties of cement powder, mix proportions, micro structure development, reduction of free water, and moisture transport phenomena. Basically, major compounds in OPC are aluminate (C_3A), alite (C_3S), belite (C_2S), ferrite (C_4AF), and gypsum ($C\dot{S}_2H$). In addition to major components in OPC, blending material such as fly ash (FA) and slag (SG) are added to produce blended cements. The hydration process of cement is modeled by considering hydration process of individual mineral component separately in this model. Furthermore, this model can be easily implemented into general purpose FE software such as ANSYS which runs on desktop computers.

Maekawa et al. [4] explain heat generation during cement hydration in terms of two material functions. These are reference heat generation rate, and thermal activity of mineral components of cement powder. Furthermore, the following effects are included in this model to make heat evaluation realistic.

1. Temperature dependency on rate of cement hydration
2. Retarding effects of fly ash and chemical admixtures (γ)
3. Availability of free water content (β_i)
4. Effect of weight percentage of clinker minerals (μ)
5. Fineness of powder materials (s_i)

6. Effects of calcium hydroxide production on reaction of fly ash and slag (λ)

The specific heat generation rate for cement powder, H_c, is explained as given in equation 3-1.

$$H_C = \sum p_i . H_i \qquad 3\text{-}1$$

Where, p is the fractional mass of i^{th} mineral component, and i represents C_3A, C_3S, C_2S, C_4AF, SG, and FA. Here specific heat generation rate for C_3A, and C_4AF are given such that $H_{C3A} = H_{C3AET} + H_{C3AMN}$, and $H_{C4AF} = H_{C4AFET} + H_{C4AFMN}$ considering heat generation during formation of ettringite (ET) reacting with $C\dot{S}_2H$, and conversion of ettringite to mono-sulfate (MN).

Specific heat generation rate, H_i, of i^{th} mineral components is defined based on Arrhenius' law as given in equation 3-2.

$$H_i = \gamma \beta_i \lambda \mu s_i H_{i,T0}(Q_i) exp\left\{ -\frac{E_i}{R}\left[\frac{1}{T} - \frac{1}{T_0} \right] \right\} \qquad 3\text{-}2$$

Where,

Q_i : Accumulated heat, and $Q_i = \int_0^{\infty} \int H_i dt$

R: Gas constant,

$\frac{E_i}{R}$: Thermal activity,

T_0 : Reference temperature, and

T: Temperature

The reference heat generation rates, $H_{i,T0}$, at reference temperature (T_0 = 293 K) for each mineral components of cement are given in Figure 3-2, and Figure 3-4.

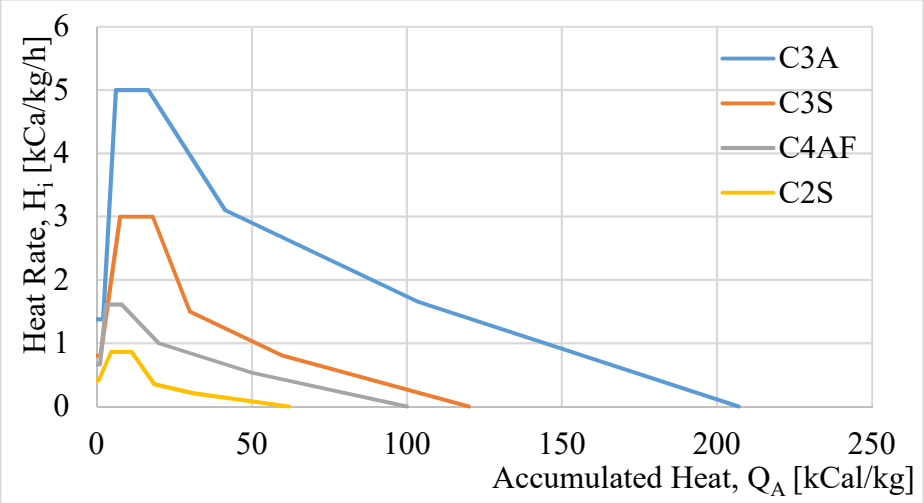

Figure 3-2: Reference heat generation curves for formation of hydrates and mono-sulfate at reference temperature, T_0 = 293 K

Source: Modelling of Concrete Performance by Maekawa et al. [4]

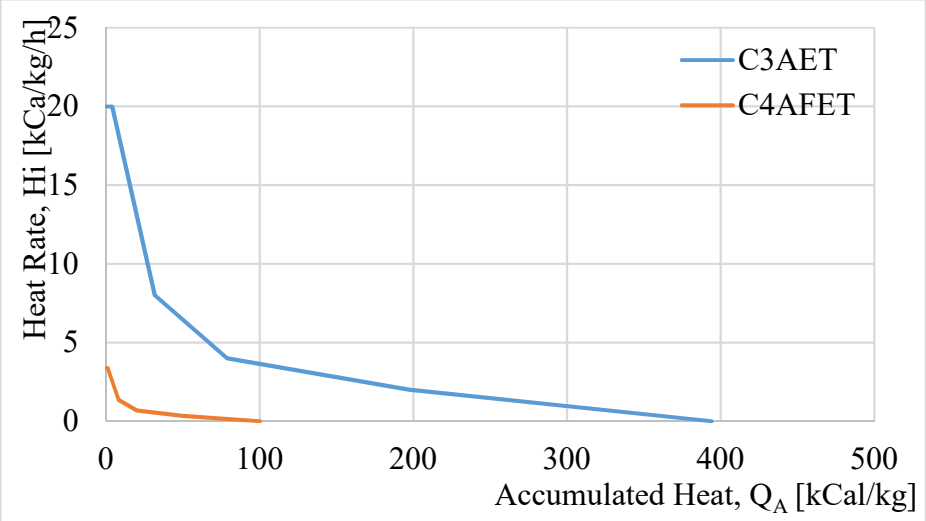

Figure 3-3: Reference heat generation rate curves for formation of ettringite at reference temperature, T_0 = 293 K

Source: Modelling of Concrete Performance by Maekawa et al. [4]

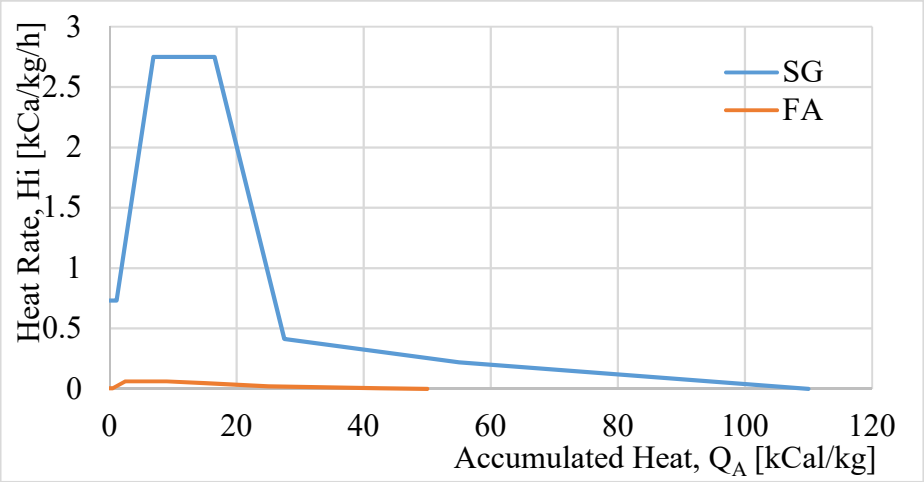

Figure 3-4: Reference heat generation rate curves for Slag & Fly ash reaction at reference temperature, T_0 = 293 K

Source: Modelling of Concrete Performance by Maekawa et al. [4]

Hydration rate depends on fineness of cement powder as finer particles react faster than coarse particles. Based on this hypothesis, Maekawa et al. [4] propose a coefficient to control rate of hydration reaction representing effects of fineness as shown in equation 3-3.

$$s_i = \frac{S_i}{S_{io}} \qquad 3\text{-}3$$

Where, S_i, S_{io} are Blaine value and Reference Blaine value of i^{th} powder component respectively.

Maekawa et al. [4] propose relationship for thermal activity of each mineral component with respect to accumulated heat as shown in Figure 3-5, relying on dependency of thermal activity with accumulated heat dissipated reported by Suzuki et al. [26] .

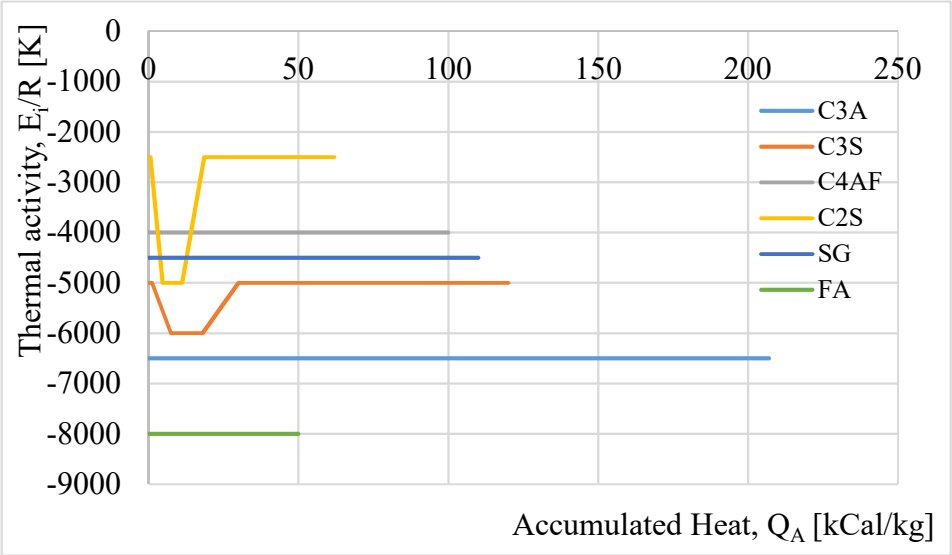

Figure 3-5: Thermal activity on reaction of cement minerals

Source: Modelling of Concrete Performance by Maekawa et al. [4]

Free water is paramount component in continuing cement hydration, and facilitates required space to precipitate the formed hydrates surround cement particles. Thus, cement hydration rate highly depends on availability of non-bound water in gel and capillary pores. Therefore, Maekawa et al. [4] propose an expression accounting retardation effect on heat generation rate with the hypothesis of availability of free water as given in equation 3-4. Further this control the reactions of clinker mineral are to be terminated with the degree of hydration reaching 100% or non-existence of free water in pores.

$$\beta_i = 1 - \exp\left\{-5.0\left[\frac{w_{free}}{100.\eta_i}.s_i^{1/2}\right]^{2.4}\right\} \qquad 3\text{-}4$$

Where,

$$w_{free} = \frac{\{w_{total} - \Sigma w_i\}}{C}$$

C : Cement content

$$\eta_i = 1 - \left(1 - \frac{Q_i}{Q_{i,\infty}}\right)^{1/3}$$

$Q_{i,\infty}$: Final heat generation of i^{th} mineral component

w_i^v : Amount of water consumed by i^{th} mineral component

w_{total} : Water content

Despite the fact that interdependence among clinker minerals are still unexplained, Maekawa et al. [4], suggest to represent this effect by factor μ as a function of C_3S/C_2S ratio as given in equation 3-5.

$$\mu = 1.4\left\{1.0 - \exp\left[-0.48\left(\frac{p_{C_3S}}{p_{C_2S}}\right)^{1.4}\right]\right\} + 0.1 \qquad 3\text{-}5$$

Where,

p_{C_3S} : Weight percentage of C_3S, and

p_{C_2S} : Weight percentage of C_2S.

The reaction rates of slag and fly ash are evaluated based on produced $Ca(OH)_2$ as a result of C_3S and C_2S hydration. Based on the study carried out by Santhikumar [84], Maekawa et al [4] express effects on rate of reaction of slag and fly ash on the amount of $Ca(OH)_2$ availability as follows.

$$\lambda = 1 - \exp\left[-2.0\left(\frac{F_{CH}}{R_{SGCH} + R_{FACH}}\right)^{5.0}\right] \qquad 3\text{-}6$$

Where, F_{CH} is the amount of $Ca(OH)_2$ produced by the hydration of C_3S & C_2S before consuming by C_4AF, and R_{SGCH} and R_{FACH} are the amount of $Ca(OH)_2$ required to continue reaction with slag and fly ash respectively expressed in equation 3-6.

In the original model proposed by Maekawa et al. [4], factors γ introduce to take into account the effects of addition of chemical admixtures and supplementary cementations materials (i.e. fly ash and slag) respectively as shown in equation 3-7. However, in this research, addition of admixture is not considered, since the intention of the present study is to model the heat of hydration of cement. Therefore, ϑSP_{ef} are considered as zero. Generally, super plasticizer delays initial setting and active heat generation. Thus, it is important to incorporate this effect into the heat of hydration model to predict the temperature rise from the time of placing of concrete. However, this effect is only applicable for the dormant period of heat generation of cement. The factor corresponds to delaying effect of admixture was obtained based on the test results as explained in section 4.3.

$$\gamma = \exp\left[\frac{-1000\left(\vartheta_{SPef} + \vartheta_{FAef}\right)}{10 p_{C_3S} s_{C_3S} + 5 p_{C_2S} s_{C_2S} + 2.5 p_{SG} s_{SG}}\right] \qquad 3\text{-}7$$

Where,

ϑ_{SPef} : Effective delaying capability of admixture

ϑ_{FAef} : Effective delaying capability of fly ash taken as 2% of fly ash replacement ratio

$p_i s_i$: Replacement ratios of C_3S, C_2S, and slag

Flow chart illustrating procedure of heat evaluation subroutine for cement hydration are shown in Figure 3-6. APDL coding of the subroutine to compute heat generation due to hydration of cement is given in APPENDIX D.

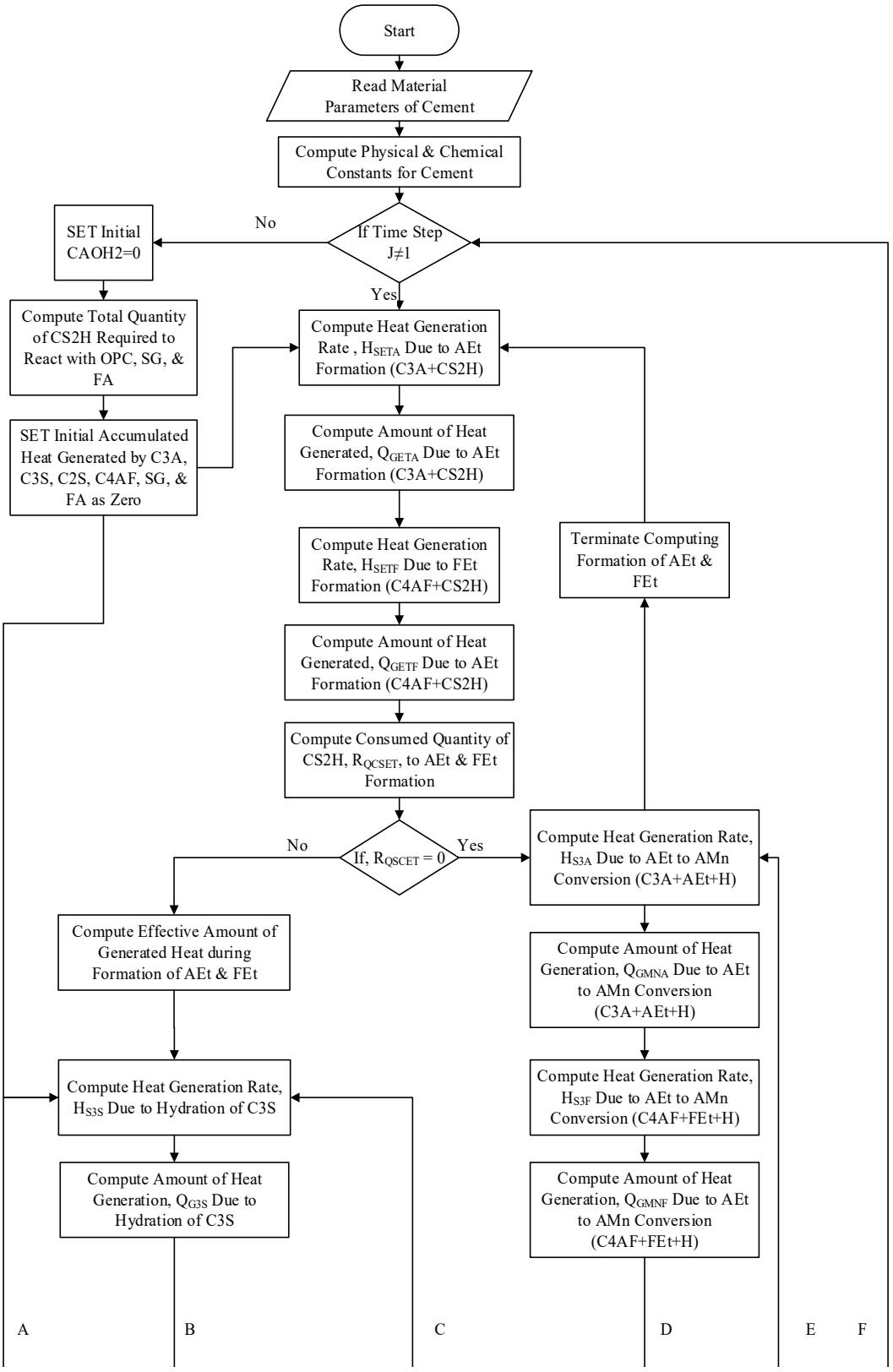

Refer next page for succeeding section of the above flow chart.

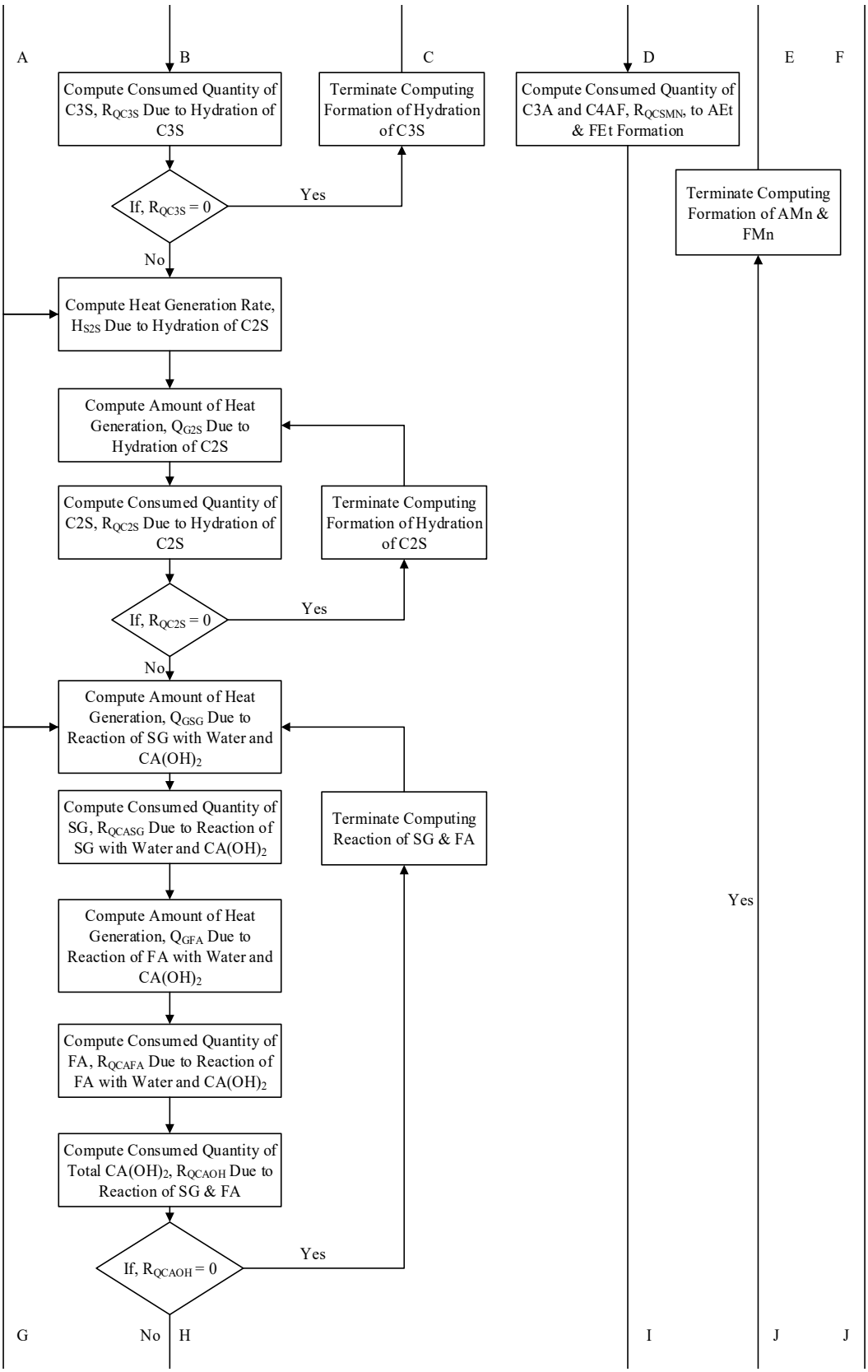

Refer next page for succeeding section of the above flow chart.

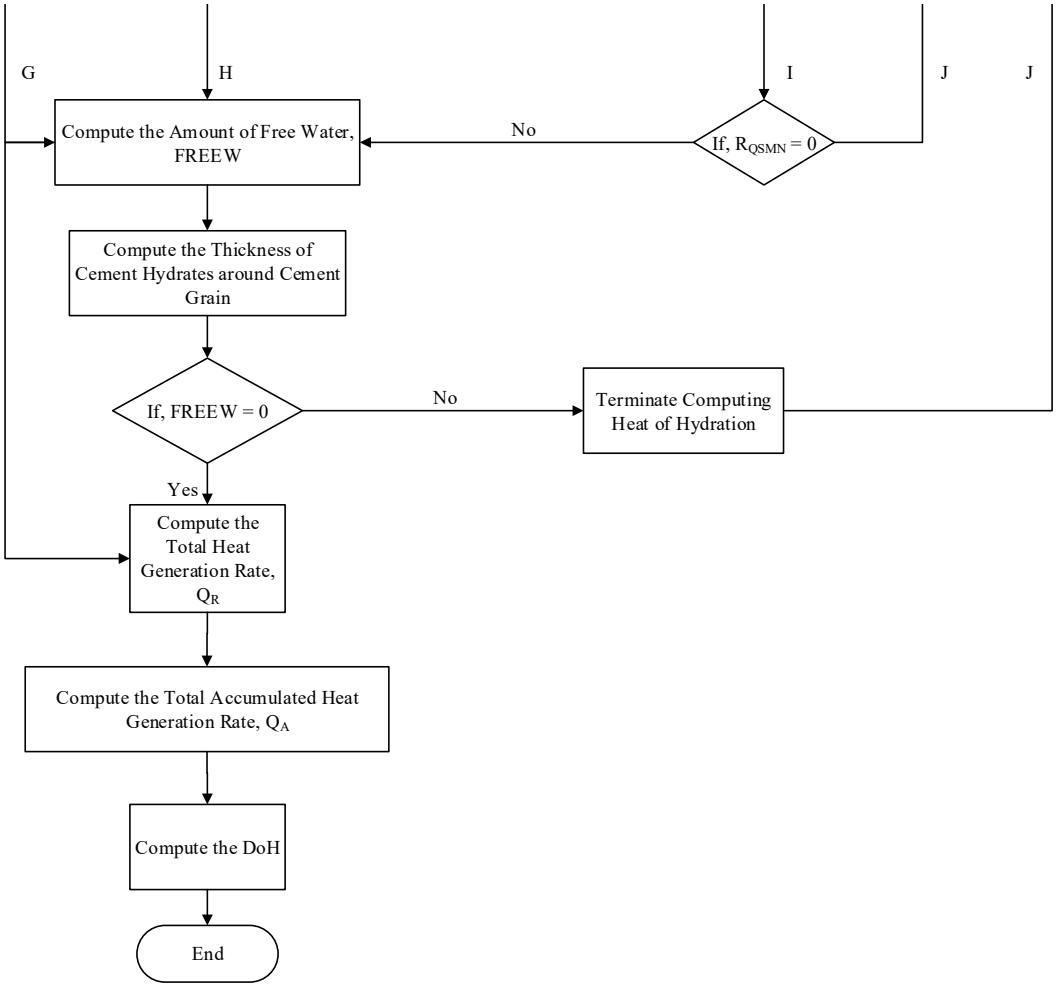

Figure 3-6: Flow Chart to Estimate Heat Generation Rate due to Cement Hydration

In the original model proposed by Maekawa et al. [4], factors γ and λ are introduced to take into account the effects of addition of chemical admixtures and supplementary cementations materials (i.e. fly ash and slag) respectively. However, in this research, addition of fly ash and slag were not considered since the intention of the present study is to model the heat of hydration of ordinary Portland cement. Therefore, λ was considered as unity. Generally, super plasticizer delays initial setting and active heat generation. Thus, it is important to incorporate this effect into the heat of hydration model to predict the temperature rise from the time of placing of concrete. However, this effect is only applicable for the dormant period of heat generation of cement. The

factor corresponds to delaying effect of admixture was obtained based on the test results as explained in section 7.

3.4 Modeling of Specific Heat Capacity of Concrete

Mixing theory is common in terms of evaluating heat capacity characteristics of composites material such as concrete. This hypothesis states that specific heat capacity of a material is given by summing the multiplication of fractional mass and specific heat capacity of material components. Major components in concrete are cement paste, fine, and coarse aggregates, mixing theory can simply be applied as given in equation 3-8 to evaluate specific heat capacity of concrete.

$$c_{ct} = \sum m_i c_i = m_{cp} c_{cp} + m_s c_s + m_g c_g \qquad 3\text{-}8$$

Where, m, c and i denote fractional mases, specific heat capacity of cement paste (cp), sand (s), and aggregate (g).

Cement paste consists un-hydrated cement powder, cement hydrates, free water, and vaporized air in capillary and gel pores as described in section 2.5. Therefore, specific heat characteristics of cement paste eventually rely on specific heat characteristics of these major components in cement paste. However, contribution to specific heat capacity of cement paste from vaporized air in pores, are insignificant with lesser fractional mass and specific heat capacity. Hence, these components are neglected in evaluation of specific heat capacity of concrete. Specific heat capacity of cement paste can be evaluated with heat evaluation principle for mixes again as given in equation 3-9.

$$c_{cp} = \sum m_j c_j = m_c c_c + m_{ch} c_{ch} + m_{fw} c_{fw} \qquad 3\text{-}9$$

Where, m, c and j denote fractional mases, and specific heat capacity of cement powder (c), cement hydrates (ch), and free water (fw).

The specific heat capacities of cement powder and hydration products are predicted using Dulong – Petit Rule (DPR) [72] and Neumann – Kopp Rule (NKR) [72] using molar heat capacities of constituent atoms initially, and applying mixing theory to obtain total specific heat capacities. Atomic heat for most of solid elemental substances presents in cement are given in Table 3-4, and this is reported by J.W. Mullin [85].

Table 3-4: Atomic Heat for Solid Elemental Substances

Elemental Substance	Atomic Heat, [cal/mol/K]
Carbon, C	1.8
Hydrogen, H	2.3
Oxygen, O	4.0
Aluminum, Al	3.5
Silicon, Si	3.8
Sulfur, S	5.4
Calcium, Ca	6.2

Specific heat capacities of cement minerals based on DPR & NKR are given in Table 3-5.

Table 3-5: Specific Heat Capacities of Cement Mineral Components

Cement Mineral	Formula	Molar mass [g/mole]	Calculation, [cal/mol/K]	Specific Heat Capacity, [kcal/kg/K]
Aluminate, C_3A	$3CaO.Al_2O_3$	270.191	3(6.2+4.0) +2x3.5 +3x4.0 = 49.6	0.1837
Alite, C_3S	$3CaO.SiO_2$	228.314	3(6.2+4.0) +3.8 +2x4.0 = 42.4	0.1857
Belite, C_2S	$2CaO.SiO_2$	172.237	2(6.2+4.0) +3.8 +2x4.0 = 32.2	0.1870
Ferrite, C_4AF	$4CaO.Al_2O_3.Fe_2O_3$	485.955	4(6.2+4.0) +2x3.5 +3x4.0+2x6.2 +3x4.0 = 84.2	0.1733
Gypsum, $C\dot{S}_2H$	$3CaSO_4.2H_2O$	136.134	3(6.2+5.4+4x4.0) +2x9.8 = 102.4	0.7522

Specific heat capacities of cement hydrates based on DPR & NKR are given in Table 3-6.

Table 3-6: Specific Heat Capacities of Cement Hydration Products

Cement Hydration Product	Formula	Molar mass [g/mole]	Calculation [cal/mole/K]	Specific Heat Capacity [kcal/kg/K]
Calcium Hydroxide, CH	$Ca(OH)_2$	74.092	6.2+ 2(4.0+2.3) = 18.8	0.2537
Calcium Silicate Hydrate, $C_3S_2H_3$	$3CaO.2SiO_2.3H_2O$	342.442	3x10.2 +2x11.8 +3x9.8 = 83.6	0.2441
Tetra calcium Aluminate Hydrate, C_3ACH	$3CaO.Al_2O_3.Ca(OH)_2.12H_2O$	560.463	3x10.2+19 +18.8+12x9.8 = 186	0.3319
Calcium Aluminoferrite Hydrate, C_6AFH_{12}	$6CaO.AI_2O_3.Fe_2O_3.12H_2O$	814.289	6x10.2+19 +24.4+12x9.8 = 222.2	0.2729
Calcium Trisulfoaluminate Hydrate (AEt), $C_3A(C\dot{S}_2)_3H_{32}$	$3CaO.AI_2O_3.3CaSO_4.32H_2O$	1255.073	3x10.2+19 +3x27.6 +32x9.8 = 446	0.3554
Calcium Trisulfoaluminoferrite Hydrate (FEt), $C_3AF(C\dot{S}_2)_3H_{32}$	$3CaO.AI_2O_3.Fe_2O_3.3CaSO_4.32H_2O$	1414.760	3x10.2+19 24.4+3x27.6+32x9.8 = 470.4	0.3325

Calcium Monosulfoaluminate Hydrate, $C_3A(C\dot{S}_2)H_{12}$	$3CaO.AI_2O_3$.$CaSO_4$. $12H_2O$	622.505	3x10.2+19+27.6 +12x9.8 = 194.8	0.3129
Calcium Monosulfoaluminoferite Hydrate, $C_3AF(C\dot{S}_2)H_{12}$	$3CaO.AI_2O_3$. $Fe_2O_3.CaSO_4.12H_2O$	782.192	3x10.2+19+24.4 +27.6+12x9.8 = 219.2	0.2802

Computational methodology illustrating steps involves in calculation of specific heat capacity of concrete are given in Figure 3-7. Specific heat capacity of concrete is applied as a constant during cement hydration as described in section 5.2. APDL program coding of subroutine to compute specific heat capacity of concrete are given in APPENDIX E.

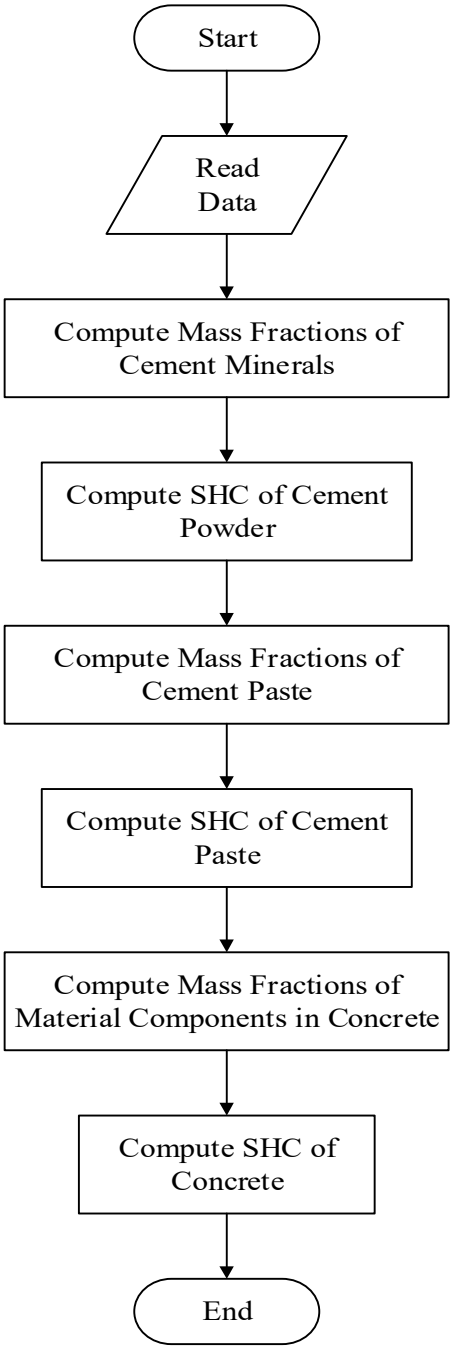

Figure 3-7: Flow Chart to Estimate Specific Heat Capacity of Concrete

3.5 Modeling of Thermal Conductivity of Concrete

Fractional volumes of major components in concrete are popular among many theories developed to predict thermal conductivity characteristics in concrete as described in section 3.5. Major components required to evaluate thermal conductivity

of concrete are basically cement paste, porosity of cement paste, fine and coarse aggregate and interfacial zone in between aggregate and cement paste. Cement paste consists of un-hydrated cement powder and cement hydrates known as cement gel, pores filled with free water and humid air as explained in section 2.5. In addition to fractional volumes, thermal conductivity, and shape of components are required in assessment of thermal conductivity of concrete. In addition to fractional volumes, temperature, pore pressure and relative humidity inside cement paste are essential in terms of predicting thermal conductivity of free water and humid air. Thermal conductivity characteristics in interfacial zone is noticeably greater than in cement gel, mainly as a result of present in rich water content and not as much of humid air, and thermal conductivity of water considerably higher than humid air [38].

Apart from many theories proposed by different authors which mostly can only be applied for two phase systems, a more general model proposed by Wang et al. [86], as given in equation 3-10, was used to evaluate thermal conductivity characteristics of cement paste (K_{cp}) with the presence of three phase system, i.e. solid, liquid, and gas in cement paste.

$$K_{cp} = \frac{\sum_{i=1}^{n} K_i \emptyset_i \frac{d_i K}{(d_i - 1)K + K_i}}{\sum_{i=1}^{n} \emptyset_i \frac{d_i K}{(d_i - 1)K + K_i}} \qquad 3\text{-}10$$

Where, K_i, ϕ_i, and d_i denote thermal conductivity, fractional volume, and shape factors for solid, free water, and humid air components in cement paste respectively. K, is thermal conductivity of continuous phase. These factors, except thermal conductivity of free water and humid air, are obtained during calibration of thermal conductivity model as described in section 5.7. Thermal conductivity of water, K_w, is computed using the expression reported by University of Purdue [87] as given in equation 3-11.

$K_w = C_0 + C_1 T + C_2 T^2$ [J/s/m/K] 3-11

Where, constants C_0, C_1, C_2 are -0.582187, 6.3613×10^{-3}, -7.9715×10^{-6} respectively, and temperature, T, is in Kelvin (K).

Expression for thermal conductivity of humid air, K_g, is reported by Tsilingiris [88] as given in equation 3-12 below. This formula is used to obtained thermal conductivity of water vapor in pores.

$$K_g = \frac{K_a + x_v(0.8536K_v - K_a)}{1 - 0.1464x_v} \text{ [J/s/m/K]} \quad 3\text{-}12$$

Where, K_a : Thermal conductivity of dry air given by the following equation.

$K_a = C_0 + C_1 T + C_2 T^2 + C_3 T^3 + C_4 T^4 + C_5 T^5$ [J/s/m/K], and constants C_0, C_1, C_2, C_3, C_4, and C_5, are -2.276501×10^{-3}, 1.2598485×10^{-4}, $-0.4815235 \times 10^{-7}$, $1.73550646 \times 10^{-10}$, $-1.066657 \times 10^{-12}$, and $2.47663035 \times 10^{-17}$ respectively. Temperature, T is in Kelvin (K) [89].

K_v : Thermal conductivity of water vapor given by the following equation.

$K_v = C_0 + C_1 T + C_2 T^2$ [J/s/m/K], and constants C_0, C_1, and C_2, are $1.48436432 \times 10^{-2}$, $-3.52786713 \times 10^{-5}$, and $1.663336663 \times 10^{-7}$ respectively. Temperature, T is in Kelvin (K) [89].

x_v : Molar fraction of vapor given by the following equation.

$x_v = R_h \frac{P_{sv}}{P_0}$ For temperatures below $100\,^0C$ [88],

P_{sv} : Saturated vapor pressure,

$P_{sv} = C_0 + C_1 T + C_2 T^2 + C_3 T^3 + C_4 T^4$ [kPa], and constants C_0, C_1, C_2, and C_4 are 0.7073034146, -2.703615165x10^{-2}, 4.36088211x10^{-3}, -4.662575642x10^{-5}, and 1.034693708x10^{-6} respectively. Temperature, T is in Kelvin (K) [89].

P_0 : Atmospheric pressure (101.325 kPa), and

R_h : Relative humidity

Microstructure development model expanded by Torban C.H. [90], which was initially explored by Powers and Brownyard [69], express fractional volumes of key components in cement paste. Total porosity (ϕ_{TP}) of cement paste is explained in terms of water to cement ratio (W/C), and degrees of hydration (DoH) as given in equation 3-13.

$$\phi_{TP} = \frac{W/C - 0.17DoH}{W/C + 0.32} \quad 3\text{-}13$$

Fractional volume of empty capillary pores (ϕ_{EP}) is given by equation 3-14.

$$\phi_{EP} = \frac{0.0575DoH}{W/C + 0.32} \quad 3\text{-}14$$

Free water content (w_{free}) is appraised during heat evaluation of cement hydration as described in section 3.3. Hence, fractional volume of free water (ϕ_{FW}) is estimated as given in equation 3-15.

$$\phi_{FW} = \frac{V_{FW}}{V_{CP}} \quad 3\text{-}15$$

Where, V_{FW} : Volume of free water, V_{CP} : Volume of cement paste which remains as a constant during concrete hardening [90],

$V_{FW} = \frac{W_{free}}{\rho_w}$, ρ_w : Density of water,

$V_{CP} = \frac{m_c + m_w}{\rho_{cp}}$, m_c : Cement content, m_w : Water content, ρ_c : Density of cement paste,

and, $\rho_c = \frac{1230}{W/C + 0.32}$

Fractional volume of solid component in cement paste is given by equation 3-16.

$$\phi_{CP} = 1 - \phi_{TP} \qquad 3\text{-}16$$

Where;

$\emptyset_{cp}$: Fractional volume of cement pastes and $\emptyset_{TP}$: Total Porosity.

Once thermal conductivity of cement paste is known, effective medium theory (EMT), for two component systems in a composite is applied to obtain effective thermal conductivity of cement mortar, i.e. for cement paste and fine aggregate [38]. The effective thermal conductivity of cement mortar is expressed as given in equation 3-17 as per EMT.

$$K_{MT} = \frac{1}{4}\left\{\left[3\phi_{SD} - 1\right]K_{SD} + \left[3\phi_{CPS} - 1\right]K_{CP} + \sqrt{\left[\left(3\phi_{SD} - 1\right)K_{SD} + \left(3\phi_{CPS} - 1\right)K_{CP}\right]^2 + 8K_{CP}K_{SD}}\right\}$$

3-17

Where,

K_{SD} : Thermal conductivity of fine aggregate

ϕ_{CPS} : Fractional volume of cement pastes in mortar

$\phi_{CPS} = \frac{V_{CP}}{V_{CP} + V_{SD}}$, V_{SD} : Volume of sand in mortar

ϕ_{SD} : Fractional volume of sand in mortar, and

$\phi_{SD} = \frac{V_{SD}}{V_{CP} + V_{SD}}$

Finally, thermal conductivity of concrete is calculated by repeating EMT for cement mortar and coarse aggregate as expressed in equation 3-18. An empirical function is introduced based on water to cement ratio and DoH to thermal conductivity of coarse aggregate to encounter effects of interfacial zone in between coarse aggregate and cement mortar.

$$K_{CT} = \frac{1}{4}\left\{\left[3\phi_{AG} - 1\right]K_{AG} + \left[3\phi_{MT} - 1\right]K_{MT} + \sqrt{\left[\left(3\phi_{AG} - 1\right)K_{AG} + \left(3\phi_{MT} - 1\right)K_{MT}\right]^2 + 8K_{MT}K_{AG}}\right\}$$

3-18

Where,

K_{MT} : Thermal conductivity of mortar

ϕ_{MT} : Fractional volume of mortar

$\phi_{MT} = \frac{V_{CP} + V_{SD}}{V_{CP} + V_{SD} + V_{AG}}$, V_{AG} : Volume of coarse aggregate in concrete

ϕ_{AG} : Fractional volume of coarse aggregate in concrete, and

$$\phi_{AG} = \frac{V_{AG}}{V_{CP} + V_{SD} + V_{AG}}$$

Computational methodology illustrating steps included in estimation of thermal conductivity of concrete, are given in Figure 3-8. Thermal conductivity of concrete is applied before starting solution for each load steps during cement hydration process. APDL program coding of subroutine to compute thermal conductivity of concrete are given in APPENDIX F.

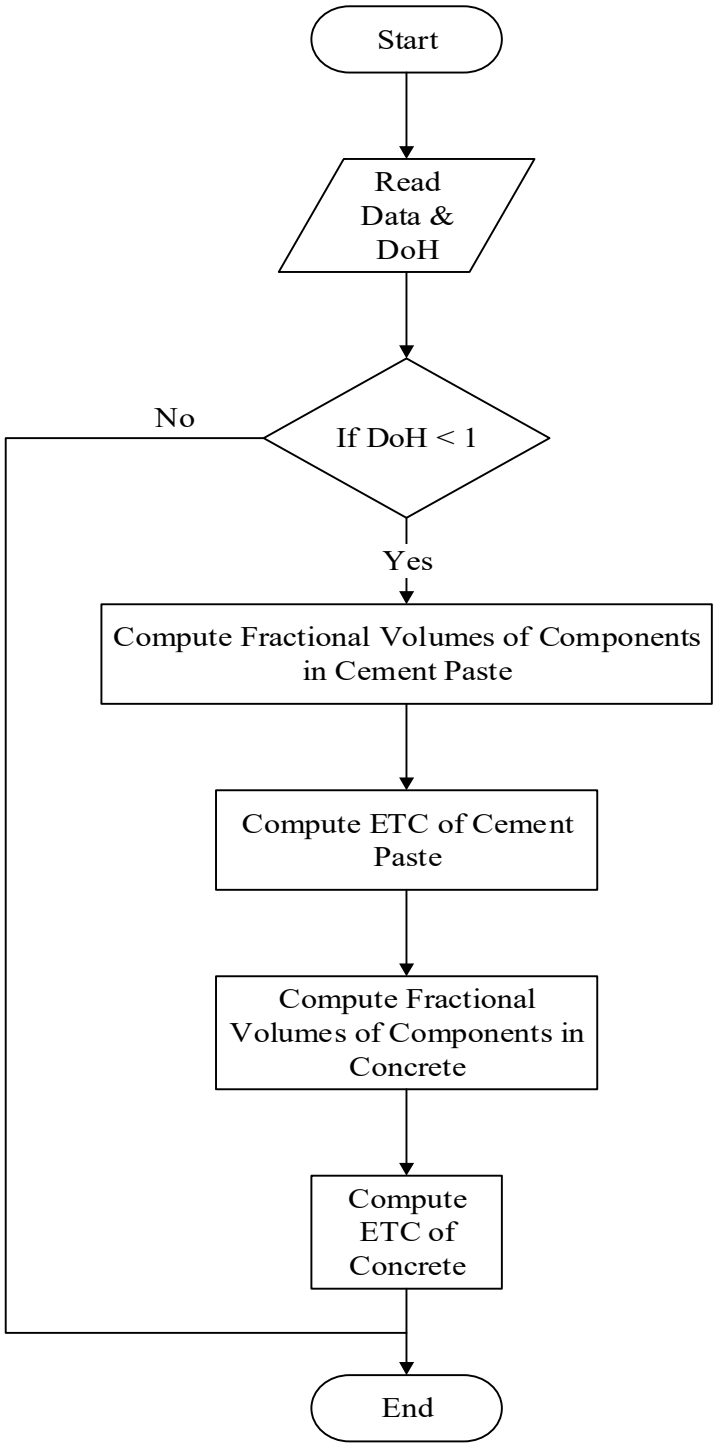

Figure 3-8: Flow Chart to Estimate Effective Thermal Conductivity of Concrete

3.6 Modeling Initial and Thermal Boundary Conditions

3.6.1 Initial Conditions

Initial temperature of concrete during concrete batching is essentially important as it affects the rate of cement hydration. Mindess et al. [56] recommends that the optimum concrete placing temperatures should be in the range of 10~15^{0}C, and should not allow to exceed 35^{0}C. Further, Mehta et al. [91] suggest that placing temperature should be maintained below 21^{0}C even in hot weather condition. Equation 3-19 is used to calculate concrete placing temperature, T_{ini}, as it is controlled by temperatures, specific heat, and weight of material components in concrete. Here, effects of moisture and entrapped air are neglected as mass fractions are negligible.

$$T_{ini} = \frac{C_{SD}T_{SD}W_{SD} + C_{AG}T_{AG}W_{AG} + C_C T_C W_C + C_W T_W W_W}{C_{SD}W_{SD} + C_{AG}W_{AG} + C_C W_C + C_W W_W} \quad 3\text{-}19$$

Where, C_{SD}, C_{AG}, C_C and C_W denote specific heat capacities of fine aggregate, coarse aggregate, cement powder, and water respectively. T, and W represent temperature and weight of above material components.

3.6.2 Thermal Boundary Conditions

There are several different heat transferring mechanisms with regards to thermal boundary conditions to describe heat transfer with respect to heat source and surrounding environment. These are conductive heat transfer to solid surfaces which are in contact, convection heat transfer from exposed concrete and form surfaces, solar absorption, and radiation from surface. Heat conduction, convection and solar absorption are only taken into account in this research as the effects of another parameter are insignificant [92]. Heat flow through evaporation and condensation mechanisms as well, were not included in this study as the effects are insignificant.

Model to predict thermal boundary conditions involves daily ambient temperature variations, wind speed, cloud cover, dew points, global horizontal solar radiation, and

extraterrestrial horizontal solar radiation. These parameters are extracted from National Climatic Data Centre in Sri Lanka, and Solar and Meteorological Surface Observation Network.

3.6.3 Heat Conduction

Thermal conduction is the heat flow when a gradient in temperature exists through a material. Generally, heat flow from high temperature to low temperature regions according to the Fourier's law [93]. In concrete structures cast directly on top of soil or surfaces exposed to air, heat due to cement hydration or heat from soil or air, exchange by means of heat conduction phenomena across the contact interfaces in between each medium. This phenomenon controls inside temperature rise in concrete, eventually cement hydration process. Further, if inside temperature is higher in respective to surrounding, heat flow occurs into soil or air, and vice versa. However, as soil underneath or surrounding air is an infinite medium, temperature rise in soil or air cannot be anticipated.

The heat flow across an interfacial medium having thickness of d_n is given in equation 3-20 [94].

$$q = \frac{(T_s - T_a)}{R_{th}} \qquad 3\text{-}20$$

Where,

q : Heat flow (J/s)

T_s : Surface temperature (^oC)

T_a : Ambient temperature (^oC)

$R_{th} = \frac{d_n}{k_n}$; Overall thermal resistance (^oC s/J), and

k_n : Thermal conductivity of interfacial layer

Here, the thickness of interfacial layer is obtained with several trials by matching surface temperature profiles of each application during model calibration. Ambient temperature, T_a is obtained using a unit function as described in section 3.6.4 below.

3.6.4 Heat Convection

Heat transferring phenomena from a body to surrounding fluid environment is called convection. This is mainly due to random diffusion and velocity of fluid transport. Convective heat transfer is expressed by the Newton's theory of cooling [94], which states the convective heat transfer in terms of convection heat transfer coefficient (h), temperatures of surface (T_s), and ambient temperature (T_a), as given in equation 3-21.

$$q = h.A.\left(T_s - T_a\right) \qquad 3\text{-}21$$

Where, q and A denote heat flow and exposed surface area, and

$T_a = (T_{a,h} - T_{a,l}).f(\mathrm{t_s})$

$T_{a,h}$: Maximum daily temperature,

$T_{a,l}$: Minimum daily temperature,

$f(t_s)$: Unit function to represent the shape of daily ambient temperature variation to be derived based on experimental data as described in section 7, and the ambient temperature is a input parameter used to estimate the thermal boundary conditions.

t_s : Time in hours in the form of serial decimal.

There are two types of convection heat transferring mechanisms, i.e. free convection and force convection. Free convection is caused with buoyancy forced applied on bulk fluid in respective to differential densities, and force convection is due to fluid transport with external force applied such as wind in air. The convection coefficient representing both free and forced convection which is proposed by Kyle et al [95] is given with equation 3-22.

$$h = 0.2782C\left[\frac{1}{T_{avg}+17.8}\right]^{0.181}\left|T_s - T_a\right|^{0.266}\sqrt{1+2.8566w} \qquad 3\text{-}22$$

Where;

C : Constant to represent heat flow, and as defined in Table 3-7 below with regards to surface orientation and hot or cool respect to the ambient temperature [95].

w : Velocity of wind

T_{avg} : Average air film temperature approximated as average of T_s and T_a, and

T_s and T_a denote surface and ambient temperature respectively.

Table 3-7: Heat flow constant, C for different surface orientations

Surface Orientation	Condition	C
Bottom Horizontal	$T_s > T_a$	10.15
Top Horizontal	$T_s < T_a$	10.15
Bottom Horizontal	$T_s < T_a$	20.4
Top Horizontal	$T_s > T_a$	20.4
Vertical	-	15.89

3.6.5 Solar absorption

Solar absorption is a heat flux that the intensity is highly depends on extraterrestrial solar radiation, atmospheric conditions, cloud cover, time of year, incidence angle of the Sun on the surface of earth, and the orientation of exposed surface [93]. Temperature rise and heat dissipation characteristics in concrete is affected significantly when concrete and form surfaces are exposed to solar absorption. John et al. [95], proposed the following equation 3-23 to 3-29 to estimate the heat flux due to solar absorption. Figure 3-9 illustrates the angles used to calculate in between components of solar radiation and particular surface where radiation is applied.

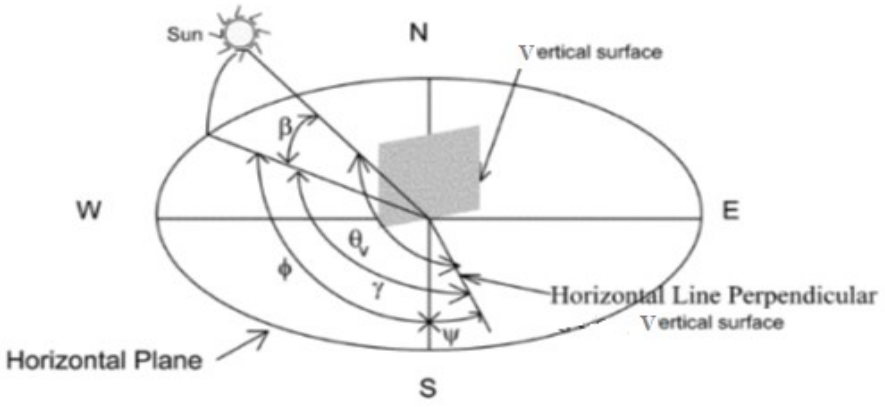

Figure 3-9: Angle used to calculate solar incidence angle on concrete surface

Source: Temperature Boundary Condition Models for Concrete Bridge Members by Kyle et al. [95]

The normal solar radiation, E_N (W/m^2) on horizontal surface is given by;

$$E_N = \frac{E_H}{Sin\beta} \qquad 3\text{-}23$$

And, the component of normal solar radiation, E_V (W/m^2) on a vertical surface is given by;

$$E_V = E_N Cos\theta_v \qquad 3\text{-}24$$

And,

$$E_H = \left[0.91 - \left(0.7C_N\right)\right] E_{TOA} \qquad 3\text{-}25$$

Where;

C_N : Cloud cover, and

E_{TOA} : Extraterrestrial horizontal solar radiation (W/m^2).

Angles marked in Figure 3-9 are given by equation 3-26 to 3-28.

$$\beta = Sin^{-1}\left(CosL_a Cos\delta CosH + SinL_a Sin\delta\right) \quad 3\text{-}26$$

$$\psi = Cos^{-1}\left[\frac{\left(Sin\beta SinL_a - Sin\delta\right)}{Cos\beta CosL_a}\right] \quad 3\text{-}27$$

$$\theta_v = Cos^{-1}\left(Cos\beta Cos\gamma\right) \quad 3\text{-}28$$

Where;

δ : Solar declination angle (degrees)

H : Apparent solar time expressed as an angle (degrees),

L_a : Latitude

L_o : Longitude, and

$$H = \frac{AST}{4}$$

AST is given by;

$$AST = LST + ET + 4(LSM - L_o)$$

3-29

LST : Local standard time and is given with minutes starting from midnight

ET : Equation of time as given in based on Julian day of the year

LSM : Local standard time meridian

Shading effects on exposed surfaces are taken into consideration, when the angle γ is in between 90^o to 270^o, which is heat flux due to solar radiation is not applied to that particular surface.

Table 3-8: Equation of time based on Julian day of the year

Range of Julian Day, D	Equation to calculate ET
$11 \le D < 106$	$ET = -14.2Sin\left[\frac{\pi(D+7)}{111}\right]$
$107 \le D < 166$	$ET = -4.0Sin\left[\frac{\pi(D-106)}{59}\right]$
$167 \le D < 246$	$ET = -6.5Sin\left[\frac{\pi(D-166)}{80}\right]$
$247 \le D < 365$	$ET = 16.4Sin\left[\frac{\pi(D-247)}{113}\right]$

3.6.6 Irradiation

Holman [94] defined that the irradiation is due to electromagnetic radiation induced by a body according to the Stefan-Boltzmann's theory. Heat flux emitted by thermal irradiation is given as equation 3-30 [13, 3].

$$\frac{q}{A} = \sigma\varepsilon\left(T_s^{\,4} - T_{sky}^{\,4}\right) \qquad 3\text{-}30$$

Where,

$\frac{q}{A}$: Heat flux per unit area (W/m^2),

σ : Stefan-Boltzmann Constant (5.669x10-8 $W/m^2/K^4$),

ε : Emissivity as given in Table 4-5,

T_s : Surface temperature (^oK), and

$$T_{sky} = \varepsilon_{sky}^{1/4} T_a \quad (3\text{-}31)$$

$$\varepsilon_{sky} = 0.787 + 0.764 \ln\left(\frac{T_{dp}}{273}\right) F_{cloud} \quad (3\text{-}32)$$

$$F_{cloud} = 1.0 + 0.024 C_N - 0.0035 C_N^{\,2} + 0.00028 C_N^{\,3} \quad (3\text{-}33)$$

T_{dp} : Dew point temperature (°K)

3.6.7 Flow Chart of Thermal Boundary Model

Initial and thermal boundary conditions estimation and setting methodology included in thermal boundary condition subroutine is illustrated by a flow chart given in the Figure 3-10. The relevant APDL programming codes are given in APPENDIX G.

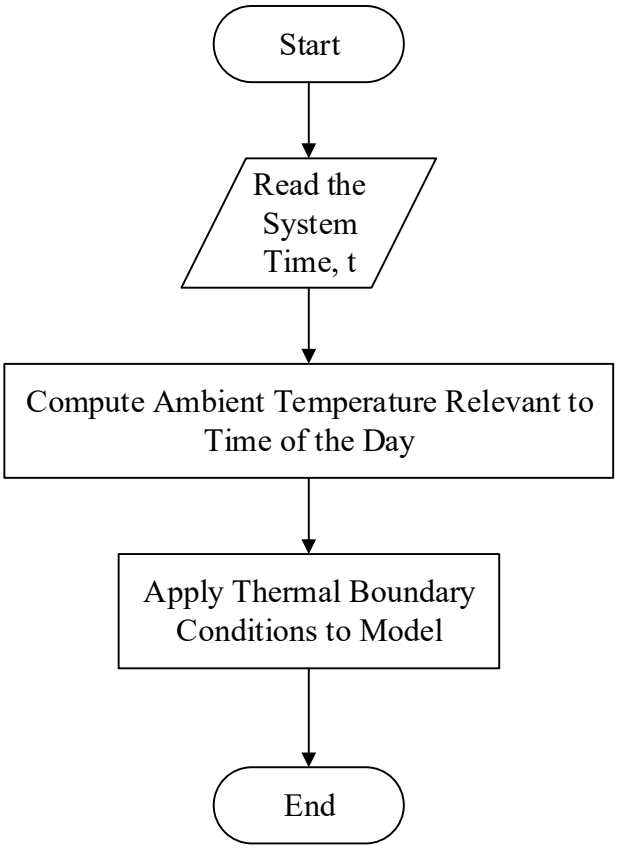

Figure 3-10: Flow Chart to Estimate Thermal Boundary Conditions

4 Experimental Investigations

4.1 Introduction

This chapter outlines the objectives and work program of experimental investigations, and chemical, physical and thermal properties of material for use in the investigation of thermal properties of concrete, and temperature rise due to heat of hydration under different thermal boundary conditions. These set of temperature rise data were processed to develop a model to predict thermal properties of concrete. Further, the predicted temperature rise using thermal property model and heat of hydration program are initially calibrated and verified with temperature rise data obtained from current experimental investigations and previous studies.

4.2 Objective

The core objectives of this experimental program are to;

a. Investigates variation of thermal properties of concrete and develop a numerical model to predict thermal properties of concrete during concrete hardening.

b. Provides independent temperature rise data due to heat of hydration of concrete with known thermal boundary conditions to calibrate heat of hydration program and thermal property models.

c. Verification of temperature rise predicted by the heat of hydration program and thermal property models for different concrete mix proportions and thermal boundary conditions.

d. Further verification with temperature rise data from previous studies conducted in the field with different structural members and thermal boundary conditions.

4.3 Experimental Program

Initially, an estimation methodology is adapted to predict specific heat capacity of concrete based on DPR, NKR, and mixing theories as briefed in section 3.4, when chemical composition of cement minerals, and mix proportions of concrete are known.

Sensitivity analysis was carried out to investigate sensitivity of thermal properties to temperature rise curve using heat conduction analysis as described in section 5.2. Furthermore, this analysis is used to identify the most sensitive portion of temperature rise curve for a particular thermal property in order to decide which thermal property of concrete is most effective parameter to be varied.

An experimental setup was planned to investigate thermal conductivity of concrete with verification of the predicted specific heat capacity of concrete. These data were then processed to develop a numerical model and computer program subroutine to predict the variation of thermal conductivity. Further, this experimental set up was planned to focus a method to monitor temperature rise inside a fresh concrete sample controlling static thermal boundary conditions and moisture movements, and how to minimize the effects of heat of hydration on temperature inside a given concrete specimen. An illustration of experimental setup, experimental plan, data analysis, and results are described in section 5.3, to 5.7. These experimental data of thermal conductivity of concrete are eventually used to calibrate and verify the program subroutine developed to predict thermal conductivity of concrete.

Finally, another experimental setup was planned to investigate temperature rise due to heat of hydration of cement in concrete by controlling semi adiabatic and ambient thermal boundary conditions. This temperature rise data are used initially to calibrate and verify the temperature rise predicted by the heat of hydration and thermal property programs. Experimental setup is described in Chapter 6 illustrating semi adiabatic and ambient thermal boundary conditions.

4.4 Ordinary Portland cement Types

In this study, thermal properties and temperature rise due to cement hydration in concrete was examined with concrete produced with Ordinary Portland Cement (OPC) available in Sri Lanka. Two types of OPC from different manufacturers are used in this experimental program for initial calibration and verification of temperature rise predicted by the program, and four different types of OPC were used for further verification of program predictions from previous experimental investigations carried out in field applications. Chemical analysis results of all OPC types were conducted using standard methods, and reported oxide compositions are given in Table 4-1.

Table 4-1: Chemical Compositions of Cement Types

Chemical Compound	Standard Notation	Cement Type					
		OPC1	OPC2	OPC3	OPC4	OPC5	OPC6
CaO	C	63.4	65.79	64.6	63.66	64.18	62.39
SiO_2	S	20.94	20.60	19.92	20.68	20.18	21.04
Al_2O_3	A	5.31	4.80	4.48	5.24	5.30	4.88
Fe_2O_3	F	3.26	3.09	3.45	3.83	3.62	3.00
MgO	M	1.22	0.76	1.28	1.89	1.20	0.62
K_2O	K	0.20	0.16	0.32	0.32	0.00	0.00
Na_2O	N	0.00	0.00	0.00	0.10	0.00	0.00
SO_3	-	2.41	2.38	2.53	2.52	1.94	1.71
Cl^-	-	0.02	0.01	0.015	0.00	0.00	0.00

The oxide compositions were analyzed to compute the percentage compositions of mineral components using Bogue analysis [14] as given in Table 4-2. Physical properties of cement types are examined and given in Table 4-3.

Table 4-2: Weight Percentage of Mineral Components of OPC

Cement Type	Weight percentage of mineral components of OPC [%]				
	C_3A	C_3S	C_2S	C_4AF	$C\dot{S}_2H$
OPC1	8.56	58.59	15.86	9.92	5.21
OPC2	7.49	67.77	7.94	9.40	5.14
OPC3	9.03	69.30	4.83	10.50	5.46
OPC4	7.41	54.07	18.50	11.66	5.44
OPC5	7.92	61.54	11.43	11.02	4.19
OPC6	7.86	52.08	21.03	9.13	3.69

Table 4-3: Physical Properties of OPC Cement Types

Cement Type	Water Demand [%]	Soundness [mm]	Setting Time [min]		Residue 45mm	Fineness [cm^2/g]
			Initial	Final		
OPC1	29.6	1.1	158.0	202.0	9.6	3093
OPC2	31.9	1.0	130.0	185.0	3.3	3335
OPC3	29.7	0.8	128.3	186.7	13.3	3950
OPC4	29.8	1.1	147.0	194.0	9.6	3450
OPC5	30.4	0.8	126.7	181.7	5.5	3370
OPC6	29.6	1.5	148.0	223.0	12.5	3800

4.5 Fine and Coarse Aggregates

Concrete mixes are produced with fine (river sand) and coarse (crushed rock) aggregate. Charnockitic gneiss or charnockite, quartzite, marble, dolomite, granulite, migmatite, gneisses and amphibolite are the common Precambrian metamorphic rocks available in Sri Lanka [96]. Therefore, thermo-physical properties of fine and coarse aggregates are in similar range as they are naturally produced from same rocks origins [97].

4.6 Physical and Thermal Properties of Material, and Thermal Boundary Parameters

Physical and thermal properties of material components in concrete, formwork, and insulation materials which are used to investigate thermal properties and temperature rise through the experimentally investigation program described in section 4.3 are given in

Table 4-4.

Table 4-4: Physical and Thermal Properties of Concrete, Formwork, and Insulations Material

Material	Density, ρ [kg/m^3]	Specific Heat Capacity, c [J/kg/K]	Thermal Conductivity, λ [J/s/m/K]
Cement Powder	3250	0.7	0.121
Hydrated Cement Paste	$\frac{1230}{W/C+0.32}$ [40]	Section 3.4	Section 3.5
Fine Aggregate	3170	1150	2.05
Coarse Aggregate	1026	1150	2.05
Water	1000	4186	Section 3.5
Atmospheric Air	-	Section 3.5	Section 3.5
Vaporized Air	-	Section 3.5	Section 3.5
Styrofoam	20	1500	0.06
Plywood	697	1256	0.46
Steel	7200	7850	1763
Subgrade Soil	1800	2100	2.18

Surface properties of concrete, formwork and insulation materials used to maintain thermal boundary conditions are given in Table 4-5 and Table 4-6. These surface parameters are used to carry out heat conduction analysis in order to predict

temperature responses due to ambient temperature, solar radiation, and wind effects…etc. as explained in section 3.6.

Table 4-5: Emissivity, and Absorptivity, for Material used in Heat Conduction Analysis

Material	Emissivity		Absorptivity	
	Found in Literature	Used in Analysis	Found in Literature	Used in Analysis
Concrete	0.88 ~ 0.93	0.92	0.23 ~ 0.59	0.4
Sand	0.93 ~ 0.92	0.92	0.40 ~ 0.60	0.4
Plywood	0.82 ~ 0.92	0.92	0.40 ~ 0.60	0.4
Steel	0.82 ~ 0.96	0.96	0.40 ~ 0.60	0.6
Styrofoam	0.82 ~ 0.92	0.92	0.40 ~ 0.60	0.4

Table 4-6: Coefficient of Thermal Convection for Material Surfaces

Material	Coefficient of Thermal Convection	
	Found in Literature	Used in Analysis
Concrete	115	115
Sand	108	108
Plywood	108	95
Steel	345	300
Styrofoam	100	90

5 Experimental Investigation of Thermal Properties of Concrete

5.1 Introduction

This chapter outlines sensitivity of thermal properties to temperature rese due to heat of hydration of cement experimental setup to investigate variation of thermal conductivity of concrete.

5.2 Sensitivity Analysis

A transient heat conduction analysis which is described in section 5.4, was conducted using ANSYS software to determine the sensitivity of thermal properties to temperature rise at the center of a concrete specimen under external heat input. The specimen was modelled as shown in Figure 5-4.

Initial inside temperature and steady state boundary temperatures were set as T_{t0} = 30 ^{o}C, and T_{o} = 40 ^{o}C respectively. Thermal conductivity and specific heat capacity of steel (0.5% Carbon) mold were considered as 54 J/s/m/K, 465 J/kg/K respectively [93].

As many authors reported [7, 8, 9, 10], the thermal conductivity of concrete was selected with an average value of 2.422 J/s/m/K.

Torban C et al. [90] reports that the degree of hydration that can be achieved within a day for OPC is 30%. Bentz [5] reveals that the specific heat capacity of saturated OPC paste with w/c of 0.3 to 0.4, linearly decreases by 14.5%, when the degree of hydration is 30%. Based on this hypothesis, the overall linear reduction in specific heat capacity of concrete including fine and coarse aggregate computed using equation 3-7, is less than 5.4% from the initial specific heat capacity of OPC concrete. Therefore, specific heat capacity of concrete was selected with the maximum value of 1339 J/kg/K adding 5.4% decrease for the sensitivity analysis (See Table 5-1).

Density of concrete was estimated based on the densities of material in concrete mixes as reported by many authors [5, 6, 73, 74, 30] using equation given in section 3.5. This remains unchanged as reported by Torban C et al. [90], due to total volumetric or mass changes do not occur thorough out the hydration process.

The specific heat capacity of gneisses and granulite type rocks are reported in the range of 670 to 1550 J/kg/K [98]. Therefore, the specific heat capacities of mix M-3 given in section 5.5, was calculated considering the specific heat capacity of aggregate reported (i.e. 670 to 1550 J/kg/K) and given in Table 5-1 below. Further, the density of concrete was estimated as 2271 kg/m^3 to calculate the thermal diffusivity of the same mix.

Table 5-1: Selected Specific Heat Capacity of Concrete assuming Thermal Conductivity as a Constant

Thermal Conductivity, k J/s/m/K	Specific Heat Capacity, c J/kg/K	Thermal Diffusivity, α m^2/s
2.422	1266.69	8.4195E-07
2.422	1339.00	7.9648E-07

Transient heat conduction analysis was performed for a 150 mm concrete cube under external temperature of 40 ^{o}C. It took nearly 1 hour and 40 minutes to reach temperature at the center to external temperature as shown in Figure 5-1. It can be also seen that change of specific heat from 1339 to 1266.69 J/kg/K (i.e. 5.4% change) has not significantly affected curve of temperature rise.

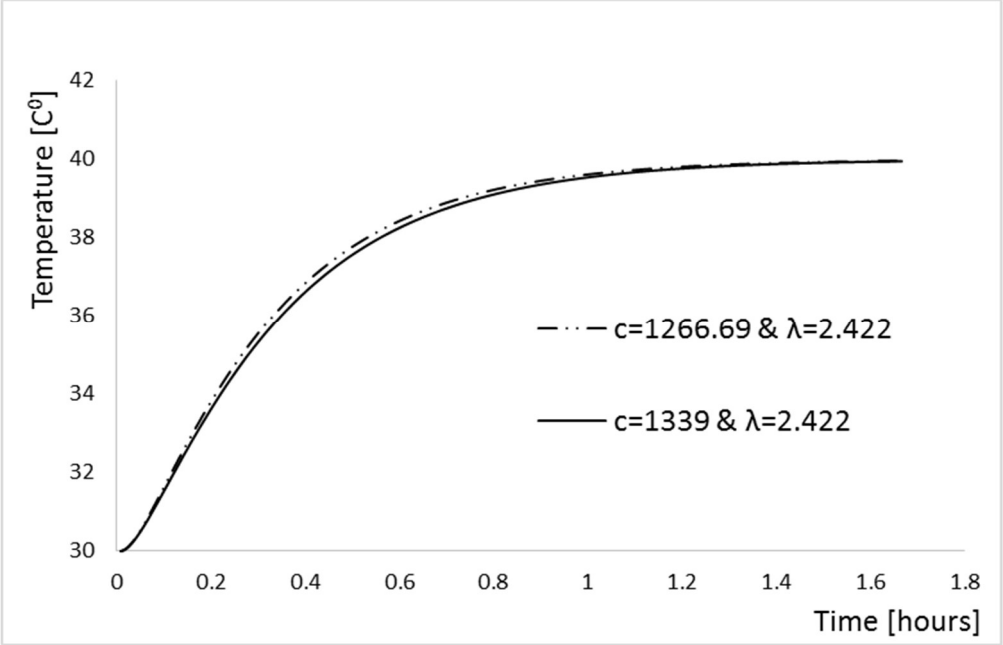

Figure 5-1: Sensitivity of Temperature Response to Specific Heat Capacity of Concrete

Further, it can be observed that 5.4% reduction in specific heat capacity affects to middle range of temperature rise curve with insignificant increase in temperature, and not for the maximum rate of temperature rise during initial stage.

Therefore, thermal conductivity of concrete can be obtained by matching the temperature variation with time obtained from experiments and transient heat conduction analysis while assuming specific heat capacity being a constant in early age concrete.

5.3 Experimental Setup

Experimental setup shown in Figure 5-2, consisted of hot water bath connected to a thermostat (TST) and thermocouple to control constant temperature T_o. Four numbers of standard steel mould were used to cast specimens, and thermocouples were placed at centers of each specimens to measure temperature rise during heating in the hot water bath as shown in Figure 5-3.

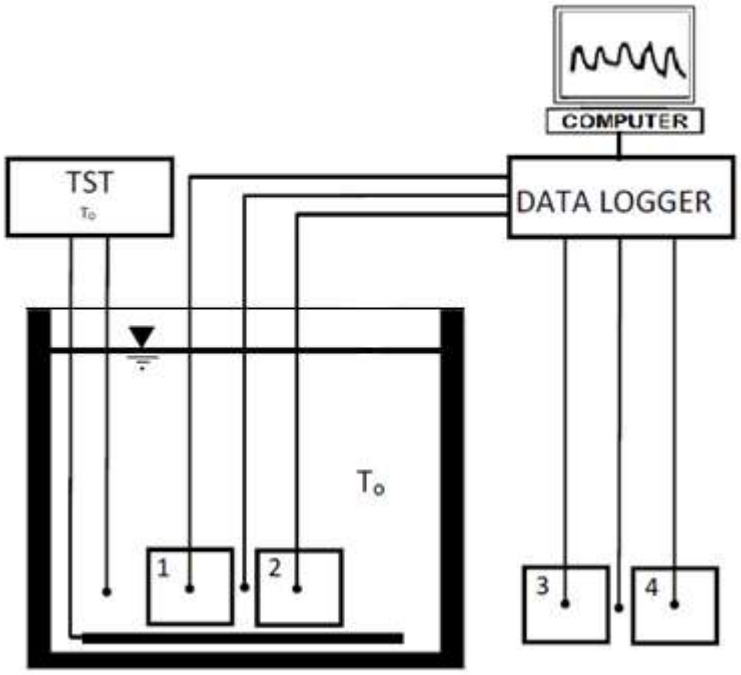

Figure 5-2: Experimental setup to measure internal temperature rise of specimens using a hot water bath

Figure 5-3: Specimens are inside Hot Water Bath

Steel molds were carefully filled with concrete continuously applying vibrations in order to minimize entrapped air. Top surface of specimens was sealed as shown in

Figure 5-4 and Figure 5-5, to avoid water movement into the specimens from water bath.

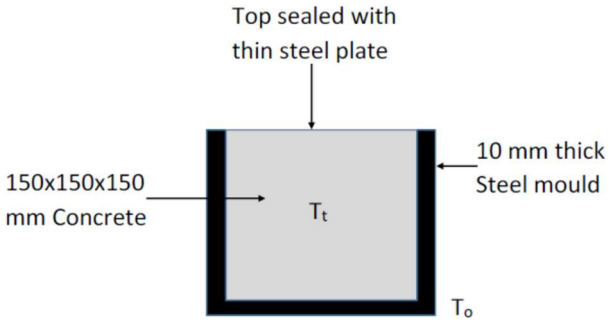

Figure 5-4: Specimen geometry, dimensions, and boundary conditions

Figure 5-5: Concrete Specimens Out Side the Hot Water Bath

Specimens 1 and 2 were immersed in hot water bath 2 hours after concrete batching, and the specimens 3 and 4 were placed outside the hot bath exposing to ambient temperature allowing them to cool. The temperature at the center of all specimens were measured at every 30 sec. intervals using a data logger. The specimen 1 & 2 were retained in hot water bath until the temperature at the centre of specimens were stabilized at the hot bath temperature (T_o). After that, specimens 1 & 2 were removed from the water bath and immersed the specimen 3 & 4 in the hot water bath. Those specimens were kept in the water bath until the temperature at the centre was stabilized.

This process was repeated for a duration of 24 hrs. Two specimens were used simultaneously for measuring the temperature response of concrete specimen at a particular age of concrete to minimize the experimental errors. Further these two set of specimens were used to measure temperature response with 10 consecutive time intervals within a day to obtain thermal property variation pattern. Temperature readings were taken at 30 sec. intervals with an accuracy of 0.01 ^{o}C, and recorded by data logger as shown in Figure 5-6.

Figure 5-6: Data Logger

5.4 Heat Conduction Analysis to Estimate Thermal Conductivity of Concrete

A macro program was written to create FEM with APDL (ANSYS Parametric Design Language) to carry out transient heat conduction analysis incorporating initial (T_i) and boundary temperatures (T_0), thermal conductivity, and specific heat capacity of concrete as input parameters to ANSYS software to predict the temperature variation with time at the center of specimen. Time interval was set as 30 seconds as per the experimental conditions.

A three-dimensional isoperimetric and eight nodes solid element was selected for the thermal analysis. In ANSYS, this element type is called SOLID70. The predicted temperature response curves were fitted with temperature response measured from the

experiment by adjusting thermal properties of concrete within the relevant time interval.

5.5 Experimental Plan

Initially, same size concrete specimens with similar arrangement were prepared for the selected mix proportions and peak temperature rise due to heat of hydration was monitored. It was found that maximum temperature difference due to hydration was 2.1 ^{o}C at around 07 hours after batching concrete. Therefore, for each time interval (approximately 90 minutes), temperature rise due to heat of hydration is approximately 0.7 ^{o}C which will not significantly affect the temperature rise due to external heat input from hot water which was kept at 10 ^{o}C above the ambient temperature.

Furthermore, keeping the temperature difference, T_o–T_i, around 10 ^{o}C helped to minimize the effect of acceleration of cement hydration process due to heating in the hot water bath [53].

The experimental plan was prepared to investigate thermal properties of fresh concrete with different cement contents, w/c, and aggregate contents as given in Table 5-2.

Table 5-2: Concrete Mix Proportions

Mix	OPC Type	Cement Content [kg/m^3]	Water Content [kg/m^3]	Fine Aggregate Contents [kg/m^3]	Coarse Aggregate Content [kg/m^3]
M-1	OPC1	395	201	1032	777
M-2	OPC1	464	178	930	758
M-3	OPC1	482	156	901	732

Mix proportions were selected by varying w/c in the range of 0.3 ~ 0.5, and total fine and coarse aggregate content in the range of 1633 ~ 2079 kg/m^3.

Hot water bath temperature for all the specimen was maintained approximately at 40 ^oC and the initial temperature for all the specimens was around 30 ^oC, which was the mean ambient temperature inside the laboratory. Core temperature of each cube was measured until the inside temperature reached the outside temperature. It took around 01 hour and 40 minutes to achieve this status.

5.6 Specific Heat Capacity of Concrete

Based on DPR, NKR, and mixing theory, the specific heat capacity of cement (OPC) was estimated using the specific heat capacities of C_3S, C_2S, C_3A, C_4AF, and $(C\dot{S})_3H_2$ as 983.3, 1013.7, 1015.5, 923.9, 1347.0 J/kg/K respectively and found as 985.6 J/kg/K for OPC1. Estimated Specific heat capacities of three mix proportions of concrete considered are given in Table 5-3.

Table 5-3: Estimated Specific Heat capacity of Concrete for three Concrete Mixes

Mix	W/C Ratio	Cement Content (kg/m^3)	Water Content (kg/m^3)	Total Aggregate Content (kg/m^3)	Specific Heat Capacity, c (J/kg/K)
M-1	0.508	395	201	1809	1377
M-2	0.384	464	178	1688	1348
M-3	0.324	482	156	1633	1323

5.7 Thermal Conductivity of Concrete

Thermal conductivity of concrete was obtained by fitting with temperature response curve predicted with transient heat conduction analysis using ANSYS, and

experimental temperature response data for mixes M-1, M-2, and M-3. Sample analytical fit with measured temperature response data of M-3 specimen 1 & 2 for the time interval between 4 hours 20 minutes ~ 6 hours are given in Figure 5-7. These curves were fitted with specific heat capacity of 1323 J/kg/K, and thermal conductivity of 2.471 J/s/m/K.

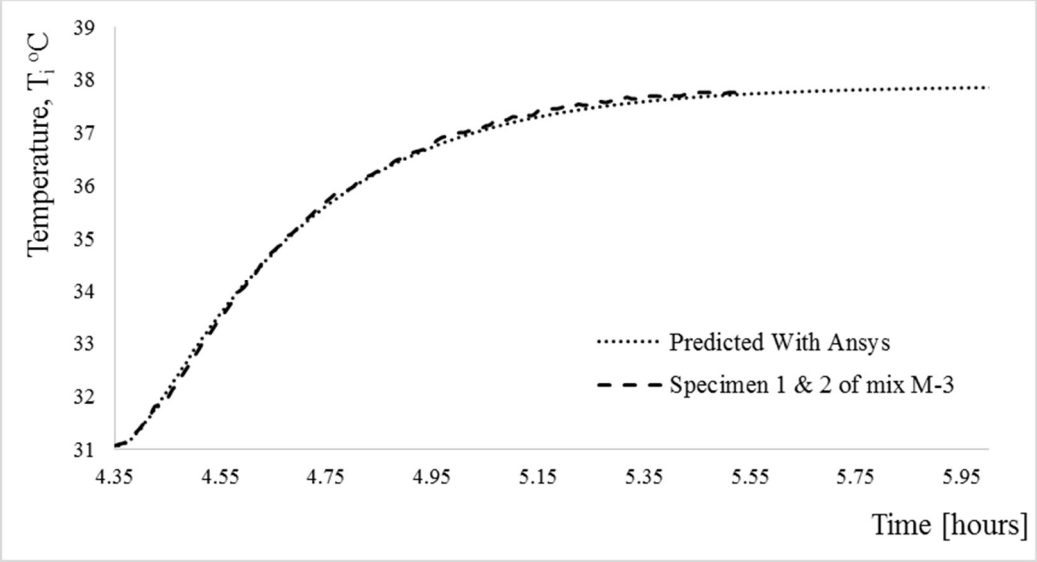

Figure 5-7: Fitted temperature response curves with relevant experimental data of M-3 specimen 1 & 2

Thermal conductivity obtained based on above described method for three Mixes are shown in Figure 5-8, and the variation of thermal conductivity with time can be expressed as nonlinear curve pattern.

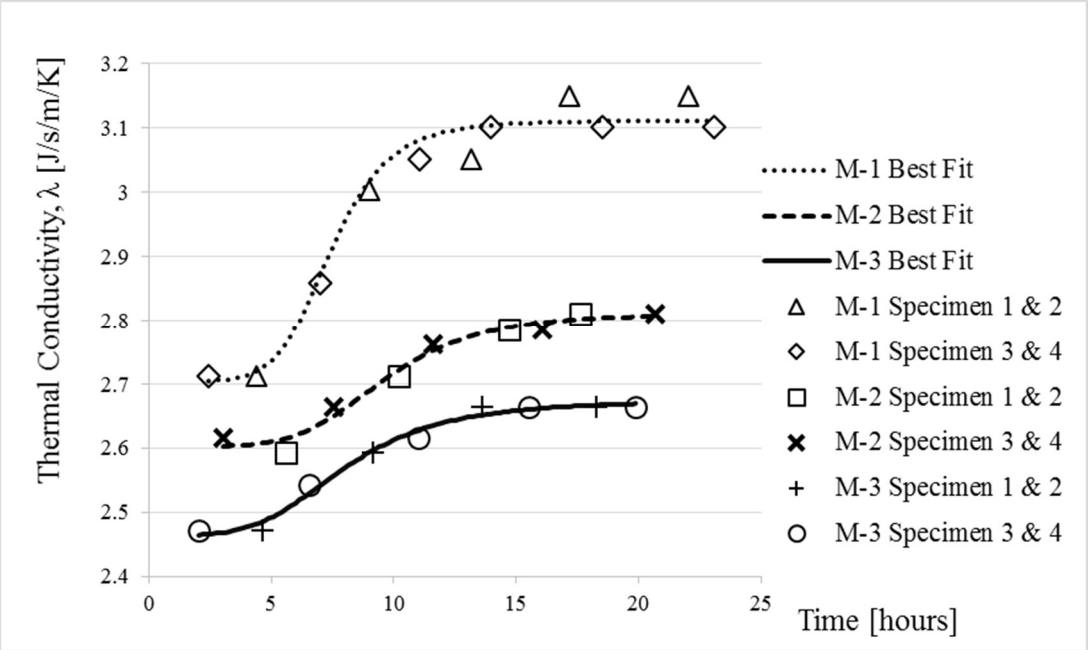

Figure 5-8: Variation of Thermal Conductivity of Concrete Mixes

It can be seen that the thermal conductivity of OPC concrete follows a unique pattern irrespective of the mix proportions, where it remains constant up to 4 ~ 5 hours and starts to increase up to a maximum value in the range of 2.62 ~ 3.10 J/s/m/K which is fairly in good agreement with values proposed by Kim et al. (2.1 ~ 3.0 J/s/m/K) [7], and Vosteen et al. [8] in previous studies for hardened concrete.

5.8 Summary

Proposed simplified method can be used to investigate thermal properties of fresh and early age concrete. Specific heat capacities of concrete mixes estimated based on the experimental investigation and rules of Dulong – Petit and Neumann– Kopp Rules are in good agreement with the previous studies.

It was found that the thermal conductivity of concrete increase rapid at early age. The variation of thermal conductivity at fresh state concrete follows a unique variation irrespective mix proportions, where it remains constant up to 4 ~ 6 hrs. and starts to increase up to a maximum value in the range of 2.62 ~ 3.10 J/s/m/K within 24 hrs.

These data can be used to study the effect of mix proportion on variation of thermal properties of concrete with hydration to develop a model to predict the variation of thermal conductivity once chemical compositions of cement, w/c, and aggregate contents is known.

6 Experimental Investigation of Temperature Rise in Concrete due to Heat of Hydration of Cement

6.1 Introduction

This chapter describes experimental setup to obtain temperature rise data with different thermal boundary conditions. In this investigation, temperature rise due to heat of hydration of concrete was monitored in a fully insulated concrete test block and partially insulated concrete test block in order to maintain different thermal boundary conditions. These temperature data were used to calibrate and verify the temperature rise predicted in concrete by the proposed model incorporating thermal properties estimated based on method described in section 5.

6.2 Experimental Setup

Experimental setup shown in Figure 6-1 consisted of data logger connected with thermocouple to record temperature rise due to heat of hydration of cement at predetermined locations for two concrete test blocks named as BLK 01 and BLK 02. Positions of thermocouples were decided in order to get maximum temperature rises, temperature rises at surfaces, and ambient temperature variations for each concrete test block as shown in Figure 6-2 and Figure 6-3. Geometric sizes of concrete test blocks BLK 01 and BLK 02 were cast with 1.0 x 1.0 x 1.0 m, and 2.5 x 1.5 x 1.5 m respectively.

Test block BLK 01 was cast with 18 mm plywood sheet formworks, and these plywood sheets were internally insulated with 100 mm thick Styrofoam sheets on all faces as shown in Figure 6-2.

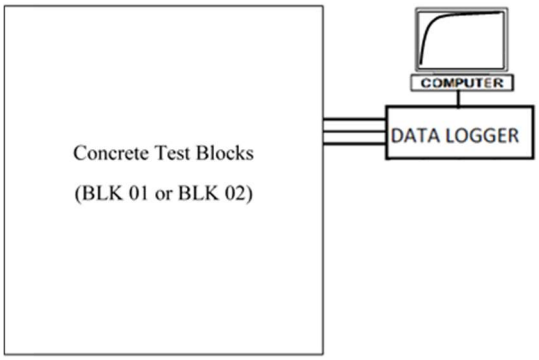

Figure 6-1: Experimental Setup to Measure Temperature Rise Due to Heat of Hydration of Cement

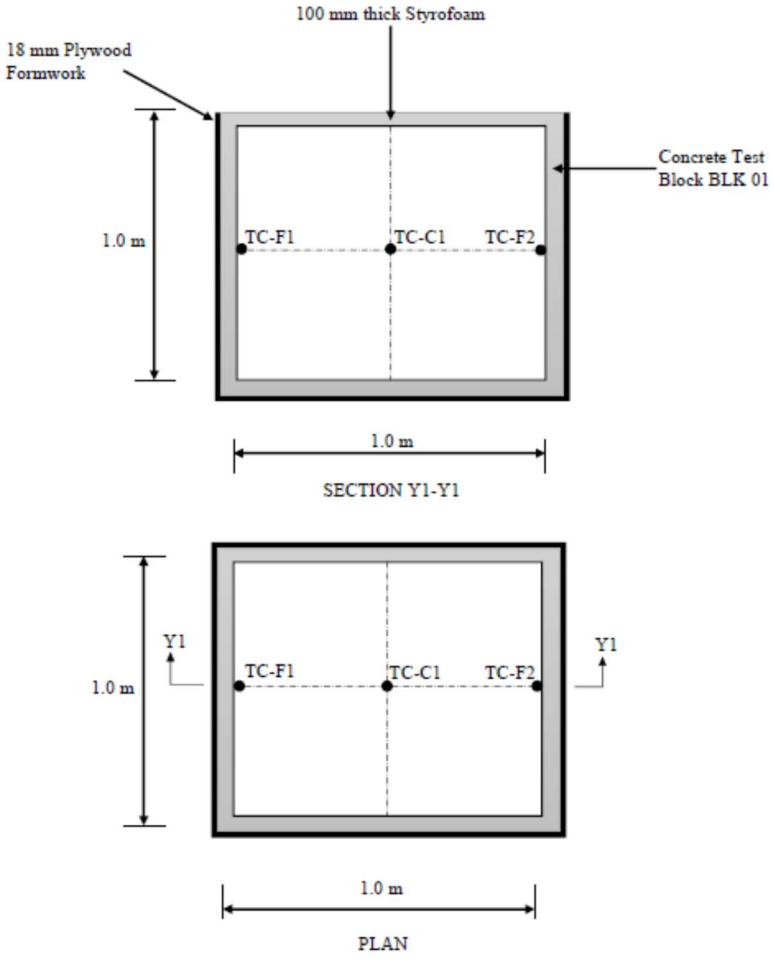

Figure 6-2: Geometry and Locations of Thermocouples for Concrete Test Block BLK 01

Test block BLK 02 was cast on 75 mm thick screed concrete with 15 mm plywood sheet formwork. Three vertical surfaces of plywood formwork were insulated internally with 50 mm thick Styrofoam sheets, and top surface was covered with 125 mm thick sand layer as shown in Figure 6-3. The adopted system of surface insulation and covering system was determined in order to maintain different thermal boundary conditions and make use temperature rise data for verification purposes of the temperature rise predicted by FE program incorporating cement hydration model described in section 3.3 and thermal properties of concrete calculated based on the method described in section 5.

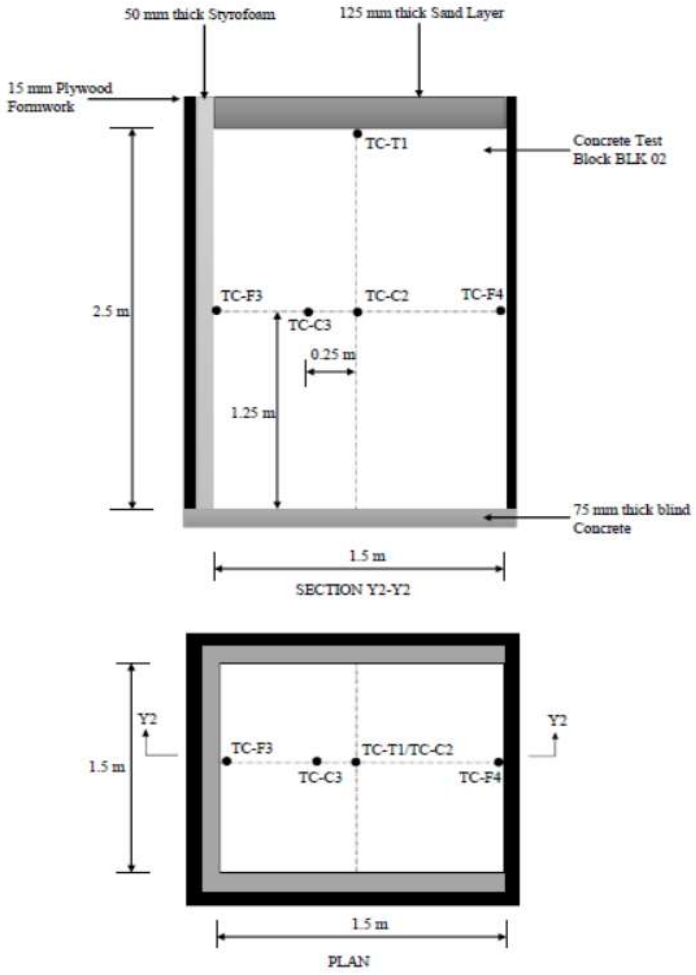

Figure 6-3: Geometry and Locations of Thermocouples for Concrete Test Block BLK 02

6.3 Experimental Plan

Experimental plan was prepared to investigate the temperature rise due to heat of hydration of cement in concrete test block BLK 01 & BLK 02 with different cement types, cement contents, w/c, and aggregate contents as given in Table 6-1. Chemical and mineral compositions, and physical properties of cement type OPC1 & OPC2 are given in Table 4-1 and Table 4-2, and respectively.

Table 6-1: Concrete Mix Proportions

Mix	Test Block Ref.	OPC Type	Cement Content [kg/m^3]	Water Content [kg/m^3]	Fine Agg. Contents [kg/m^3]	Coarse Agg. Content [kg/m^3]	Admixture [ml]
M-4	BLK 01	OPC2	400	160	800	1020	4000
M-5	BLK 02	OPC3	400	192	743	1026	3000

Mix proportions were selected by varying w/c in the range of 0.4 ~ 0.5, and total fine and coarse aggregate content in the range of 1769 ~ 1820 kg/m^3.

Near adiabatic thermal boundary condition was maintained by minimizing heat flow into surrounding environment with 100 mm thick Styrofoam sheet insulation for all surfaces of concrete test block BLK 01. Temperature rise at the center and surfaces were monitored and recorded with a data logger as shown in Figure 6-2 for approximately 2.5 days. Here, one thermocouple was used at the center (TC-C1) and two thermocouples (TC-F1/TC-F2) on two opposite faces of block BLK 01. A data logger was used to record temperature rise at selected locations at 5 minutes intervals. These data were used to calibrate temperature rise at core due to heat of hydration, and specific heat capacity of concrete predicted by heat of hydration and thermal property simulation program.

Semi adiabatic thermal boundary conditions were set with 50 mm thick Styrofoam for three vertical surfaces, cast on 75 mm thick screed concrete, and 125 mm thick sand layer placed on top surface of concrete test block BLK 02 after casting. Temperature rise due to heat of hydration at locations shown in Figure 6-3 were monitored and recorded in data logger for approximately 7.0 days. Here, thermocouples were placed at center (TC-C2), at 250 mm offset from center (TC-C3), at insulated face (TC-F3), and top face (TC-T1) as shown in Figure 6-3. These data were used to further verify temperature rise due to heat of hydration, and thermal property simulation program.

Temperature readings were recorded with an accuracy of 0.01 ^{o}C, using a data logger for concrete test blocks BLK 01 & BLK 02. Further, ambient temperatures were also monitored using a separate thermocouple (TC-A1/TC-A2) for block BLK 01 & BLK 02 respectively.

6.4 Experimental Results

Temperature rise due to heat of hydration of cement in concrete with M-4 concrete mix given in Table 5-2 above, and ambient temperature variation with time measured for test blocks BLK 01 are shown in Figure 6-4. Relevant data file extracted from data logger is annexed in APPENDIX I.

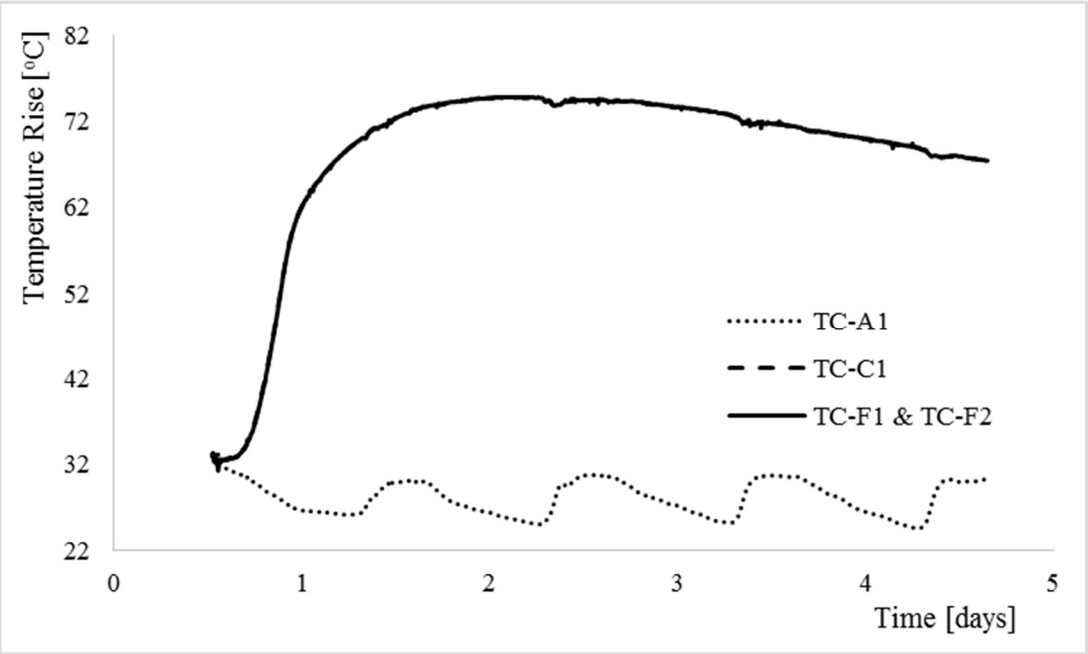

Figure 6-4: Temperature Rise and Ambient Temperature Variation with Time - Test Block BLK 01

Table 6-2 gives date, time of concrete starting and finishing, fresh concrete temperature at the time of placing of concrete, maximum temperature recorded at each thermocouple, and time taken to reach the maximum temperature for concrete test block BLK 01.

Results given in Figure 6-4 & Table 6-2 indicate that temperature distribution across the block BLK 01 is nearly uniform since the temperature profile from TC-C1 and TC-F1 & TC-F2 overlaps each other. This confirms the effectiveness of Styrofoam insulation provided and the size of the test block to achieve nearly adiabatic condition at center.

Table 6-2: Maximum Temperature at Center & Insulated Faces, and Time of Concreting - Test Block BLK 01

Date	Concreting			TC ref.	Max. Temp.	Time to reach max. Temp.
	Start time	Finish time	Placing temp.			
09/01/2012	12:33 PM	12:46 PM	33.01 ^{0}C	TC-C1	78.20 ^{0}C	1.344 days
				TC-F1	76.10 ^{0}C	
				TC-F2	75.70 ^{0}C	

Temperature rises due to heat of hydration of cement in concrete with M-5 concrete mix given in Table 5-2 above, and ambient temperature variation with time measured from test blocks BLK 02 are shown in Figure 6-5. Relevant data file extracted from data logger is annexed in APPENDIX I.

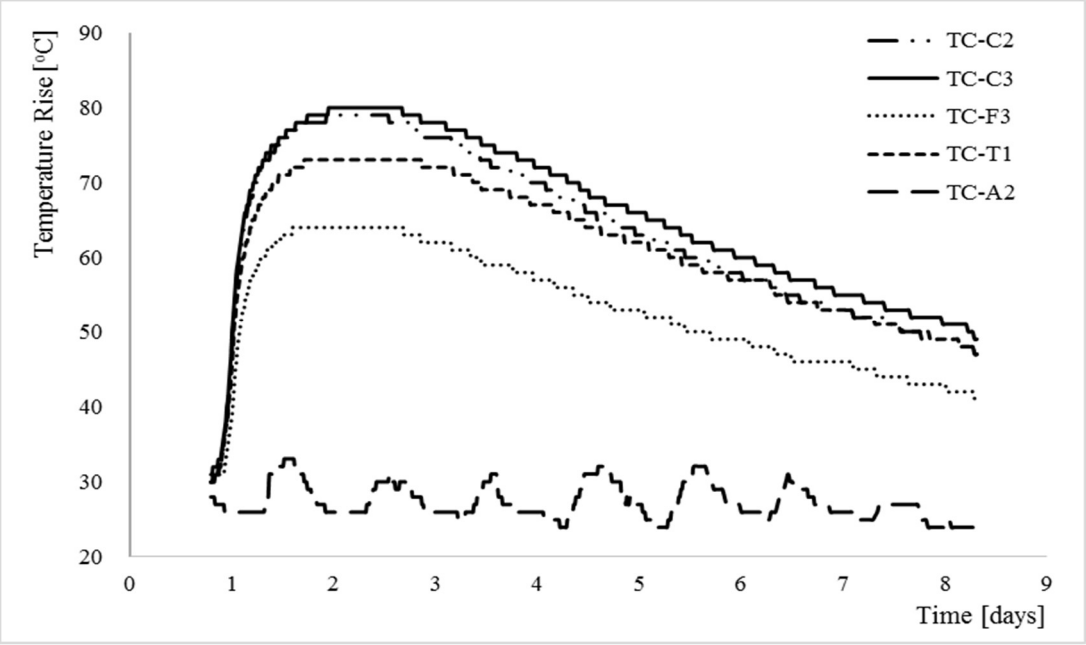

Figure 6-5: Temperature Rise and Ambient Temperature Variation with Time - Test Block BLK 02

Table 6-3 gives date, time of concrete starting and finishing, fresh concrete temperature at the time of placing of concrete, maximum temperature recorded at each thermocouple, and time taken to reach the maximum temperature for concrete test block BLK 02.

Table 6-3: Maximum Temperature at Center & Faces, and Time of Concreting - Test Block BLK 02

Date	Concreting			TC ref.	Max. Temp.	Time to reach max. Temp.
	Start time	Finish time	Placing temp.			
18/11/2011	18:50 PM	19:45 PM	32.90 ^{0}C	TC-C2	80.0 ^{0}C	1.167 days
				TC-C3	79.0 ^{0}C	
				TC-F3	73.0 ^{0}C	
				TC-F4	58.0 ^{0}C	
				TC-T1	64.0 ^{0}C	

The highest temperature of 80 °C was recorded near the center (TC-C2) approximately 1.167 days after placing of concrete.

6.5 Summary

Temperature rise data from concrete test block BLK 01 are with nearly adiabatic thermal boundary conditions, and can be used to calibrate the temperature predictions by the heat of hydration and thermal property prediction model initially.

Experimental data from the test block BLK 02 are with surfaces exposing to different thermal boundary conditions and can be used to verify initially the calibrated heat of hydration and thermal property prediction models further.

7 Calibration and Verification of Simulation Program

7.1 Introduction

This chapter briefly describes, about initial calibration and verification of thermal property model and temperature rise predicted by heat of hydration model in combination with thermal boundary conditions using experimentally investigated data described in Chapter 4, 5, and 6 above. Temperature rise data collected from previous studies carried out in field are used for further verification purposes of thermal responses predicted by the FEM simulation program.

7.2 Thermal Conductivity Model

Initial calibration of thermal conductivity model was conducted using middle level set of data obtained from concrete mix M-2 given in Table 5-2.

Thermal conductivity of cement paste is depending on thermal conductivity, volume fraction, and shape of each components in cement paste as described in section 3.5 briefly. The components in cement paste, i.e. cement hydration products and non-reacted cement powder, free water in pores, and vaporized air in empty pores, exist in solid, liquid, and gas phases. Since the thermal conductivity characteristics of cement paste is evaluated based on general model proposed by Wang et al. [86], as described in section 3.5.

Fractional volumes of each components of cement paste were calculated as described in section 3.5, and their variations are as shown in Figure 7-1.

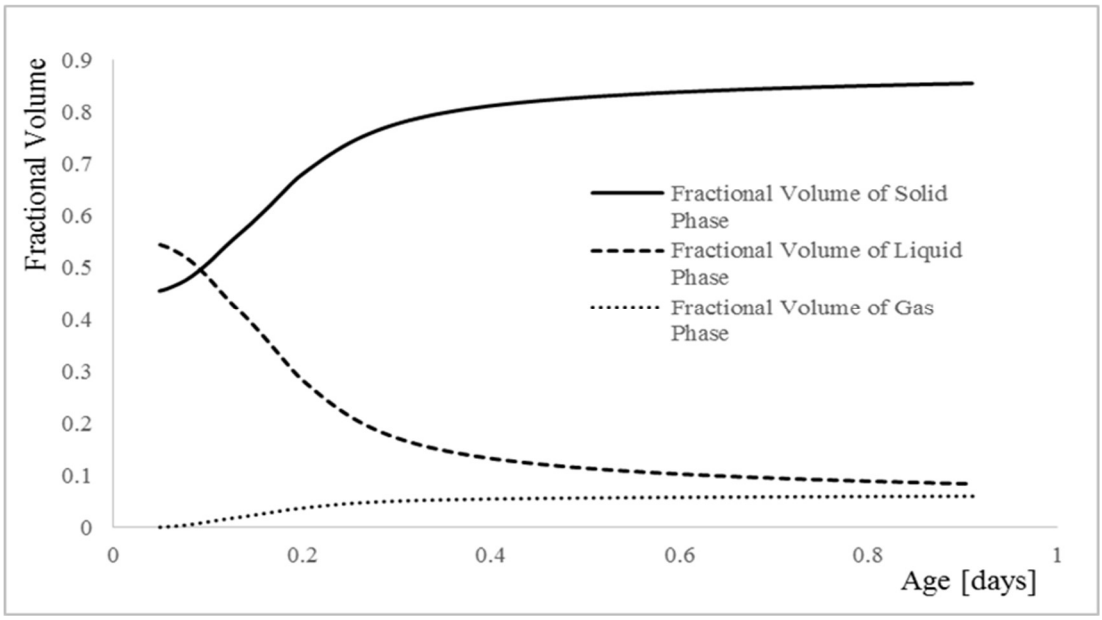

Figure 7-1: Variation of Fractional Volumes of each components in Cement Paste for mix M-2 during initial stages

Shape of each components were evaluated assuming shape parameters as described in Table 7-1.

Table 7-1: Phases and Shapes of Components in Cement Paste

Component in cement paste	Phase	Shape	Remarks
Hydrated and non-reacted cement particles	Solid	Discontinuous medium with complicated variation in shape	An empirical formula was introduced to represent variation in shape during hydration process to use in thermal conductivity model
Free water in gel and capillary pores	Liquid	Continuous medium with complicated in shape during initial stages	Factor is not required for the continuous medium as per thermal conductivity model
Humid air in empty pores	Gas	Discontinuous medium with complicated variation in shape	Assume to be similar to solid phase in shape to use in thermal conductivity model

The empirical formula given in equation 7-1 was obtained with several trials from heat conduction analysis using FEM program described in section 5.4.

$$d_{s\&g} = 1.5 + 0.5DoH^{10}\left[\frac{3}{1-(W/C)^{2.7}}\right]^{2.7} \qquad 7\text{-}1$$

Where, $d_{s\&g}$, DoH, W/C denote shape factor for cement hydration products and non-reacted cement particles, degree of hydration, and water to cement ratio of cement paste respectively. Respective variation of degrees of hydration, and shape factor for solid and gas phases generated by the model are shown in Figure 7-2 and Figure 7-3 respectively for concrete mix M-2.

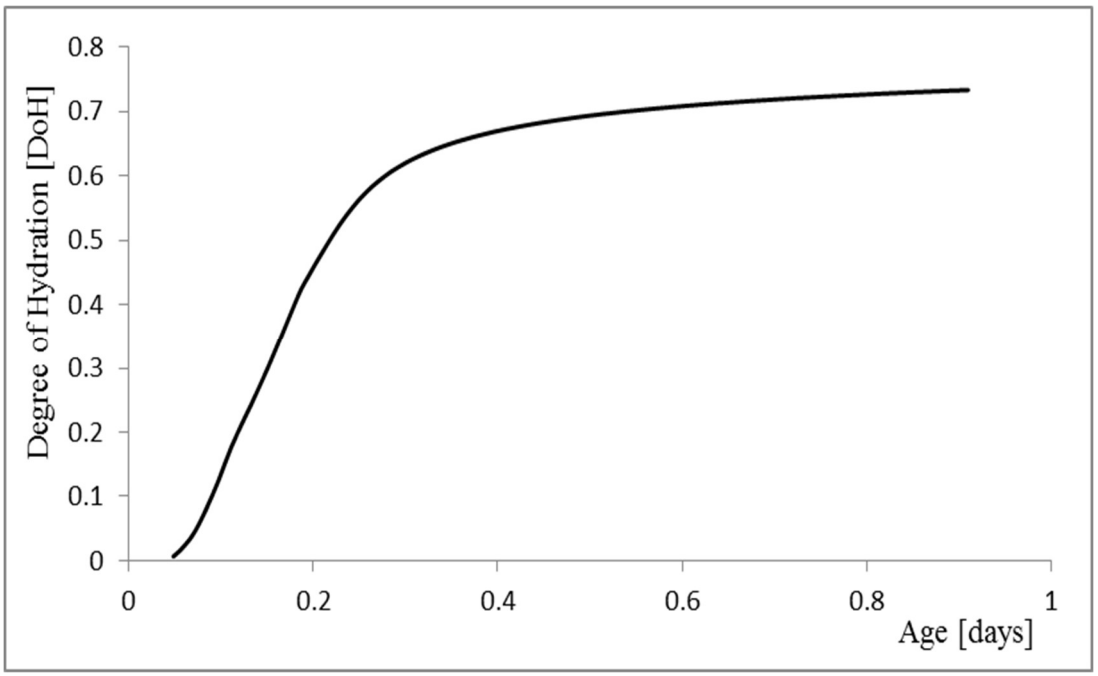

Figure 7-2: Variation of Degrees of Hydration [DoH] for mix M-2 during initial stages

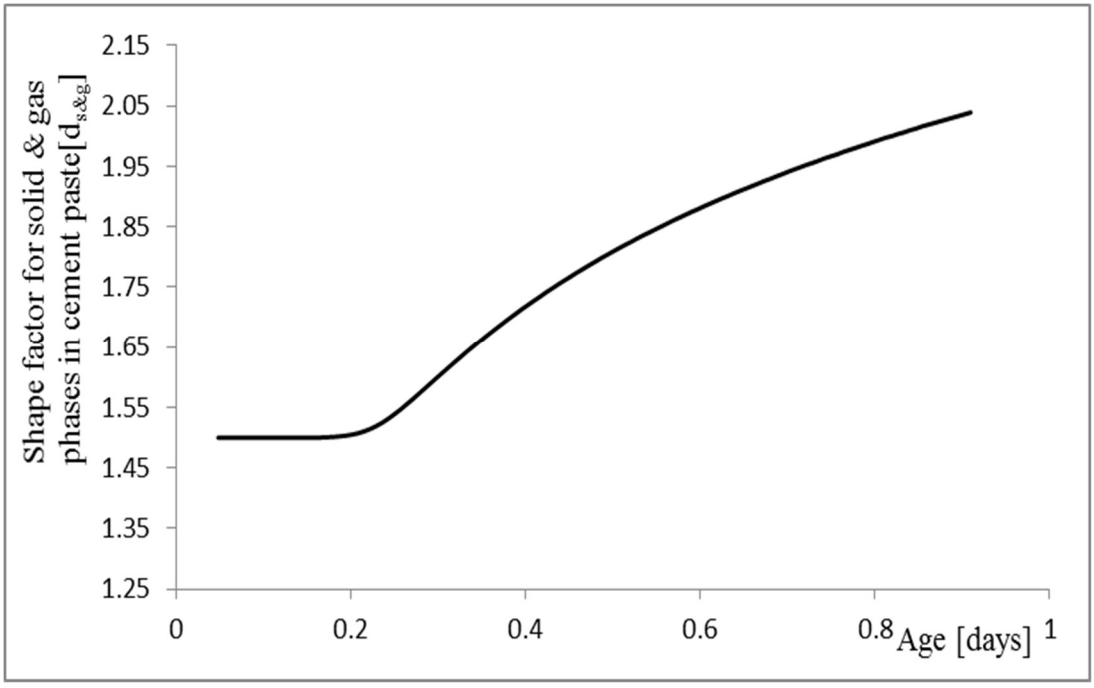

Figure 7-3: Variation of shape factor for solid and gas phases in cement paste [$d_{s\&g}$] for mix M-2 during initial stages

Thermal conductivity of hydrated products and non-reactive cement particles in cement paste were assumed as 54.8 kcal/day/m/K, and the variation of thermal conductivity of free water and gas are given in Figure 7-4. Here relative humidity of vaporized air inside pores was assumed as 95%, and thermal conductivity of free water and humid air were estimated as described in section 3.5, and varies as shown Figure 7-4 in due to rise in temperature.

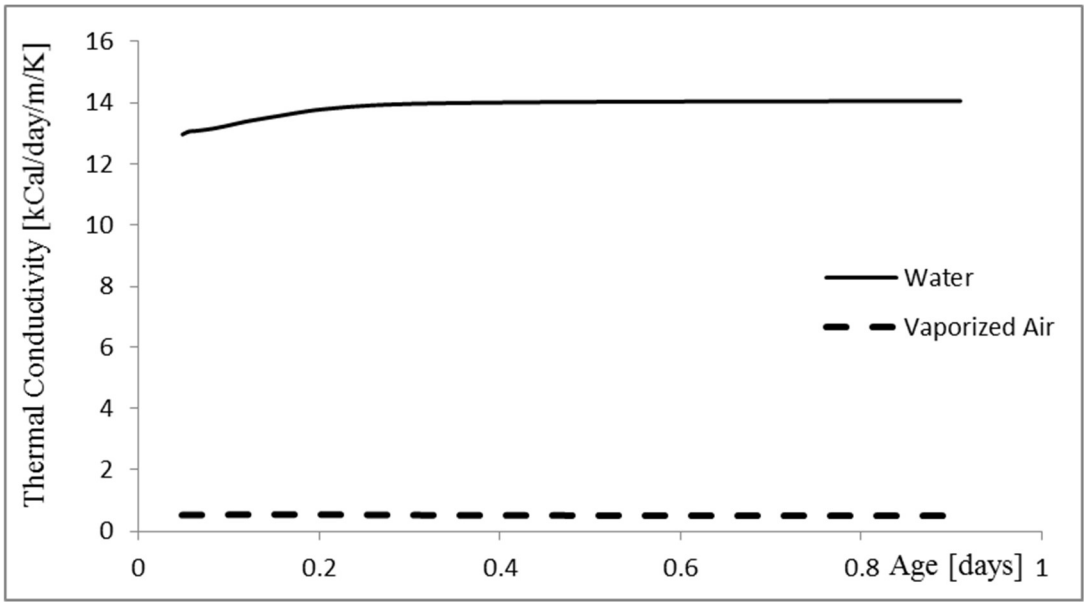

Figure 7-4: Variation of thermal conductivity of water and vaporized air in pores of cement paste of mix M-2 during initial stages

Thermal conductivity of cement pastes of concrete mix M-2 was obtained and the variation with the age of concrete is shown in Figure 7-5.

Once, the thermal conductivity of cement pastes of concrete mix M-2 was estimated, the effective medium theory (EMT) for two phase systems described in section 3.5, was applied to obtain the thermal conductivity of cement mortar, i.e. cement paste and fine aggregate. Here, the thermal conductivity of fine aggregate was assumed as 42.4 kcal/day/m/K during initial calibration of thermal conductivity model. Thermal

conductivity of cement mortar was obtained and the variation with the age of concrete is shown in Figure 7-5.

Again, the EMT was applied to estimate the thermal conductivity of concrete by considering two phase system of cement mortar and coarse aggregate. Here as the size of aggregate is comparatively larger than fine aggregate, effect of interfacial zone formed in between coarse aggregate and cement mortar affects the thermal conductivity characteristics of coarse aggregate. Empirical formula was obtained as given in equation 7-2 by several trials of thermal conductivity analysis to add the effects of interfacial zone to the thermal conductivity of coarse aggregate.

$$\lambda_{magg} = \lambda_{agg}\left[5.9315\left(W/C\right)^2 - 3.0328(W/C) + 1.41\right] \qquad 7\text{-}2$$

Where, λ_{magg} , λ_{agg} , and W/C denote thermal conductivity of aggregate after addition of interfacial zone's effects, thermal conductivity of coarse aggregate, and water to cement ratio respectively. Here, the thermal conductivity of coarse aggregate was assumed as 41.6 kcal/day/m/K to calibrate the model initially. Predicted variation of thermal conductivity of concrete with mix M-2 is shown in Figure 7-5.

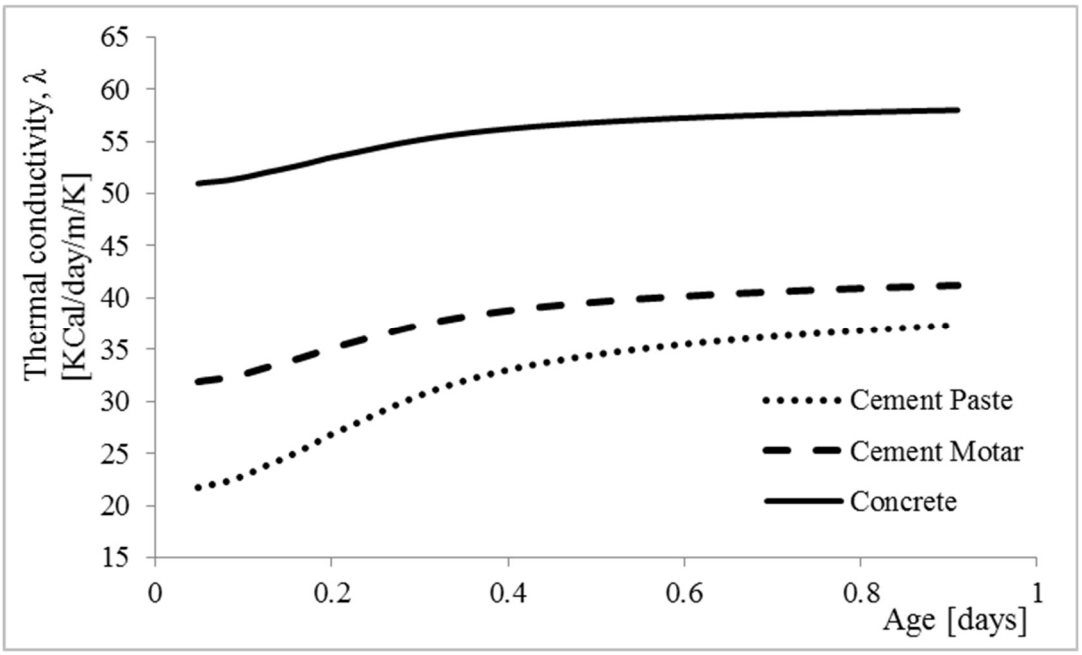

Figure 7-5: Variation of Thermal Conductivity of Cement Paste, Mortar, and Concrete for mix M-2

Finally, the calibrated model was used to predict the variation of thermal conductivity of concrete mixes M-1 & M-3. The obtained results are shown in Figure 7-6.

Furthermore, variation of fractional volumes, shape factors, and thermal conductivity of each components in concrete mixes M-1, and M-3, during initial verification, are given in APPENDIX I.

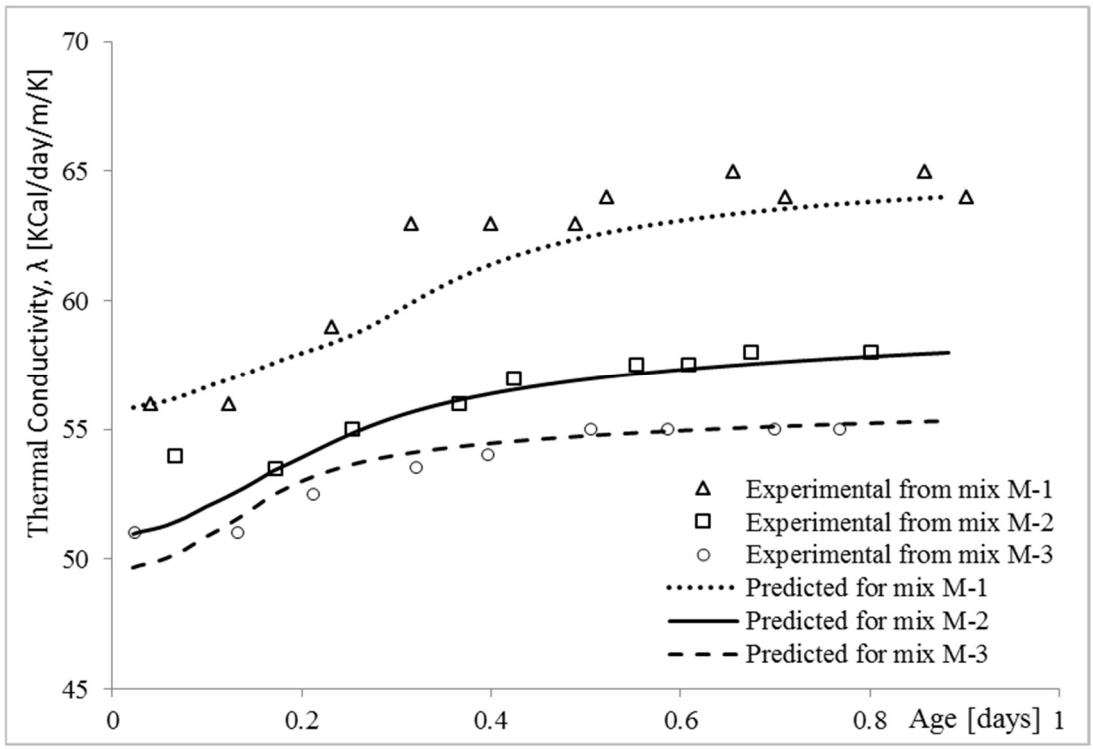

Figure 7-6: Experimentally Investigated and Predicted Variation of Thermal Conductivity of Concrete Mixes M-1, M-2, and M-3

7.3 Thermal Analysis by FEM

Heat of hydration model described in section 3.3 and model to predict thermal properties were incorporated in ANSYS software to perform thermal analysis. A three-dimensional isoperimetric and eight nodes solid element was selected for the thermal analysis. In ANSYS, this element type is called SOLID70.

The hydration model computes the heat generated rate due to heat of hydration of cement based on element temperature, mineral composition of cement, amount of gypsum added, cement content, water content, admixtures, and initial temperature of the element. Then the corresponding heat generation rate for each element, thermal properties relevant to degrees of hydration and system temperature, and relevant thermal boundary conditions are then applied, and perform thermal analysis using ANSYS to get the temperature history. The updated temperature is then read by the

heat generation program and starts to calculate heat generation rate for the next step based on revised element temperature for each and every element. The whole computational process is described with flowcharts in section 3.2.

7.4 Initial Calibration with Experimental Data from Test Block BLK 01

Initially, temperature rise predicted by the heat of hydration and thermal conductivity model was calibrated with temperature rise data obtained from concrete test block BLK 01.

Specific heat capacity of concrete mix M-4 was estimated as described in section 3.4, and found as 0.302 kcal/kg/K. Variation of thermal conductivity of concrete mix M-4 was predicted using thermal conductivity model described in section 7.2, and predicted variation is shown in Figure 7-7. It was found that thermal conductivity of concrete for mix M-4 varies in the range of 46 ~ 53.9 kcal/day/m/K during a period of 04 days which is approximately 17% increase.

Thermal and physical properties of insulation, and form material were selected are given in Table 4-4.

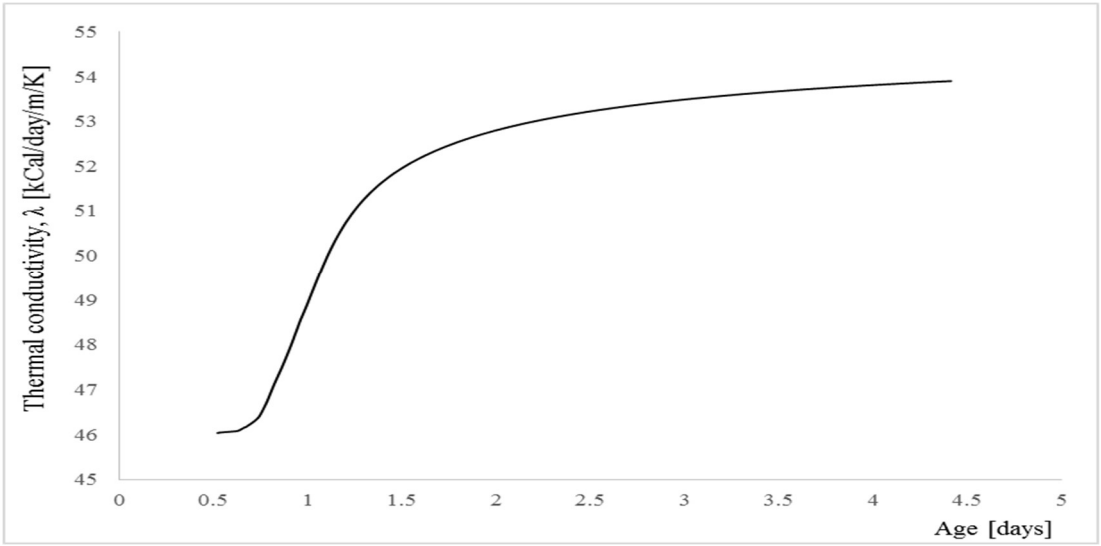

Figure 7-7: Variation of Thermal Conductivity of Concrete Mix M-4 Predicted by Thermal Conductivity Model

Effects of solar radiation on the exposed surfaces were taken into account and respective horizontal solar radiation estimated based on 9th Julian day of year 2012, and geometric orientation of test block is shown in Figure 7-8. Furthermore, shading effects for solar radiation on vertical surfaces of the test block was also taken into account considering geometric orientation as shown in Figure 7-8. Cloud factor is reported as 0.6 for the date of conducting the experiment of block BLK 01. Here, S1 to S4 are top, and vertical surfaces at X = 0, X = L, Z = 0, and Z = W of test block respectively. X, Y, and Z axes are considered direction of east to west, altitude and south to north.

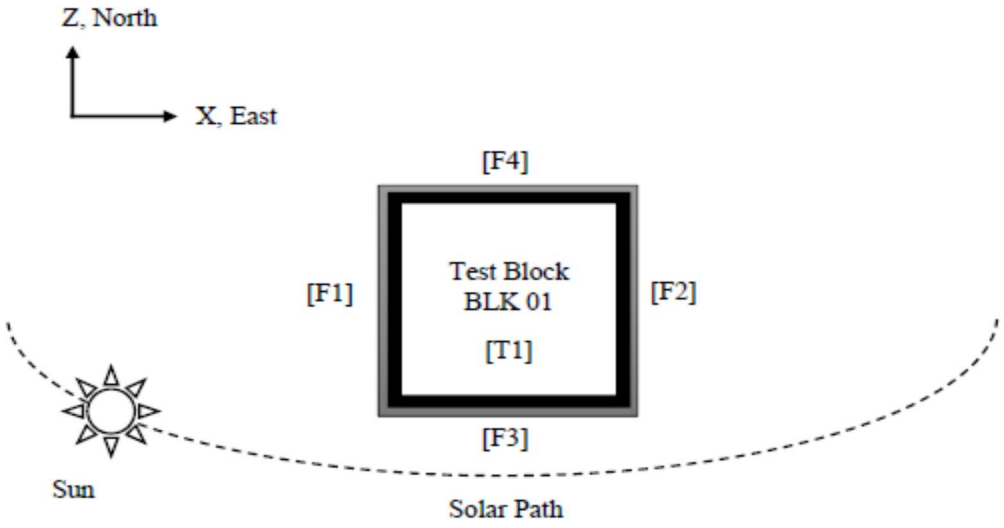

Figure 7-8: Plan View - Geometric Orientation of Test Block BLK 01

Ambient temperature was modeled with 5th order polynomial function based on the experimental data measured as follows, and implemented into thermal boundary conditions setting program to simulate ambient temperature variation for the test block BLK 01.

$$T_{AMB} = C_0 + C_1 t + C_2 t^2 + C_3 t^3 + C_4 t^4 + C_5 t^5$$

Where, constants C_0, C_1, C_2, C_3, C_4, and C_5 were found as -11.269, 253.559, -570.224, 604.580, -314.710, and 64.849 respectively. T_{AMB}, and t denote ambient temperature

in K, and time in days. Measured and predicted ambient temperature variation is shown in Figure 7-10.

Surface thermal loads were applied maintaining ambient thermal boundary conditions considering, convection, and irradiation, solar radiation with shading effects from top and vertical surfaces, and heat conduction to subgrade soil through bottom surface of test block as described in section 3.6

Furthermore, the model was calibrated in order to add the delaying effects of admixture, and parameter for delaying effects for concrete mix M-4 was found as 0.13.

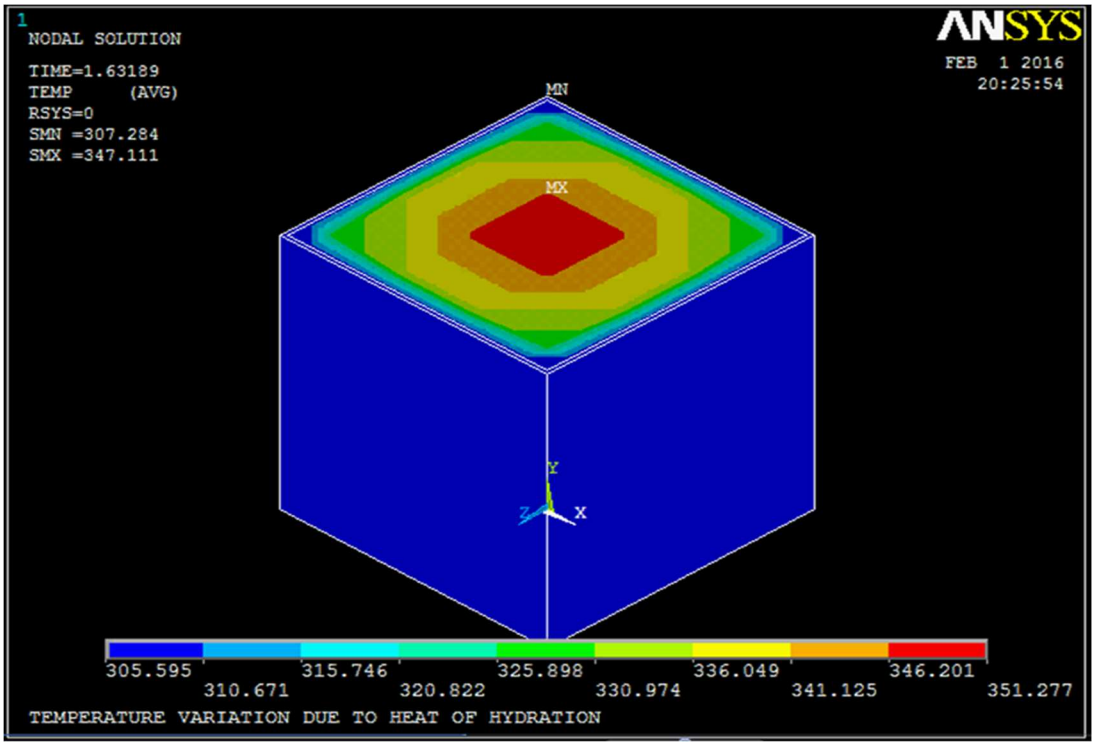

Figure 7-9: Picture from Thermal Analysis of BLK 1 using ANSYS

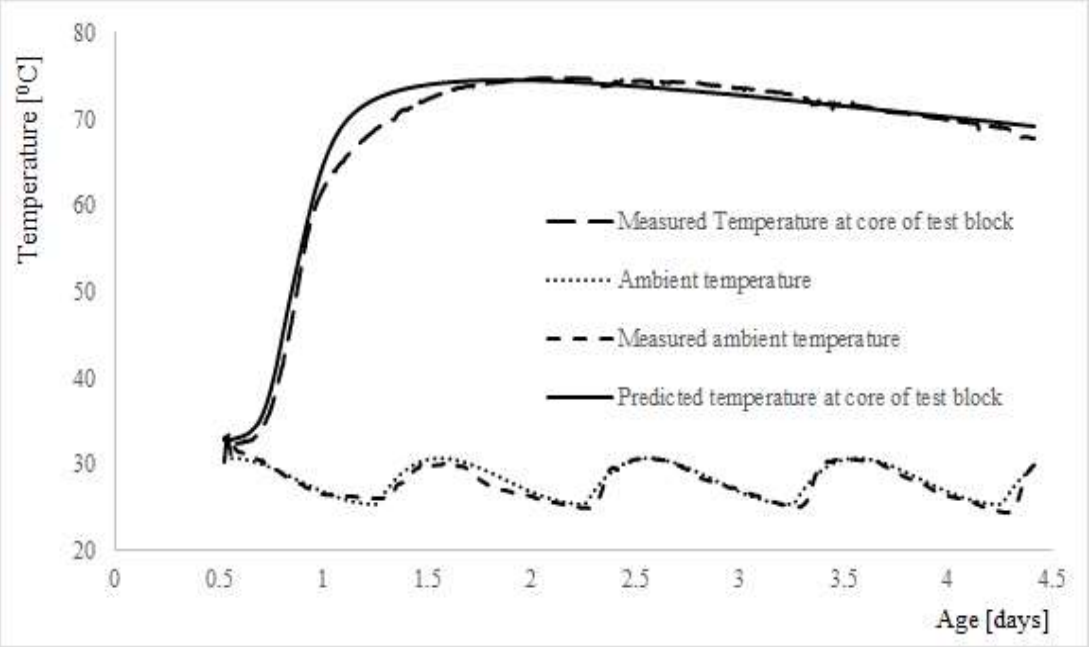

Figure 7-10: Temperature Rise and Ambient Temperature Variation Predicted and Measured from Test Block BLK 01

Figure 7-9 shows a snap shot of thermal analysis simulation by ANSYS for BLK 01. Heat of hydration model was calibrated indicating overall match with measured temperature rise data at the core of test block BLK 01 as shown in Figure 7-10. Further, it was noted that effects variation of thermal boundary conditions insignificant as Styrofoam behaves as a thermal barrier to heat dissipations as well as heat absorption phenomena.

7.5 Initial Verification with Experimental Data from Test Block BLK 02

The calibrated heat of hydration program, and model for thermal properties was further verified with temperature rise data investigated from test block BLK 02.

Specific heat capacity of concrete for mix M-5 was computed as 0.299 kcal/kg/K, and variation of thermal conductivity as shown in Figure 7-11. It was found that thermal conductivity of concrete for mix M-5 varies in the range of 49.5 ~ 59.3 kcal/day/m/K during a period of 04 days which approximately 20% increase. Thermal and physical

properties of insulations, screed concrete, top covering, and form material were selected as defined in Table 4-4.

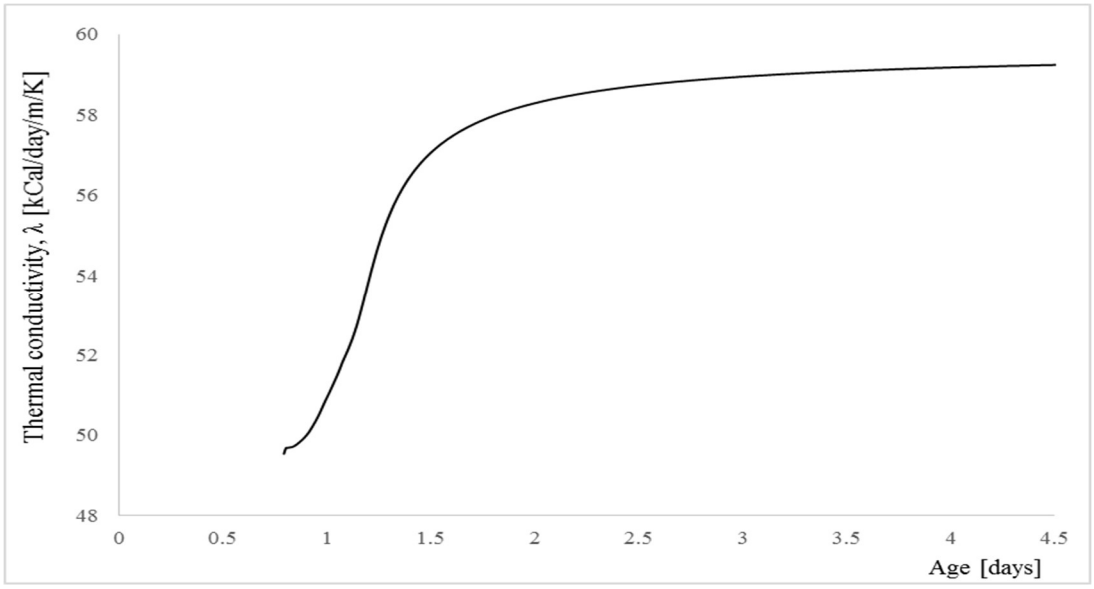

Figure 7-11: Variation of Thermal Conductivity of Concrete Mix M-5 Predicted by Thermal Conductivity Model

Thermal boundary conditions were applied similarly in section 7.4, and the variation of applied surface thermal loads considering geometrical orientation of test block BLK 02 were as shown in Figure 7-12. Solar radiation was computed based on 322nd Julian day of year 2011 [99]. These surface thermal loads were estimated and applied by the subroutine for thermal boundary conditions as described in section 3.6.

Constant parameter to simulate ambient temperature variation were derived by matching data recorded the thermocouple placed outside the test block, and found constants C_0, C_1, C_2, C_3, and C_4 as -2.5135, 13.034, -23.758, 16.547, and -2.8836 respectively. Measured and applied ambient temperature variation is given in Figure 7-14.

Further, it was found with several trials of heat simulation, the parameter for delaying effects of admixture in concrete mix M-5 as 0.06.

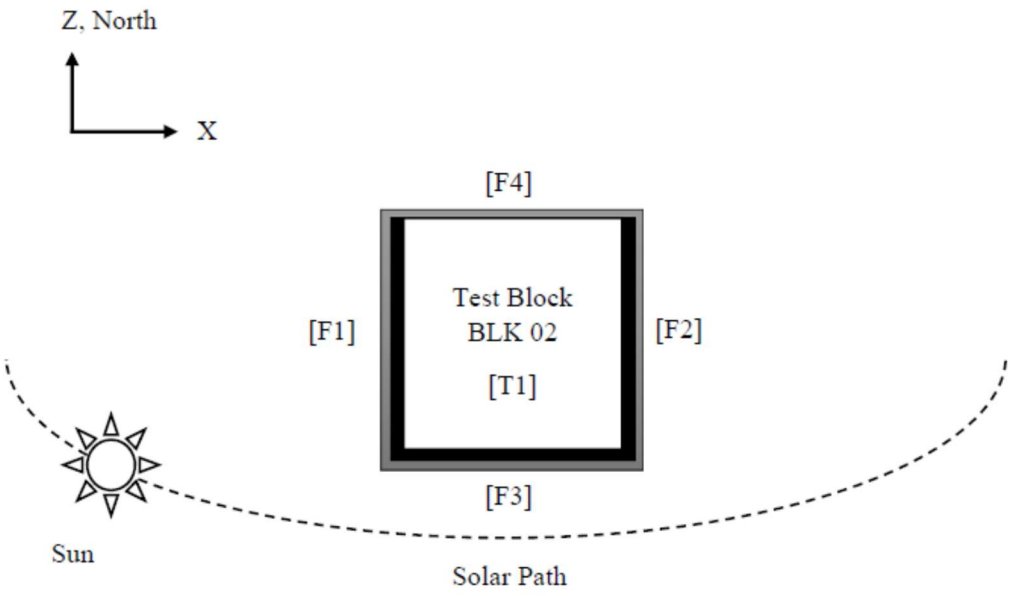

Figure 7-12: Plan View - Geometric Orientation of Test Block BLK 02

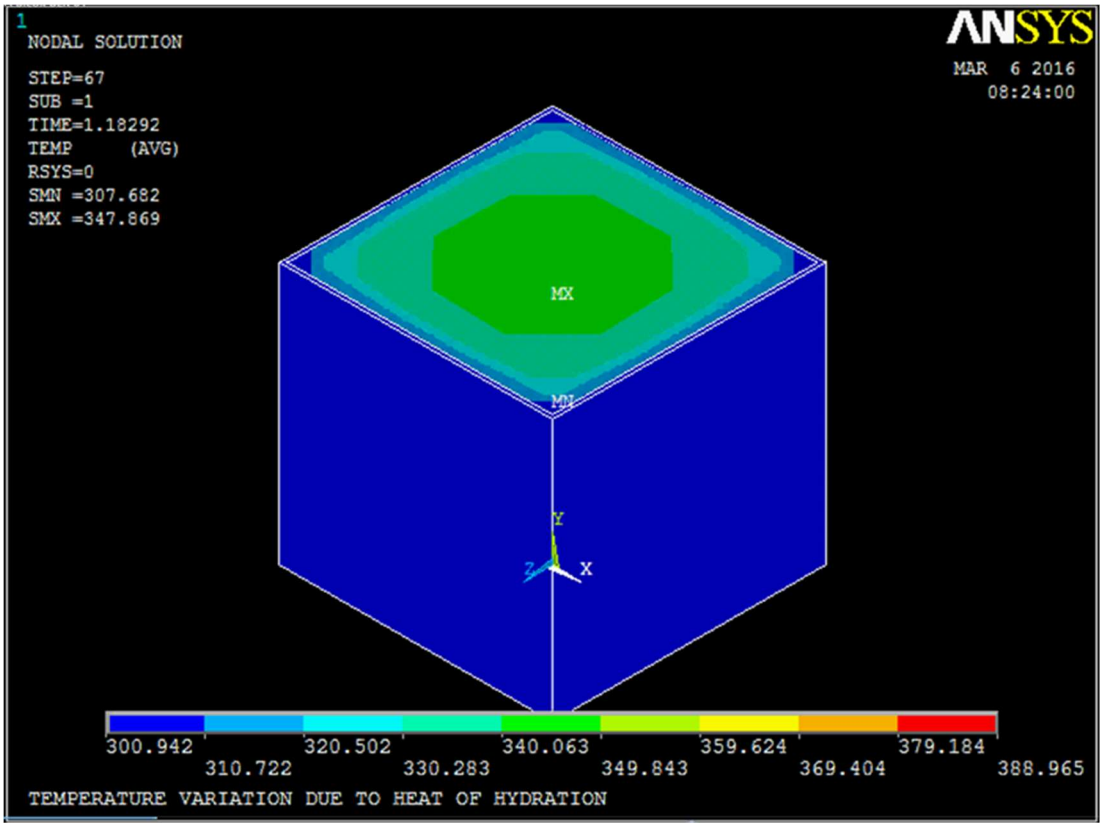

Figure 7-13: Picture from Thermal Analysis of BLK 2 using ANSYS

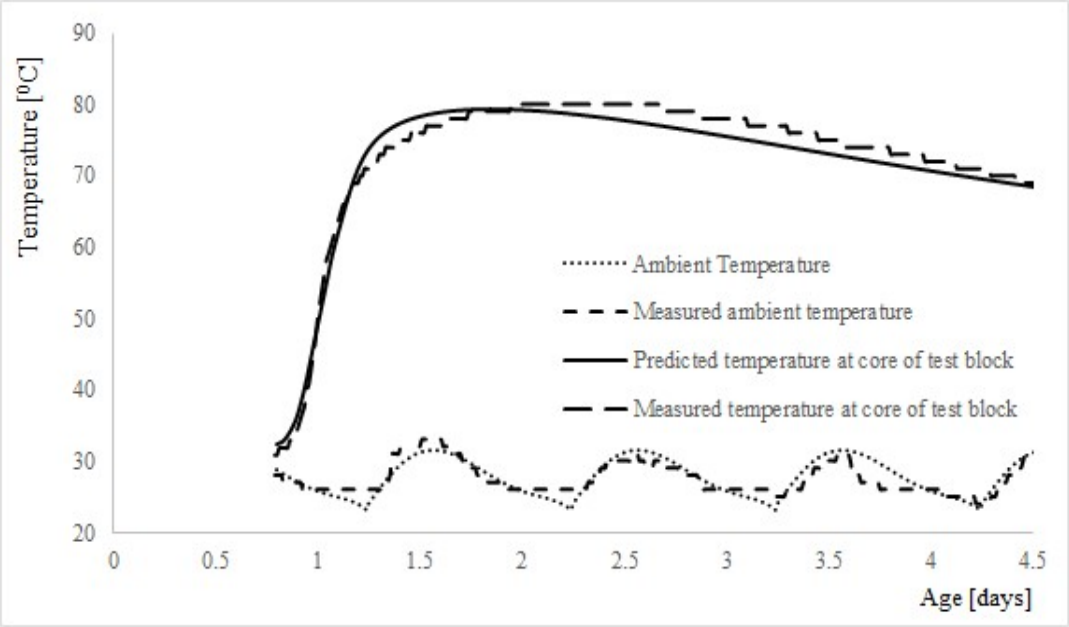

Figure 7-14: Temperature Rise and Ambient Temperature Variation Predicted and Measured from Test Block BLK 02

Figure 7-9 shows a snap shot of thermal analysis simulation by ANSYS for BLK 02. The calibrated heat of hydration model predicted temperature rise, matches with measured temperature rise data at the core of test block BLK 02 as shown in Figure 7-14. Further, it was noted that effect of variation of thermal boundary conditions significantly affects temperature rise despite of Styrofoam insulation on three vertical surfaces.

7.6 Further Verification with Temperature Rise Data from Previous Field Investigation

Temperature rise due to heat of hydration, thermal properties and their variations, variations of thermal boundary conditions, and thermal properties of formwork materials were further verified by predicting temperature rise curves compared with temperature rise data from a previous study [99]. Table 7-2 provides details with regards to project, member sizes, concrete mix reference, and type of formwork used in the field application extracted from the study.

Table 7-2: Details of Field Test

Project[1]	Structure	Structural Member	Size of Member	Type of formwork	Concrete Mix Ref.
1	Intake	wall	300mm	12mm thick plywood	M-6
2	Reservoir	wall	500mm	12mm thick plywood	M-7
3	Reservoir	wall	750mm	12mm thick plywood	M-8
4	Intake	wall	300mm	4mm thick steel	M-9

Note 1

1. Group Town water supply project
2. Ragama Reservoir in Medical faculty
3. Greater Galle water supply project
4. Polgolla water supply project

Table 7-3 shows concrete mix data of each field application, and chemical and mineral compositions data for each types of OPC are presented in Table 4-1 and Table 4-2 respectively.

Table 7-3: Concrete Mix Proportions used in Field Test

Mix Ref.	OPC Type	Cement Content [kg/m^3]	Water Content [kg/m^3]	Fine Aggregate [kg/m^3]	Coarse Aggregate [kg/m^3]
M-6	OPC4	400	174	883	1013
M-7	OPC5	370	152	893	1020
M-8	OPC6	395	170	858	982
M-9	OPC4	361	181	848	1037

Thermal and physical properties of concrete mix M-6 to M-9 were estimated as given in Table 7-4.

Table 7-4: Thermal and Physical Properties Predicted by the model for Concrete Mixes used in Field Test

Mix Ref.	W/C [%]	Total Aggregate Content [kg/m^3]	Density [kg/m^3]	Specific Heat Capacity [kcal/kg/K]	Thermal Conductivity	
					Period [days]	Range [kcal/day/m/K]
M-6	43.50	1896	2470	0.319	2.68	47.77~54.15
M-7	41.08	1913	2435	0.305	2.23	45.32~51.11
M-8	43.04	1840	2404	0.302	1.75	47.77~54.67
M-9	50.14	1885	2427	0.306	1.50	47.77~54.15

Figure 7-15 to Figure 7-17 show temperature rises at center of wall from thermal analysis using calibrated and verified hydration model including the model for thermal

properties, and thermal boundary condition. Here actual temperature variations records were extracted from previous study [99] measured in different field applications given in Table 7-2 above.

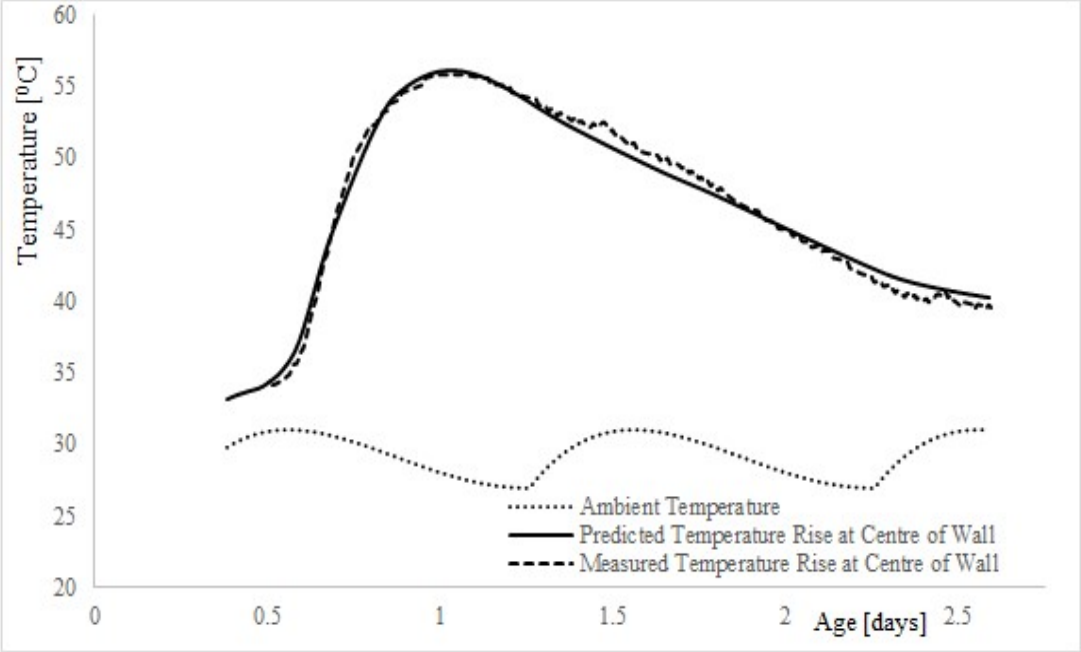

Figure 7-15: Temperature Rise and Ambient Temperature Variation Predicted and Measured from 300mm Thick Wall in Project 1.

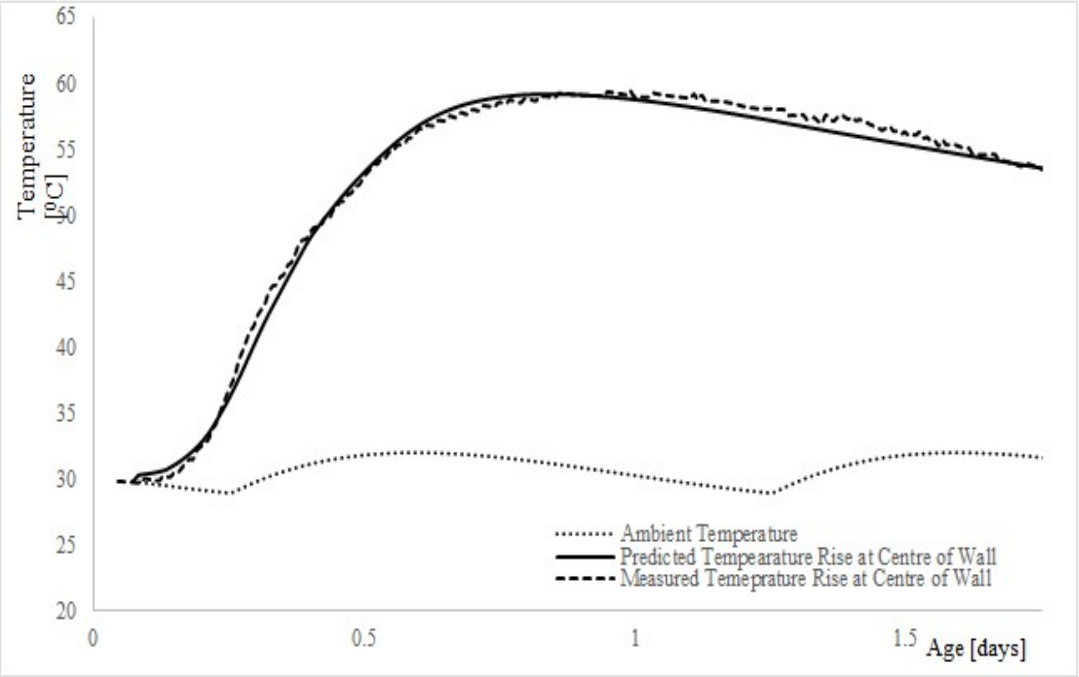

Figure 7-16: Temperature Rise and Ambient Temperature Variation Predicted and Measured from 500mm Thick Wall in Project 2.

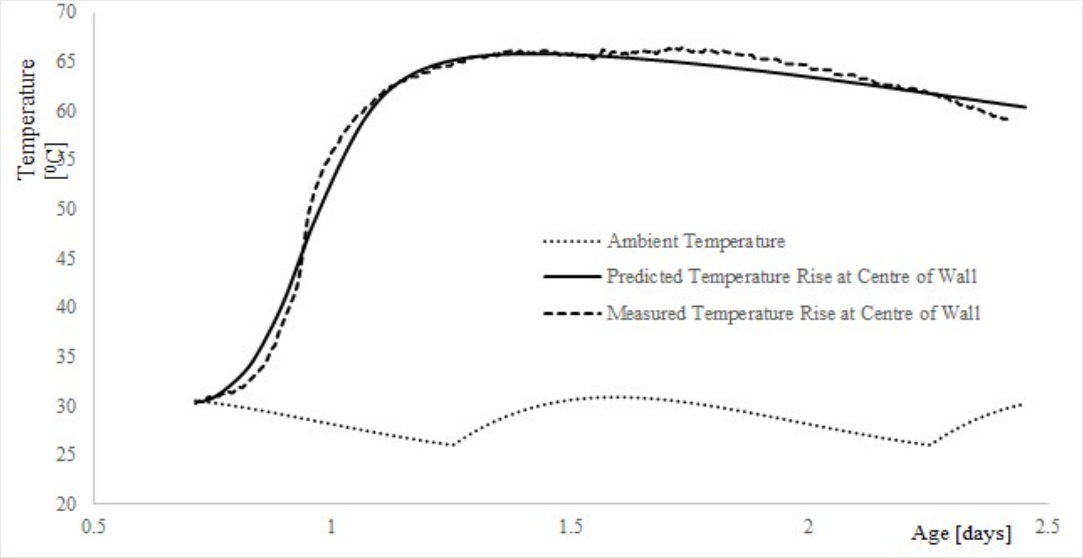

Figure 7-17: Temperature Rise and Ambient Temperature Variation Predicted and Measured from 750mm Thick Wall in Project 3.

Table 7-5: Summary of Measured and Predicted Maximum Temperatures and Time to Reach the Maximum Temperature for each Field Test

Project	Concreting		Measured		Predicted		Percentage Difference in Prediction of Temp. [%]
	Start time	Placing Temp. [^{0}C]	Max. Tem. [^{0}C]	Time to reach max. Temp. [days]	Max. Tem. [^{0}C]	Time to reach max. Temp. [days]	
1	09:00 AM	29.50	55.80	0.66	56.11	0.65	0.56
2	01:07 AM	29.80	59.36	0.88	59.20	0.85	-0.27
3	05:08 PM	30.17	66.20	0.73	65.79	0.70	-0.62
4	08:19 PM	30.00	42.33	0.65	41.60	0.64	-0.02

It can be seen that the hydration model effectively predicts the temperature history of the wall for each field test, and the time to reach the peak temperature rise is approximately similar to actual data retrieved from field test. Results of the analysis (i.e. maximum temperature) and measured maximum temperature for each case are given in Table 7-5. It can be seen from the results given in Table 7-5, that the accuracy achieved with the hydration model is sufficient to propose appropriate values of the temperature rise between the hydration peak and ambient temperature, (T_1) for any formwork type.

8 Applications of Developed Model

8.1 Effects of Variation of Mineral Composition

Chemical composition of OPC available in the local market was extracted from a market survey carried out recently, and are given in Table 8-1. The mineral compositions were determined by Bouge analysis [14], and present with equivalent type of cement as per ASTM C150, and EN197-1 standards in Table 8-2. The corresponding cement type as per ASTM C150, and EN197-1 were determined as described in section 2.7.

The adiabatic temperature rise for each cement product was predicted assuming 400kg/m^3 cement content with 40% w/c ratio, 30^0C initial temperature, and specific heat capacity of 0.30 kcal/kg/K for 2.75 days. Variation of thermal conductivity is not effective for heat conduction analysis under adiabatic conditions as there is no heat dissipation to surrounding, and hence the variations of thermal conductivity with the degrees of hydration was ignored. Predicted adiabatic temperature rise for concrete with OPC products are shown in Figure 8-1.

Table 8-1: Chemical Composition of OPC Available in Local Market

Chemical Compound	Cement Type				
	OPC-P1	OPC-P2	OPC-P3	OPC-P4	OPC-P5
CaO	64.2	64.1	64.1	64.2	63.1
SiO_2	20.5	20.0	21.3	20.9	19.8
Al_2O_3	4.7	4.9	5.2	5.2	4.8
Fe_2O_3	3.3	3.8	3.9	4.0	3.4
MgO	1.0	1.4	1.3	1.5	2.3
K_2O	0.2	0.4	0.3	0.3	0.7
Na_2O	0.0	0.0	0.0	0.0	0.0
SO_3	2.4	2.1	1.9	1.8	2.6
Cl^-	0.015	0.0	0.0	0.0	0.0

Table 8-2: Mineral Composition, Powder Fineness, and Equivalent ASTM and European Cement Types of OPC Available in Local Market Products

Market product	Mineral Components [%]					Fineness [cm^2/g]	ASTM C150	EN197-1
	C_3A	C_4AF	C_3S	C_2S	$C\dot{S}H_2$			
OPC-P1	6.87	10.04	62.37	11.72	5.18	3468	IV	CEM I
OPC-P2	6.56	11.56	64.56	8.64	4.52	3479	IV	
OPC-P3	7.18	11.87	53.09	21.02	4.10	3364	II	
OPC-P4	7.01	12.17	56.68	17.16	3.89	3093	II	
OPC-P5	6.97	10.35	61.83	10.12	5.62	3704	IV	
Average	6.92	11.20	59.71	13.73	4.66	3422	IV	

Temperature rise under adiabatic conditions was also predicted using C660 [21] method for same mix proportions with CEM I cement catogory, as the variation of chemical composition of cement can not be simulated by this method. Predicted temperature rise under adiabatic conditions using C660 method is shown in Figure 8-1 below.

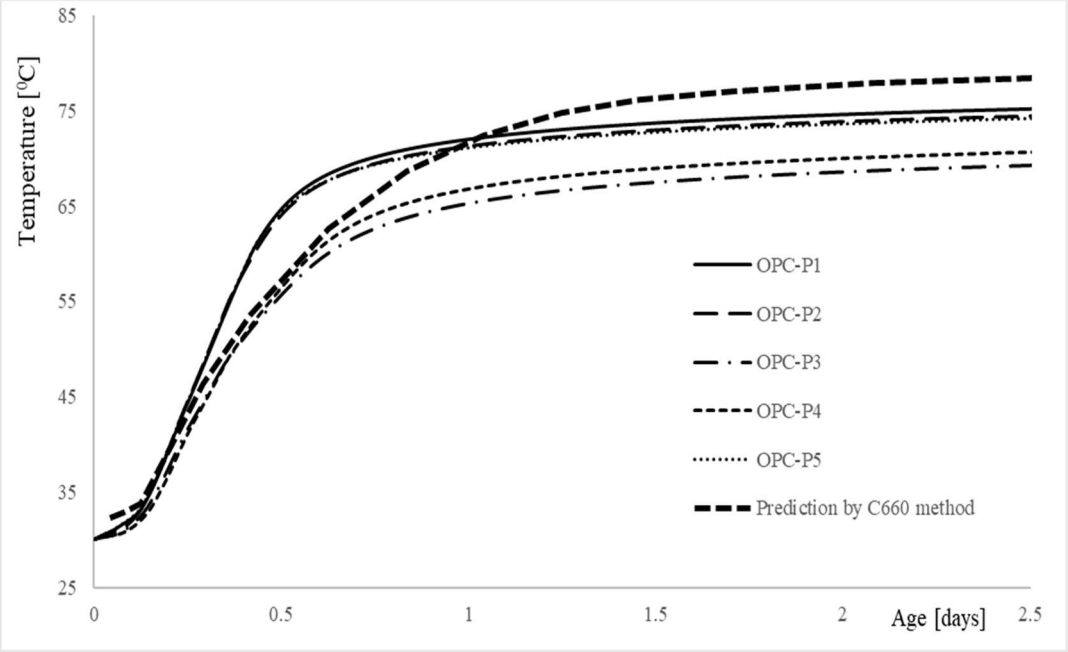

Figure 8-1: Predicted Adiabatic Temperature Rise for OPC Products Available in Local Market

It can be noted that the maximum adiabatic temperature reported by C660 method is slightly higher than the predictions using the proposed hydration model.

OPC-P1 reported the highest adiabatic temperature rise while the lowest by OPC-P3. It can be seen that there is a considerable difference in the temperature rise (7 ~8 °C) due to change in chemical composition of ordinary Portland cement.

8.2 Recommendations for T_1

Design of water retaining structures is based on crack control in immature and mature concrete. In order to control cracking in immature concrete it is necessary to provide reinforcement considering the temperature and moisture effects at early age of concrete.

According to the recommendation given in BS8007, the main factor which determine the reinforcement requirement to control early age thermal cracking is the fall in temperature between hydration peak and mean ambient temperatureT_1. T_1 depends on many factors such as thickness of the section, size of the member, cement content, chemical composition of cement, type of formwork, concrete placing temperature and ambient temperature. Typical values of T_1 for UK conditions are given in BS8007 which are not applicable to local conditions. Therefore, the proposed cement hydration model with thermal property models for concrete was used to predict appropriate T_1 values.

In order to predict fall in temperature between hydration peaks and mean ambient temperature, T_1, for wall and ground slab panels, the temperature rise in panels were analyzed with ANSYS incorporating the calibrated hydration and thermal property models.

Since heat dissipation is effective through the two opposite faces perpendicular to the thickness of wall, the size of wall panel used in the analysis does not affect the

temperature rise. Thickness of the wall panels, type of formwork and cement contents were selected to cover typical values given in Table A2 of BS 8007 [100].

Since it is difficult to produce grade 35A concrete with less than 380 kg/m^3 under local conditions [101], only two cement contents, 380 and 400 kg/m^3 were selected for the analysis.

Furthermore, thermal properties of formworks and initial conditions given in Table 8-3 were used in the analysis. Concrete placing temperature and mean ambient temperature were assumed as 32 ^{o}C and 28 ^{o}C respectively.

Maximum temperature rise estimated by C660 method were also included in Table 8-3 for comparison.

Table 8-3: T_1 Values for Different Wall Thickness and Formwork Materials

Wall Thickness (mm)	4mm thick steel formwork		12mm thick plywood formwork		18mm thick plywood formwork	
	Cement content		Cement content		Cement content	
	380 kg/m^3	400 kg/m^3	380 kg/m^3	400 kg/m^3	380 kg/m^3	400 kg/m^3
300	17 [26]	18 (15) [27] []	31	34	32 [32]	34 (31) [34]
500	27 [33]	29 (27) [35] [	38	40	38 [37]	40 (43) [39]
700	34 [38]	36 (39) [40]	41	44	42 [40]	44 (49) [42]
1000	40 [42]	42 (49) [44]	44	47	44 [43]	47 (56) [45]

Concrete placing temperature = 32 ^{0}C

Mean ambient temperature = 28 ^{0}C

( ) BS 8007 values

[ ] Estimated values using C660 method

Considering an average value for the chemical composition of cement, the walls were analyzed with steel and plywood formwork (12mm and 18mm thick) as well and all the T_1 values calculated are summarized in Table 8-3 above. The values given in () bracket are corresponding values given in BS 8007, and [] brackets are based on C660 method.

It can be seen that there is no significant effect to T_1 when thickness of plywood form works vary from 12mm to 18mm. However, T_1 values recommends by BS8007 are higher than the predicted results with local conditions except for thin walls with average mineral composition of cement.

Further, T_1 predictions by C660 method gives comparatively high values for thin sections and low values for thick sections.

9 Discussion & Conclusions

Specific heat capacity of cement powder estimated based on Dulong-Petit Rule (DPR) and Neumann-Kopp Rule (NKR) and mixing theory described in section3.4 are in the range of 700 ~ 950 J/kg/K which is in good agreement with values reported by many researchers [5, 73, 74]. Specific heat capacities of concrete were estimated following the same method and found that the all temperature response curves obtained from experiments can be predicted with the specific heat capacity of aggregates, 1150 J/kg/K, which is in agreement with the specific heat capacity range reported by Julia C [98].

Further, according to the model's predictions there is only insignificant variation (4%) in specific heat capacity of concrete for considerable variation of w/c (0.3 ~ 0.5) and cement contents (395- 482 kg/m^3).

Also, specific heat capacity of concrete mixes estimated based on the experimental investigation and rules of Dulong – Petit and Neumann– Kopp are in good agreement with the previous studies. Therefore, this method can be used to estimate specific heat capacity of concrete with an acceptable accuracy.

According to experimental investigations, the thermal conductivity of OPC concrete follows a unique pattern with increasing trend irrespective of the mix proportions. It remains constant upto 4 ~ 5 hours and starts to increase upto a maximum value in the range of 2.62 ~ 3.10 J/s/m/K which is in good agreement with values proposed by Kim et al. (2.1 ~ 3.0 J/s/m/K) [7], and Vosteen et al. [8] in previous studies for hardened concrete. Further, it was found that the thermal conductivity of concrete increases about 20% with the hydration process during first 4 ~ 5 hours and remains unchanged afterward.

Since thermal conductivity measured by the proposed experimental methodology are in good agreement with previous studies, the proposed simplified experimental

method can be used to investigate thermal conductivity of fresh and early age concrete effectively without using sophisticated experimental tools.

Furthermore, it can be stated that the calibrated model predicts thermal conductivity of concrete effectively and estimate variation of thermal conductivity with respective to the mix proportions, degrees of hydrations, aggregate shape etc. This model can be effectively used in heat conduction analysis program to carry out thermal analysis of concrete in fresh and hardened states.

In BS 8007, T_1 (i.e. temperature drop between hydration peak and ambient temperature) values are given for concrete placing temperature of 25 °C and mean daily temperature of 15°C. It is expected that due to high ambient temperature in Sri Lanka, T_1 values should be higher than the values given in BS 8007. However, according to the results of the analysis with local materials and environment conditions, all the T_1 values given in BS 8007 are higher than values obtained for local condition except for 300 mm wall for which calculated T_1 values are slightly higher than the corresponding BS 8007 values.

Finally, the following conclusions can be made as a result of this study.

1. Specific heat capacity of concrete can be considered as constant thermal property during the hydration process of cement in concrete.
2. Thermal conductivity of concrete varies with the hydration process during early stage of concrete hardening and it is essential to consider this variation of thermal conductivity in thermal analysis in order to predict temperature rise in concrete.
3. Temperature rise due to heat of hydration of cement in concrete can be effectively predicted by the hydration model proposed by Maekawa et. al, proposed model for thermal conductivity and proposed method to estimate specific heat capacity for a given concrete mix, type of formwork, type of cement, and thermal boundary conditions, etc.

10 Recommendations

As the model proposed by Maekawa et al. [4] can be used to predict temperature rise due to heat of hydration of blended cement, and admixtures as well, this model should be further calibrated and verified with experimental data of blended cements and admixtures. Furthermore, thermal properties model should also be developed further incorporating same effects.

Also, this method of analysis shall further be developed to simulate thermal analysis of a progressive concrete construction to predict temperature response in concrete.

Another aspect which shall recommend to develop is, this program should be used to simulate complete structure minimizing use of computer memory (may be with another platform such as ABACUS) to investigate overall thermal and structural behaviors due to heat of hydration of cement.

References

[1] Blanks and Robert F., "Comparison of Selected Portland Cements in Mass Concrete Tests," Michigan, 1933.

[2] ACI 207.1R-96, "Mass Concrete," Farmington Hills, Mich., 1996.

[3] Bentz D.P., "CEMHYD3D: A Three-Dimensional Cement Hydration and Microstructure Development Modelling Package. Version 2.0," *NISTIR 6485,* 2000.

[4] Maekawa K., Chaube R. and Kish T., Modeling of concrete performance: hydration, microstructure formation and mass transport, London: E and FN SPON, 1999.

[5] Bentz D.P., "Transient plane source measurements of the thermal properties in hydrating cement pastes," *Materials and Structures,* 2007.

[6] Ukrainczyk N. and Matusinovic T., "Thermal properties of hydrating calcium aluminate cement pastes," *Cement and Concrete Research,* 2010.

[7] Kim K.H., Jeon S.E., Kim J.K. and Yang S., "An experimental study on thermal conductivity of concrete," *Cement Concrete Res.,* 2003.

[8] Vosteen H.D. and Schellschmidt R., "Influence of temperature on thermal conductivity, thermal capacity, and thermal diffusivity for different types of rocks," *Phys Chem Earth 28:499–509,* 2003.

[9] Bouguerra A., Laurent J.P., Goual M.S. and Queneudec M., "The measurement of the thermal conductivity of solid aggregates using the transient plane source technique," *J Phys D: Appl Phys 30:2900–2904,* 1997.

[10] Horai K., "Thermal conductivity of rock-forming minerals," *J Geophys Res 76(5):1278–1308,* 1971.

[11] Hewlett P.C., Lea's Chemistry of Cement and Concrete, 4th ed., Oxford, Ed., Elsevier Ltd., 2004.

[12] Groberty B., *Portland Cement,* 2013.

[13] Zhi Ge, "Predicting temperature and strength development of the field concrete," Iowa State University, Ames, Iowa, 2005.

[14] Bouge R.H., The Chemistry of Portland Cement, New York: Reinhold Publishing Corporation, 1947.

[15] ASTM C 150, Standard specification for Portland cement, vol. 4.02, Annual Book of ASTM Standards, 2002.

[16] Tetmayer T., "Deucsche Topfer-und Ziegler-Atg.," 1883.

[17] Rastrup E., "Winter Concreting," in *Proceeding of the RILEM Symposium*, Copenhagen, 1956.

[18] Paine K.A., Dhir R.K. and Zheng L., "Predicting early-age temperatures of blended-cement concrete," in *Proceedings of the Institution of Civil Engineers*, 2006.

[19] Paine K.A., Zheng L. and Dhir R.K., "Experimental study and modelling of heat evolution of blended cements," 2005.

[20] Harrison T.A., "Early-age Thermal Crack Control in Concrete," London, 1992.

[21] Bamforth P.B., "Early-age Thermal Crack Control in Concrete," London, 2007.

[22] ASTM C595-03, "Standard Specification for Blended Hydraulic Cements," in *Annual Book of ASTM Standards V 04.01*, USA, ASTM International, 2004, pp. 340-346.

[23] AS 3972:1997, "Portland and Blended Cements," in *Standards Australia*, Homebush, 1997.

[24] GB 200: 2003, "Moderate heat Portland cement," in *low heat Portland cement, and low heat Portland slag cement*, Beijing, Inspection and Quarantine of the People's Republic of China, 2003.

[25] Van Breugel K., "Simulation of hydration and formation of structure in hardening cement based materials," *Meinema,* 1991.

[26] Suzuki Y., Harada Y., Maekawa K. and Tsuji Y., "Quantification of heat of hydration generation process in concrete," *JSCE,* 1990.

[27] Lu H.R., Swaddiwudhipong S. and Wee T.H., "Evaluation of Thermal Crack by a Probabilistic Model Using The Tensile Strain Capacity," *Magazine of Concrete Research,* vol. 53, pp. 25-30, 2001.

[28] Boulder Canyon Project Report, "Thermal properties of concrete," 1940.

[29] C. A. D. and T. C.P., "The thermal conductivity of concrete," *Magazine of Concrete Research,* 1963.

[30] Harmathy T.Z., "Thermal properties of concrete at elevated temperatures," *Journal of Materials,* 1970.

[31] Bhattacharjee B. and Krishnamurthy S., "A model for thermal conductivity of porous building materials".

[32] Glatzmaier G.C. and Ramirez W.F., *Rev. Sci. Instrum. 56,* 1985.

[33] Bkkstron G., *J. Phys E: Sci. Znstrum.15,* 1982.

[34] Cull J. P., *J. Phys E: Sci. Znstrum.7,* 1974.

[35] Gustafsson S.E., Karawacki E. and Khan M.N., *J. Phys. D: Appl. Phys. 12,* 1979.

[36] Gustafsson S.E., *Rev. Sci. Instrum. 62,* 1991.

[37] Bouguerra A., Ait Mokhtar A., Amiri O. and Diop M.B., "Measurement of thermal conductivity, thermal diffusivity, and heat capacity of highly porous building materials using transient plane source technique," *Int. Comm. Heat Mass Transfer,* vol. 28, pp. 1065-1078, 2001.

[38] Daniel P.H., "Thermal Conductivity of Fibre-Reinforced Lightweight Cement Composites," 2013.

[39] Synder K.A., Interfacail zone percolation in cement aggregate composites, Interface in Cementitious Composites, J. M. (Ed.), Ed., London: E&FN Spon, 1990.

[40] Powers T.C. and Brownyard T.L., "Studies of the Physical Properties of Hardened Portland cement Paste," 1948.

[41] Bruanauer S., Emmett P.H. and Teller E., "Adsorption of Gases in Multimolecular Layers," *Journal of the American Chemical Society,* p. 2, 1938.

[42] Jennings H.M. and Tennis P.D., "Model for the Developing Microstructure in Portland Cement Paste," *Journal of the Americal Ceramic Society,* 1994.

[43] Jeffrey W.B., Hamlin M. J., Richard A. L., Andre N., George W. S., Jeffrey S. S., Karen L. S. and Jeffrey J. T., "Mechanism of Cement Hydration," *Cement and Concrete Research,* 2010.

[44] Glasstone S., Laidler K.J. and Eyring H., "The Theory of Rate Processes," *McGraw-Hill,* 1941.

[45] Kaschiev D. and Van Rosmalen G.M., "nucleation in solutions revisited," Cryst. Res. Technol. 38, 2003.

[46] Dove P.M. and Han N., "Kinetics of mineral dissolution and growth as reciprocal microscopic surface processes across chemical driving force," in *AIP Conference Proceedings*, 2007.

[47] Dove P.M., Han N. and Yoreo J.J.D., "Mechanisms of classical crystal growth theory explain quartz and silicate dissolution behavior," 2005.

[48] Mills R. and Lobo V.M.M., "Self-Diffusion in Electrolyte Solutions," *Elsevier,* 1989.

[49] Somorjai G.A., "Introduction to Surface Chemistry and Catalysis," *Wiley-Interscience,* 1994.

[50] Adamson A.W. and Gast A.P., Physical Chemistry of Surfaces, 6th ed., New York: Wiley-Interscience, 1997.

[51] Stumm W. and Morgan J.J., Aquatic Chemistry, New York: Wiley-Interscience, 1972.

[52] Garrault S. and Nonat A., "Hydrated layer formation on tricalcium and dicalcium silicate surfaces: experimental study and numerical simulations," *Langmuir 17,* 2001.

[53] Mataraarachchi A.I.G.K., Nanayakkara S.M.A and Asamoto S., "Investigation of temperature rise due to heat of hydration of cement and annual temperature variation related to control of thermal cracking in concrete water retaining structures," *Society of Structural Engineers,* 2012.

[54] Scrivener K.L., "The development of microstructure during hydration of portland cement," University of London, 1984.

[55] Youyuan Lu, Jinrui Ahang and Zongjin Li, "Study on hydration process of early -age concrete using embedded active acoustic and non-contact complex resistivity method," *Construction and Building Material,* p. 191, 2013.

[56] Mindess S. and Young J.F., Concrete, N.J., Englewood Cliffs: Prentice-Hall Inc., 1981.

[57] Lerch W. and Bogue R.H., "Heat of Hydration of Portland cement pastes," *Journal of Research of National Bureau Standads,* vol. 12, pp. 645-664, 1934.

[58] Lerch W., "The influence of gypsum on the hydration and properties of Portland cement pastes," in *Proceedings of American Society for Testing Materials*, 1946.

[59] Lerch W., Ashton F.W. and Bogue R.H., "The sulfoaluminated of calcium," *Journal of Research of National Bureau Standards,* vol. 2, pp. 715-731, 1929.

[60] A. 207.2R-7, "Report on Thermal and Volume Change Effects on Cracking of Mass Concrete," American Concrete Institute, Farmington Hills, 2007.

[61] Shuhua Liu, Lu Wang, Yuxin Gao, Baoying Yu and Wan Tang, "Influence of fineness of hydration kinetics of supersulfated cement," *Thermochimica Acta,* pp. 39-42, 2015.

[62] RILEM 42-CEA, "Properties of set concrete at early ages," Material and Strucutures, 1981.

[63] Escalante G., Sharp J.I. and Sharp J.H., "The effects of temperature on the early hydration of Portland cement and blended cements," *Advances in cement Research,* vol. 12, pp. 121-130, 2000.

[64] Kondo R. and Kodama M., "Hydration kinetics of cement," *Semento Gijutsu Nenpo 21,* pp. 77-82, 1967.

[65] Pommersheim J.M. and Clifton J.R., "Mathematicl modeling of tricalcium silicate hydration," *Cement Concrete Research,* pp. 765-770, 1979.

[66] Pommersheim J.R., Clifton G. and Frohnsdorff G., "Mathematical modeling of tricalcium silicate hydration," *Cement Concrete Research,* pp. 765-772, 1982.

[67] Williamson R.B., "Solidification of Portland cement," *Prog. Mater. Sci.,* pp. 189-286, 1972.

[68] Jennings H.M. and Johnson S.K., "Simulation of microstructure development during the hydration of a cement compound," *Journel of American Ceramic Society,* pp. 790-795, 1986.

[69] Powers T.C. and Brownyard T.L., "Studies of the Physical Properties of Hardened Portland Cement Paste," *Detroit,* 1948.

[70] Jeffrey J. T., Joseph J. B., Jeffrey W.B., Shashank B., Jorge S.D., George W.S. and Andreas L., "Modeling and simulation of cement hydration kinetics and microstructure development," *Cement and Concrete Reseearch,* pp. 1257-1278, 2011.

[71] Andreas K. and Helge S., "Specific Heat Capacity of Metals," *TFY4165 Termisk fysikk,* 2014.

[72] Jindrich L., Pavel C, David S., Ales S. and Peter A., "Estimation of heat capacities of solid mixed oxides," *Thermochimica Acta 395,* pp. 27-46, 2003.

[73] Yunsheng Xu and Chung D.D.L., "Cement of high specific heat and high thermal conductivity, obtained by using silane and silica fume as admixtures," *Cement and Concrete Research,* 2000.

[74] Todd S.S., "Low-Temperature heat capacities and entropies at 298.16 K of crystalline calcium orthosilicate, zinc orthosilicate, and tricalcium silicate," *Journel of American Chemistry Soceity,* p. 3277–3278, 1951.

[75] ASTM C177, Standard method for steady state heat flux measurements and theamal transmission properties by means of the guarded hot plate appratus, 2004.

[76] ASTM C 518, Standard test method for steady state transmission properties by means of the heat flow meter appratus, PA: ASTM, 2004.

[77] ASTM C1114, Standard method for steady state transmission properties by means of the thin heater apparatus, PA: ASTM, 2006.

[78] ASTM E1225, Standard test method for thermal conductivity of solids by means of the guarded comparative longitudinal heat flow technique, PA: ASTM, 2004.

[79] ASTM D5930, "Standard test method for thermal conductivity of plastics by means of a transient line source technique," ASTM, PA, 209.

[80] ASTM C113, "Standard test method for thermal conductivity of refractories by hot wire (Platinum resistance thermometer technique)," ASTM, PA, 2009.

[81] Parker W.J., Jenkins R.J., Butler C.P. and Abbott G.L., "Flash method of determining the thermal diffusivity, heat capacity, and thermal conductivity," *Journal of Applied Physics,* vol. 32, pp. 1679-1684, 1960.

[82] T. S. W. Karol Pietrak, "A review of models for effective thermal conductivity of composite materials," *Journal of Power Technologies ,* 2015.

[83] L. F. J. D. P. H. Hasselman, " Effective thermal conductivity of composites with interfacial thermal barrier resistance," *J. Compos. Mater.,* (1987.

[84] Santhikumar S., "Temperature dependent heat generation model for mixed cement concrete with mutual interaction among constituent minerals," 1993.

[85] Mullin J.W., in *Crystalization*, 4th ed., London, Butterworth Henneman, 2001, p. 51.

[86] Wang J., Carson J.K., North M.F. and Cleland D.J., "A new approach to modelling the effective thermal conductivity of heterogeneous materials," *International J. of Heat and Mass Transfer,* vol. 49, pp. 3075-3083, 2006.

[87] Purdue University, "Thermophysical Properties of Matter: Thermal Conductivity; Nonmetallic Liquids and Gases," 1970.

[88] Tsilingiris P.T., "Thermophysical and Transport Properties of Humid Air at Temperature Range Between 0 and 100ºC.," *Energy Conservation and Management,* Septermber 2008.

[89] Rohsenow W.M., Hartnett J.P. and Cho Y.I., Handbook of Heat Transfer, New York: McGraw-Hill, 1998.

[90] Torban C.H., "Physical Structure of Hardened Cement Paste. A Classical Approach," *Construction Material,* vol. 19.

[91] Mehta P.K. and Paulo J.M.M., Concrete Structures, Properties, and Materials, N.J., Englewood Cliffs: Prentice-Hall, 1993.

[92] Michael E.R., "Predicting Temperature Rise and Thermal Cracking in Concrete," PCA, 2007.

[93] John H. L., Heat Transfer Text Book, Massachusetts: Cambridge, 2000.

[94] Holman J.P., Heat Transfer, 7th ed., New York: McGraw Hill, 1990.

[95] Kyle A.R., Jonathan L.P., Anton K.S., Maria C.G.J. and Kevin J.F., "Temperature Boundary Condition Model for Concrete Bridge Member," *ACI Material Journal,* vol. 104, pp. 379-387, July - August 2007.

[96] Jayawardena U.S., "Correlations between some strength properties of metamorphic rocks of Sri Lanka," *Journal of Geological Society of Sri Lanka,* vol. 14, pp. 65-66, 2011.

[97] Fernando L.J.D., "Mineral resources of Sri Lanka," *Natural Resources, Energy and Science Authority,* 1986.

[98] Julia C., "Thermal properties of concrete with different Swedish aggregate materials," 2013.

[99] Perera S.K.H., "Field measurements of early age temperature rise and seasonal temperature variation in concrete," March 2007.

[100] BS8007, Design of concrete structures for retaining aqueous liquid, London: British Standards Institution, 1987.

[101] Nanayakkara S.M.A and Liyanage W.W., "Use of Grade 25 concrete in Design of Water Retaining Structures Based on BS 8007 Recommendations," *IESL Transactions,* pp. 1-8, 2003.

APPENDIX A : APDL Codes of Geometric Model

```
/PREP7              ! ENTER PREPROCESSOR
/UNITS,USER,1,1,1/(86400),1,0,1,1,1/4185.8   ! SET SI UNIT SYSTEM
MP,KXX,3,9.977      ! SPECIFY THERMAL CONDUCTIVITY OF PLYWOOD [MAT 2] [KCAL/DAY/M/K]
MP,KYY,3,9.977      ! SPECIFY THERMAL CONDUCTIVITY OF PLYWOOD [MAT 2] [KCAL/DAY/M/K]
MP,KZZ,3,9.977      ! SPECIFY THERMAL CONDUCTIVITY OF PLYWOOD [MAT 2] [KCAL/DAY/M/K]
MP,C,3,0.387        ! SPECIFY SPECIFIC HEAT OF PLYWOOD [MAT 2] [KCAL/KG/K]
MP,DENS,3,530       ! SPECIFY DENSITY OF PLYWOOD [MAT 2] [KG/M3]
MP,KXX,4,42.4       ! SPECIFY THERMAL CONDUCTIVITY OF SAND [MAT 4] [KCAL/DAY/M/K]
MP,KYY,4,42.4       ! SPECIFY THERMAL CONDUCTIVITY OF SAND [MAT 4] [KCAL/DAY/M/K]
MP,KZZ,4,42.4       ! SPECIFY THERMAL CONDUCTIVITY OF SAND [MAT 4] [KCAL/DAY/M/K]
MP,C,4,0.235        ! SPECIFY SPECIFIC HEAT OF SAND [MAT 4] [KCAL/KG/K]
MP,DENS,4,1800      ! SPECIFY DENSITY OF SAND [MAT 4] [KG/M3]
MP,KXX,5,45         ! SPECIFY THERMAL CONDUCTIVITY OF LEAN CONCRETE [MAT 5] [KCAL/DAY/M/K]
MP,KYY,5,45         ! SPECIFY THERMAL CONDUCTIVITY OF LEAN CONCRETE [MAT 5] [KCAL/DAY/M/K]
MP,KZZ,5,45         ! SPECIFY THERMAL CONDUCTIVITY OF LEAN CONCRETE [MAT 5] [KCAL/DAY/M/K]
MP,C,5,0.26         ! SPECIFY SPECIFIC HEAT OF LEAN CONCRETE [MAT 5] [KCAL/KG/K]
MP,DENS,5,2100      ! SPECIFY DENSITY OF LEAN CONCRETE [MAT 5] [KG/M3]
MP,KXX,2,1.629      ! SPECIFY THERMAL CONDUCTIVITY OF STYROFOAM [MAT 4] [KCAL/DAY/M/K]
MP,KYY,2,1.629      ! SPECIFY THERMAL CONDUCTIVITY OF STYROFOAM [MAT 4] [KCAL/DAY/M/K]
MP,KZZ,2,1.629      ! SPECIFY THERMAL CONDUCTIVITY OF STYROFOAM [MAT 4] [KCAL/DAY/M/K]
```

```
MP,C,2,0.358          ! SPECIFY SPECIFIC HEAT OF STYROFOAM [MAT 4] [KCAL/KG/K]
MP,DENS,2,15          ! SPECIFY DENSITY OF STYROFOAM [MAT 4] [KG/M3]
ET,1,70               ! SPECIFY ELEMENT TYPE AS SOLID70
L=1.5                 ! SPECIFY LENGTH OF CONCRETE
W=1.5                 ! SPECIFY WIDTH OF CONCRETE
H=2.5                 ! SPECIFY THICKNESS OF CONCRETE
TS=0.050              ! SPECIFY THICKNESS OF STYROFORM
TF=0.015              ! SPECIFY THICKNESS OF FORMWORK
TL=0.050              ! SPECIFY THICKNESS OF LEAN CONCRETE
*DIM,GEO,ARRAY,3,2        ! SPECIFY 2D ARRAY TO PASS GEMETRIC PARAMETERS
*VFILL,GEO(1,1),DATA,-L/2-TS-TF
*VFILL,GEO(1,2),DATA,L/2+TS+TF
*VFILL,GEO(2,1),DATA,0
*VFILL,GEO(2,2),DATA,TL+H+TS*2.5
*VFILL,GEO(3,1),DATA,-W/2-TS-TF
*VFILL,GEO(3,2),DATA,W/2+TS+TF
K,1,-L/2-TS-TF,0,-W/2-TS-TF       ! SPECIFY KEY POINT 1
K,2,-L/2-TS,0,-W/2-TS-TF          ! SPECIFY KEY POINT 2
K,3,-L/2,0,-W/2-TS-TF             ! SPECIFY KEY POINT 3
K,4,L/2,0,-W/2-TS-TF          ! SPECIFY KEY POINT 4
K,5,L/2+TS,0,-W/2-TS-TF           ! SPECIFY KEY POINT 5
K,6,L/2+TS+TF,0,-W/2-TS-TF        ! SPECIFY KEY POINT 6
K,7,-L/2-TS-TF,0,-W/2-TS          ! SPECIFY KEY POINT 7
K,8,-L/2-TS,0,-W/2-TS             ! SPECIFY KEY POINT 8
K,9,-L/2,0,-W/2-TS            ! SPECIFY KEY POINT 9
K,10,L/2,0,-W/2-TS            ! SPECIFY KEY POINT 10
K,11,L/2+TS,0,-W/2-TS         ! SPECIFY KEY POINT 11
K,12,L/2+TS+TF,0,-W/2-TS          ! SPECIFY KEY POINT 12
K,13,-L/2-TS-TF,0,-W/2        ! SPECIFY KEY POINT 13
K,14,-L/2-TS,0,-W/2           ! SPECIFY KEY POINT 14
```

```
K,15,-L/2,0,-W/2        ! SPECIFY KEY POINT 15
K,16,L/2,0,-W/2         ! SPECIFY KEY POINT 16
K,17,L/2+TS,0,-W/2      ! SPECIFY KEY POINT 17
K,18,L/2+TS+TF,0,-W/2       ! SPECIFY KEY POINT 18
K,19,-L/2-TS-TF,0,W/2       ! SPECIFY KEY POINT 19
K,20,-L/2-TS,0,W/2      ! SPECIFY KEY POINT 20
K,21,-L/2,0,W/2         ! SPECIFY KEY POINT 21
K,22,L/2,0,W/2          ! SPECIFY KEY POINT 22
K,23,L/2+TS,0,W/2       ! SPECIFY KEY POINT 23
K,24,L/2+TS+TF,0,W/2        ! SPECIFY KEY POINT 24
K,25,-L/2-TS-TF,0,W/2+TS    ! SPECIFY KEY POINT 25
K,26,-L/2-TS,0,W/2+TS       ! SPECIFY KEY POINT 26
K,27,-L/2,0,W/2+TS      ! SPECIFY KEY POINT 27
K,28,L/2,0,W/2+TS       ! SPECIFY KEY POINT 28
K,29,L/2+TS,0,W/2+TS        ! SPECIFY KEY POINT 29
K,30,L/2+TS+TF,0,W/2+TS         ! SPECIFY KEY POINT 30
K,31,-L/2-TS-TF,0,W/2+TS+TF     ! SPECIFY KEY POINT 31
K,32,-L/2-TS,0,W/2+TS+TF        ! SPECIFY KEY POINT 32
K,33,-L/2,0,W/2+TS+TF       ! SPECIFY KEY POINT 33
K,34,L/2,0,W/2+TS+TF        ! SPECIFY KEY POINT 34
K,35,L/2+TS,0,W/2+TS+TF         ! SPECIFY KEY POINT 35
K,36,L/2+TS+TF,0,W/2+TS+TF      ! SPECIFY KEY POINT 36
K,37,-L/2-TS-TF,TL,-W/2-TS-TF       ! SPECIFY KEY POINT 37
K,38,-L/2-TS,TL,-W/2-TS-TF      ! SPECIFY KEY POINT 38
K,39,-L/2,TL,-W/2-TS-TF         ! SPECIFY KEY POINT 39
K,40,L/2,TL,-W/2-TS-TF          ! SPECIFY KEY POINT 40
K,41,L/2+TS,TL,-W/2-TS-TF       ! SPECIFY KEY POINT 41
K,42,L/2+TS+TF,TL,-W/2-TS-TF        ! SPECIFY KEY POINT 42
K,43,-L/2-TS-TF,TL,-W/2-TS      ! SPECIFY KEY POINT 43
K,44,-L/2-TS,TL,-W/2-TS         ! SPECIFY KEY POINT 44
```

```
K,45,-L/2,TL,-W/2-TS        ! SPECIFY KEY POINT 45
K,46,L/2,TL,-W/2-TS         ! SPECIFY KEY POINT 46
K,47,L/2+TS,TL,-W/2-TS      ! SPECIFY KEY POINT 47
K,48,L/2+TS+TF,TL,-W/2-TS   ! SPECIFY KEY POINT 48
K,49,-L/2-TS-TF,TL,-W/2     ! SPECIFY KEY POINT 49
K,50,-L/2-TS,TL,-W/2        ! SPECIFY KEY POINT 50
K,51,-L/2,TL,-W/2           ! SPECIFY KEY POINT 51
K,52,L/2,TL,-W/2            ! SPECIFY KEY POINT 52
K,53,L/2+TS,TL,-W/2         ! SPECIFY KEY POINT 53
K,54,L/2+TS+TF,TL,-W/2      ! SPECIFY KEY POINT 54
K,55,-L/2-TS-TF,TL,W/2      ! SPECIFY KEY POINT 55
K,56,-L/2-TS,TL,W/2         ! SPECIFY KEY POINT 56
K,57,-L/2,TL,W/2            ! SPECIFY KEY POINT 57
K,58,L/2,TL,W/2             ! SPECIFY KEY POINT 58
K,59,L/2+TS,TL,W/2          ! SPECIFY KEY POINT 59
K,60,L/2+TS+TF,TL,W/2       ! SPECIFY KEY POINT 60
K,61,-L/2-TS-TF,TL,W/2+TS   ! SPECIFY KEY POINT 61
K,62,-L/2-TS,TL,W/2+TS      ! SPECIFY KEY POINT 62
K,63,-L/2,TL,W/2+TS         ! SPECIFY KEY POINT 63
K,64,L/2,TL,W/2+TS          ! SPECIFY KEY POINT 64
K,65,L/2+TS,TL,W/2+TS       ! SPECIFY KEY POINT 65
K,66,L/2+TS+TF,TL,W/2+TS    ! SPECIFY KEY POINT 66
K,67,-L/2-TS-TF,TL,W/2+TS+TF  ! SPECIFY KEY POINT 67
K,68,-L/2-TS,TL,W/2+TS+TF   ! SPECIFY KEY POINT 68
K,69,-L/2,TL,W/2+TS+TF      ! SPECIFY KEY POINT 69
K,70,L/2,TL,W/2+TS+TF       ! SPECIFY KEY POINT 70
K,71,L/2+TS,TL,W/2+TS+TF    ! SPECIFY KEY POINT 71
K,72,L/2+TS+TF,TL,W/2+TS+TF  ! SPECIFY KEY POINT 72
K,73,-L/2-TS-TF,TL+H,-W/2-TS-TF  ! SPECIFY KEY POINT 73
K,74,-L/2-TS,TL+H,-W/2-TS-TF  ! SPECIFY KEY POINT 74
```

```
K,75,-L/2,TL+H,-W/2-TS-TF      ! SPECIFY KEY POINT 75
K,76,L/2,TL+H,-W/2-TS-TF       ! SPECIFY KEY POINT 76
K,77,L/2+TS,TL+H,-W/2-TS-TF    ! SPECIFY KEY POINT 77
K,78,L/2+TS+TF,TL+H,-W/2-TS-TF      ! SPECIFY KEY POINT 78
K,79,-L/2-TS-TF,TL+H,-W/2-TS    ! SPECIFY KEY POINT 79
K,80,-L/2-TS,TL+H,-W/2-TS      ! SPECIFY KEY POINT 80
K,81,-L/2,TL+H,-W/2-TS         ! SPECIFY KEY POINT 81
K,82,L/2,TL+H,-W/2-TS          ! SPECIFY KEY POINT 82
K,83,L/2+TS,TL+H,-W/2-TS       ! SPECIFY KEY POINT 83
K,84,L/2+TS+TF,TL+H,-W/2-TS    ! SPECIFY KEY POINT 84
K,85,-L/2-TS-TF,TL+H,-W/2      ! SPECIFY KEY POINT 85
K,86,-L/2-TS,TL+H,-W/2         ! SPECIFY KEY POINT 86
K,87,-L/2,TL+H,-W/2          ! SPECIFY KEY POINT 87
K,88,L/2,TL+H,-W/2           ! SPECIFY KEY POINT 88
K,89,L/2+TS,TL+H,-W/2    ! SPECIFY KEY POINT 89
K,90,L/2+TS+TF,TL+H,-W/2      ! SPECIFY KEY POINT 90
K,91,-L/2-TS-TF,TL+H,W/2       ! SPECIFY KEY POINT 91
K,92,-L/2-TS,TL+H,W/2          ! SPECIFY KEY POINT 92
K,93,-L/2,TL+H,W/2           ! SPECIFY KEY POINT 93
K,94,L/2,TL+H,W/2         ! SPECIFY KEY POINT 94
K,95,L/2+TS,TL+H,W/2        ! SPECIFY KEY POINT 95
K,96,L/2+TS+TF,TL+H,W/2          ! SPECIFY KEY POINT 96
K,97,-L/2-TS-TF,TL+H,W/2+TS      ! SPECIFY KEY POINT 97
K,98,-L/2-TS,TL+H,W/2+TS       ! SPECIFY KEY POINT 98
K,99,-L/2,TL+H,W/2+TS          ! SPECIFY KEY POINT 99
K,100,L/2,TL+H,W/2+TS          ! SPECIFY KEY POINT 100
K,101,L/2+TS,TL+H,W/2+TS       ! SPECIFY KEY POINT 101
K,102,L/2+TS+TF,TL+H,W/2+TS       ! SPECIFY KEY POINT 102
K,103,-L/2-TS-TF,TL+H,W/2+TS+TF      ! SPECIFY KEY POINT 103
K,104,-L/2-TS,TL+H,W/2+TS+TF      ! SPECIFY KEY POINT 104
```

```
K,105,-L/2,TL+H,W/2+TS+TF                ! SPECIFY KEY POINT 105
K,106,L/2,TL+H,W/2+TS+TF                 ! SPECIFY KEY POINT 106
K,107,L/2+TS,TL+H,W/2+TS+TF              ! SPECIFY KEY POINT 107
K,108,L/2+TS+TF,TL+H,W/2+TS+TF           ! SPECIFY KEY POINT 108
K,109,-L/2-TS-TF,TL+H+TS*2.5,-W/2-TS-TF  ! SPECIFY KEY POINT 109
K,110,-L/2-TS,TL+H+TS*2.5,-W/2-TS-TF     ! SPECIFY KEY POINT 110
K,111,-L/2,TL+H+TS*2.5,-W/2-TS-TF        ! SPECIFY KEY POINT 111
K,112,L/2,TL+H+TS*2.5,-W/2-TS-TF         ! SPECIFY KEY POINT 112
K,113,L/2+TS,TL+H+TS*2.5,-W/2-TS-TF      ! SPECIFY KEY POINT 113
K,114,L/2+TS+TF,TL+H+TS*2.5,-W/2-TS-TF   ! SPECIFY KEY POINT 114
K,115,-L/2-TS-TF,TL+H+TS*2.5,-W/2-TS     ! SPECIFY KEY POINT 115
K,116,-L/2-TS,TL+H+TS*2.5,-W/2-TS        ! SPECIFY KEY POINT 116
K,117,-L/2,TL+H+TS*2.5,-W/2-TS           ! SPECIFY KEY POINT 117
K,118,L/2,TL+H+TS*2.5,-W/2-TS            ! SPECIFY KEY POINT 118
K,119,L/2+TS,TL+H+TS*2.5,-W/2-TS         ! SPECIFY KEY POINT 119
K,120,L/2+TS+TF,TL+H+TS*2.5,-W/2-TS      ! SPECIFY KEY POINT 120
K,121,-L/2-TS-TF,TL+H+TS*2.5,-W/2        ! SPECIFY KEY POINT 121
K,122,-L/2-TS,TL+H+TS*2.5,-W/2           ! SPECIFY KEY POINT 122
K,123,-L/2,TL+H+TS*2.5,-W/2              ! SPECIFY KEY POINT 123
K,124,L/2,TL+H+TS*2.5,-W/2               ! SPECIFY KEY POINT 124
K,125,L/2+TS,TL+H+TS*2.5,-W/2            ! SPECIFY KEY POINT 125
K,126,L/2+TS+TF,TL+H+TS*2.5,-W/2         ! SPECIFY KEY POINT 126
K,127,-L/2-TS-TF,TL+H+TS*2.5,W/2         ! SPECIFY KEY POINT 127
K,128,-L/2-TS,TL+H+TS*2.5,W/2            ! SPECIFY KEY POINT 128
K,129,-L/2,TL+H+TS*2.5,W/2               ! SPECIFY KEY POINT 129
K,130,L/2,TL+H+TS*2.5,W/2                ! SPECIFY KEY POINT 130
K,131,L/2+TS,TL+H+TS*2.5,W/2             ! SPECIFY KEY POINT 131
K,132,L/2+TS+TF,TL+H+TS*2.5,W/2          ! SPECIFY KEY POINT 132
K,133,-L/2-TS-TF,TL+H+TS*2.5,W/2+TS      ! SPECIFY KEY POINT 133
K,134,-L/2-TS,TL+H+TS*2.5,W/2+TS         ! SPECIFY KEY POINT 134
```

```
K,135,-L/2,TL+H+TS*2.5,W/2+TS                ! SPECIFY KEY POINT 135
K,136,L/2,TL+H+TS*2.5,W/2+TS                 ! SPECIFY KEY POINT 136
K,137,L/2+TS,TL+H+TS*2.5,W/2+TS              ! SPECIFY KEY POINT 137
K,138,L/2+TS+TF,TL+H+TS*2.5,W/2+TS           ! SPECIFY KEY POINT 138
K,139,-L/2-TS-TF,TL+H+TS*2.5,W/2+TS+TF       ! SPECIFY KEY POINT 139
K,140,-L/2-TS,TL+H+TS*2.5,W/2+TS+TF          ! SPECIFY KEY POINT 140
K,141,-L/2,TL+H+TS*2.5,W/2+TS+TF             ! SPECIFY KEY POINT 141
K,142,L/2,TL+H+TS*2.5,W/2+TS+TF              ! SPECIFY KEY POINT 142
K,143,L/2+TS,TL+H+TS*2.5,W/2+TS+TF           ! SPECIFY KEY POINT 143
K,144,L/2+TS+TF,TL+H+TS*2.5,W/2+TS+TF        ! SPECIFY KEY POINT 144
*DO,J,1,3,1
*DO,I,1,5,1
V,I+(J-1)*36,I+1+(J-1)*36,I+7+(J-1)*36,I+6+(J-1)*36,I+36+(J-1)*36,I+37+(J-1)*36,I+43+(J-1)*36,I+42+(J-1)*36
V,I+6+(J-1)*36,I+7+(J-1)*36,I+13+(J-1)*36,I+12+(J-1)*36,I+42+(J-1)*36,I+43+(J-1)*36,I+49+(J-1)*36,I+48+(J-1)*36
V,I+12+(J-1)*36,I+13+(J-1)*36,I+19+(J-1)*36,I+18+(J-1)*36,I+48+(J-1)*36,I+49+(J-1)*36,I+55+(J-1)*36,I+54+(J-1)*36
V,I+18+(J-1)*36,I+19+(J-1)*36,I+25+(J-1)*36,I+24+(J-1)*36,I+54+(J-1)*36,I+55+(J-1)*36,I+61+(J-1)*36,I+60+(J-1)*36
V,I+24+(J-1)*36,I+25+(J-1)*36,I+31+(J-1)*36,I+30+(J-1)*36,I+60+(J-1)*36,I+61+(J-1)*36,I+67+(J-1)*36,I+66+(J-1)*36
*ENDDO
*ENDDO
ELSIZE=0.3
/VIEW,1,1,1,1
LESIZE,ALL,ELSIZE
MSHKEY,1
MAT,1
VMESH,38,39
MAT,2
VMESH,32,34
```

```
VMESH,37
VMESH,42,44
VMESH,57,59
VMESH,62
VMESH,64
VMESH,67,69
MAT,4
VMESH,63
MAT,3
VMESH,26,31
VMESH,35,36
VMESH,40,41
VMESH,45,56
VMESH,60,61
VMESH,65,66
VMESH,70,75
MAT,5
VMESH,1,25
FINISH
```

APPENDIX B : APDL Codes of Parameter Inputs

```
!----------------START INPUT OF CEMENT CHEMICAL COMPOSITION DATA----------------------
*DIM,CD,ARRAY,90,1      ! DEFINE 1D ARRAY CD TO STORE CEMENT COPOSITION DATA
WC=400                  ! UNIT WEIGHT OF CEMENT IN CONCRETE (KG PER CUBIC METER)
*VFILL,CD(1,1),DATA,WC
P3A=9.03                ! WEIGHT PERCENTAGE OF ALUMINATE (C3A)
*VFILL,CD(2,1),DATA,P3A
P3S=69.30               ! WEIGHT PERCENTAGE OF ALITE (C3S)
*VFILL,CD(3,1),DATA,P3S
P4AF=10.5               ! WEIGHT PERCENTAGE OF FERRITE (C4AF)
*VFILL,CD(4,1),DATA,P4AF
P2S=4.83                ! WEIGHT PERCENTAGE OF BELITE (C2S)
*VFILL,CD(5,1),DATA,P2S
PPCS2H=5.46             ! WEIGHT PERCENTAGE OF GYPSUM (CS2H)
*VFILL,CD(6,1),DATA,PPCS2H
PPC=96.13               ! WEIGHT PERCENTAGE OF OPC
*VFILL,CD(7,1),DATA,PPC
BLN=3950                ! BLAINE VALUE OF OPC
*VFILL,CD(8,1),DATA,BLN
PSG=0.0                 ! WEIGHT PERCENTAGE OF SLAG
*VFILL,CD(9,1),DATA,PSG
BLNSG=3300              ! BLAINE VALUE OF SLAG
*VFILL,CD(10,1),DATA,BLNSG
SGCS2H=0.0              ! WEIGHT PERCENTAGE OF SULFATE IN SLAG
*VFILL,CD(11,1),DATA,SGCS2H
WSGMOL=0.0
*VFILL,CD(12,1),DATA,WSGMOL
PFA=0.0                 ! WEIGHT PERCENTAGE OF FLY ASH
*VFILL,CD(13,1),DATA,PFA
BLNFA=3280              ! BLAINE VALUE OF FLY ASH
```

```
*VFILL,CD(14,1),DATA,BLNFA
FACS2H=0.0              ! WEIGHT PERCENTAGE OF SULFATE IN FLY ASH
*VFILL,CD(15,1),DATA,FACS2H
WFAMOL=0.0
*VFILL,CD(16,1),DATA,WFAMOL
PLS=0.0                 ! WEIGHT PERCENTAGE OF SUPERPLASTICIZER
*VFILL,CD(17,1),DATA,PLS
BLNLS=7000              ! BLAINE VALUE OF SUPERPLASTICIZER
*VFILL,CD(18,1),DATA,BLNLS
WP=48.0                 ! WATER TO POWDER RATIO BY WEIGHT
*VFILL,CD(19,1),DATA,WP
QSP=0.25                ! CONSTANT FOR THE EFFECT OF SUPERPLASTICIZER DOSSAGE
*VFILL,CD(20,1),DATA,QSP
QSPAD=0.06              ! CONSTANT FOR THE EFFECT OF SUPERPLASTICIZER DOSSAGE
*VFILL,CD(21,1),DATA,QSPAD
CHARSP=5.0              ! CONSTANT FOR THE EFFECT OF SUPERPLASTICIZER DOSSAGE
*VFILL,CD(22,1),DATA,CHARSP
QSGMX=110.0             ! FINAL ACCUMULATED HEAT GENERATION OF SLAG
(KCAL/KG)
*VFILL,CD(23,1),DATA,QSGMX
RSGW1=0.30              ! WEIGHT PERCENTAGE OF CONSUMED WATER OF SLAG
*VFILL,CD(24,1),DATA,RSGW1
RSGCA=0.22              ! WEIGHT PERCENTAGE OF CONSUMED CA(OH)2 WHEN
REACTION OF SLAG
*VFILL,CD(25,1),DATA,RSGCA
QFAMX=50.00             ! FINAL ACCUMULATED HEAT GENERATION OF FLY ASH
(KCAL/KG)
*VFILL,CD(26,1),DATA,QFAMX
RFAW1=0.10              ! WEIGHT PERCENTAGE OF CONSUMED WATER OF FLY ASH
*VFILL,CD(27,1),DATA,RFAW1
```

RFACA=1.00 ! WEIGHT PERCENTAGE OF CONSUMED CA(OH)2 WHEN REACTION OF FLY ASH

*VFILL,CD(28,1),DATA,RFACA

RH3AMN=0.67 ! MONOSULFATE CONVERSION FACTOR

*VFILL,CD(29,1),DATA,RH3AMN

RHAFMN=1.0 ! MONOSULFATE CONVERSION FACTOR

*VFILL,CD(30,1),DATA,RHAFMN

SLLDED=0.033 ! DEFALTED TIME DURATION AT INITIAL STAGE (DAY)

*VFILL,CD(31,1),DATA,SLLDED

ALPHA=1.00 ! MODEL CONSTANT FOR CLUSTER

*VFILL,CD(32,1),DATA,ALPHA

ITLEN=0.3

*VFILL,CD(34,1),DATA,ITLEN ! INITIAL TIME LENGTH

TSMIN=0.01

*VFILL,CD(35,1),DATA,TSMIN ! MIN TIME STEP SIZE

TSMAX=0.01

*VFILL,CD(36,1),DATA,TSMAX ! MAX TIME STEP SIZE

DICP=1.5

*VFILL,CD(64,1),DATA,DICP ! FACTOR TO REPRESENT SHAPE OF PARTICLES IN CEMENT PASTE (WATER + CEMENT POWDER)

DISD=3.0

*VFILL,CD(65,1),DATA,DICPAG ! FACTOR TO REPRESENT SHAPE OF PARTICLES IN CONCRETE (WATER + CEMENT POWDER + SAND + AGGREGATE)

!-------------------------------------START SETTING INITIAL TIME--

H=19 ! HOURS (24 HOUR CYCLE)

M=0 ! MINUTES

ITIME=(H+M/60)/24 ! STARTING TIME OF THE DAY (DAYS)

*VFILL,CD(37,1),DATA,ITIME

!---------------------------------------END SETTING INITIAL TIME--

!-------------------------------START SETTING INITIAL TEMPERATURE---------------------------------

ITEMP=25.8+273 ! GET INITIAL MIXING TEMPERATURE

```
*VFILL,CD(38,1),DATA,ITEMP     ! SET INITIAL MIXING TEMPERATURE
!--------------------------------END SETTING INITIAL TEMPERATURE-----------------------------------
QTOT=((CD(7,1)-
CD(6,1))*CD(1,1)/10**4)*(CD(2,1)*207+CD(3,1)*120+CD(4,1)*100+CD(5,1)*62)
! TOTAL AMOUNT OF HEAT INCLUDES IN OPC
*VFILL,CD(39,1),DATA,QTOT
!---------------------------------START INPUT CONCRETE MIX DATA--------------------------------
!-------------------------------------------CEMENT POWEDER-------------------------------------------
DENSC=3650            ! DENSITY OF CEMENT POWDER [kg/m3]
*VFILL,CD(41,1),DATA,DENSC
KC=2.5                ! THERMAL CONDUCTIVITY OF CEMENT POWDER [Kcal/day/m/K]
*VFILL,CD(53,1),DATA,KC
!-----------------------------------------------------WATER-----------------------------------------------
CW=1              ! SPECIFIC HEAT CAPACITY OF WATER [Kcal/kg/K]
*VFILL,CD(42,1),DATA,CW
DENSW=1000            ! DENSITY OF WATER [kg/m3]
*VFILL,CD(43,1),DATA,DENSW
!-----------------------------------------------------SAND------------------------------------------------
CS=0.24               ! SPECIFIC HEAT CAPACITY OF SAND [Kcal/kg/K]
*VFILL,CD(44,1),DATA,CS
DENSS=3170          ! DENSITY OF SAND [kg/m3]
*VFILL,CD(45,1),DATA,DENSS
WS=743              ! UNIT WEIGHT OF SAND IN CONCRETE (kg/m3)
*VFILL,CD(46,1),DATA,WS
KS=42.4             ! THERMAL CONDUCTIVITY OF SAND [Kcal/day/m/K]
*VFILL,CD(55,1),DATA,KS
!-----------------------------------------COURSE AGGREGATE-----------------------------------------
CG=0.24               ! SPECIFIC HEAT CAPACITY OF AGGREGATE [Kcal/kg/K]
*VFILL,CD(47,1),DATA,CG
DENSG=3010            ! DENSITY OF AGGREGATE [kg/m3]
```

```
*VFILL,CD(48,1),DATA,DENSS
WG=1026             ! UNIT WEIGHT OF AGGREGATE IN CONCRETE (kg/m3)
*VFILL,CD(49,1),DATA,WG
KG=41.6             ! THERMAL CONDUCTIVITY OF AGGREGATE [Kcal/day/m/K]
*VFILL,CD(56,1),DATA,KG
!-----------------------------------------------CEMENT HYDRATES-----------------------------------------------
DENSCP=1.23*1000/(CD(19,1)/100+0.32)    ! DENSITY OF CEMENT HYDRATES [kg/m3]
*VFILL,CD(51,1),DATA,DENSCP
WCP0=(1+CD(19,1)/100)*CD(1,1)     ! UNIT WEIGHT OF CEMENT HYDRATES [kg/m3]
*VFILL,CD(52,1),DATA,WCP0
KCP=54.8          ! THERMAL CONDUCTIVITY OF CEMENT HYDRATES [Kcal/day/m/K]
*VFILL,CD(57,1),DATA,KCP
VCP=CD(1,1)/CD(41,1)+(CD(19,1)/100)*CD(1,1)/CD(43,1)
*VFILL,CD(59,1),DATA,VCP       ! VOLUME OF CEMENT PASTE
!-------------------------------------END INPUT CONCRETE MIX DATA---------------------------------
!---------------------------------START INPUT THERMAL BOUNDARY DATA--------------------------
JDAY=322
*VFILL,CD(68,1),DATA,JDAY       ! JULIAN DAY OF THE DATE OF TESTING
LSM=15*5.5
*VFILL,CD(69,1),DATA,LSM      ! LOCAL STANDARD TIME MERIDIAN
WINDV=3.0
*VFILL,CD(70,1),DATA,WINDV      ! VELOCITY OF WIND [m/S]
NCLD=0.5
*VFILL,CD(71,1),DATA,NCLD      ! CLOUD COVER [10-1]
TDP=22+273
*VFILL,CD(72,1),DATA,TDP       ! DEW POINT [DEGREE CELCIUS]
BOUDT=1
*VFILL,CD(78,1),DATA,BOUDT      ! APPLY THERMAL BOUNDARY CONDITION FOR TOP SURFACE [1 FOR "YES", 0 FOR "NO"]
BOUDB=1
```

*VFILL,CD(79,1),DATA,BOUDB ! APPLY THERMAL BOUNDARY CONDITION FOR BOTTOM SURFACE [1 FOR "YES", 0 FOR "NO"]

BOUDX0=1

*VFILL,CD(80,1),DATA,BOUDX0 ! APPLY THERMAL BOUNDARY CONDITION FOR SURFACE AT X=0 [1 FOR "YES", 0 FOR "NO"]

BOUDXL=1

*VFILL,CD(81,1),DATA,BOUDXL ! APPLY THERMAL BOUNDARY CONDITION FOR SURFACE AT X=L [1 FOR "YES", 0 FOR "NO"]

BOUDZ0=1

*VFILL,CD(82,1),DATA,BOUDZ0 ! APPLY THERMAL BOUNDARY CONDITION FOR SURFACE AT Z=0 [1 FOR "YES", 0 FOR "NO"]

BOUDZW=1

*VFILL,CD(83,1),DATA,BOUDZW ! APPLY THERMAL BOUNDARY CONDITION FOR SURFACE AT Z=W [1 FOR "YES", 0 FOR "NO"]

RFT=1.72 ! ROUGHNESS MULTIPLIER FOR CONVECTION FROM TOP SURFACE [CONCRETE = 1.52, STEEL AND SMOOTH = 1]

*VFILL,CD(87,1),DATA,RFT

RFV=1.52 ! ROUGHNESS MULTIFPLIER FOR CONVECTION FROM VERTICAL SURFACES [CONCRETE = 1.52, STEEL AND SMOOTH = 1]

*VFILL,CD(88,1),DATA,RFV

EMSTY=0.96

*VFILL,CD(73,1),DATA,EMSTY ! EMISSIVITY OF SURFACE

GAMAFT=0.6

*VFILL,CD(75,1),DATA,GAMAFT ! SOLAR ABSORPTIVITY OF SURFACE

TSIFZL=0.05

*VFILL,CD(84,1),DATA,TSIFZL ! THICKNESS OF INTERFACIAL ZONE IN BETWEEN BOTTOM SURFACE AND SOIL

KSOIL=42

*VFILL,CD(85,1),DATA,KSOIL ! THERMAL CONDUCTIVITY OF SOIL [Kcal/day/m/K]

TSOIL=25+273

*VFILL,CD(86,1),DATA,TSOIL ! TEMPERATURE IN SOIL [K]

LATD=6.9270786

```
*VFILL,CD(89,1),DATA,LATD       ! LATITUDE OF TESTING LOCATION
LONT=79.861243
*VFILL,CD(90,1),DATA,LONT       ! LONGITUDE OF TESTING LOCATION
!-----------------------------END INPUT THERMAL BOUNDARY DATA-----------------------------------
/EOF
```

APPENDIX C : APDL Codes of Heat Conduction Analysis Program

```
/TITLE, TEMPERATURE VARIATION DUE TO HEAT OF HYDRATION
*USE,MODEL320.MAC
/CONFIG,NRES,1000
/SOLU                                   ! ENTER SOLUTION PROCESSOR
ANTYPE,4                                ! DEFINE ANALYSIS TYPE AS TRANSIENT
SOLCONTROL,ON           ! ACTIVATE OPTIMIZED NONLINEAR SOLU DEFAULTS
CNVTOL,TEMP,0,0.005,2,0.01
*USE,PARADEF320.MAC
DELTIM,CD(36,1),CD(35,1),CD(36,1),ON    ! SPECIFY TIME STEP SIZE PARAMETERS
NLS=390
*GET,ECOUNT,ELEM,0,COUNT                ! RETRIEVE MAXIMUM ELEMENT NO
*DIM,ND,ARRAY,169,ECOUNT,NLS    ! DEFINE 3D ARRAY ND() TO STORE PARAMETERS
*DIM,MI,ARRAY,ECOUNT,NLS                ! DEFINE 2D ARRAY MI() TO STORE
MATERIAL INDEX NUMBERS
*DIM,ET,ARRAY,8,ECOUNT                  ! DEFINE 2D ARRAY ET() TO STORE ELEMENT
NODE NO DATA
*DIM,TNOD,ARRAY,8,ECOUNT,NLS            ! DEFINE 3D ARRAY TNOD() TO STORE NODAL
TEMPERATURE AT EACH LOAD STEP
*DIM,TIME,ARRAY,NLS                     ! DEFINE 1D ARRAY TIME() TO STORE TIME
*DIM,KXYZ,ARRAY,3,NLS                   ! DEFINE 2D ARRAY KXYZ() TO STORE
CUMULATIVE K VALUES AND RELEVANT NUMBERS OF ELEMENTS
*DIM,ETCI,ARRAY,3,1                     ! DEFINE 2D ARRAY KXYZ() TO STORE
INITIAL AND FINAL K VALUES
*VGET,MI(1),ELEM,1,ATTR,MAT,,,0         ! GET ELEMENT MATERIAL INFORMATION
AND FILL ARRAY MI()
*GET,NCOUNT,NODE,0,COUNT
*DIM,NCSX,ARRAY,NCOUNT                  ! DEFINE 1D ARRAY NCSX() TO STORE X -
CORDINATES OF EACH NODE
```

```
*DIM,NCSY,ARRAY,NCOUNT                ! DEFINE 1D ARRAY NCSY() TO STORE Y - CORDINATES OF EACH NODE

*DIM,NCSZ,ARRAY,NCOUNT                ! DEFINE 1D ARRAY NCSZ() TO STORE Z - CORDINATES OF EACH NODE

*DIM,NODT,ARRAY,NCOUNT,NLS            ! DEFINE 2D ARRAY NODT() TO STORE TEMPERATURE OF EACH NODE AND EVERY TIME STEP

*DIM,TATS,ARRAY,24,NLS                ! DEFINE 2D ARRAY TATS() TO STORE AMBIENT AND AVERAGE SURFACE TEMPERATURE DATA

*VFILL,CD(67,1),DATA,NCOUNT           ! STORE NUMBER OF NODES INTO CD

*VGET,NCSX(1),NODE,1,LOC,X,,,0        ! STORE X COORDINATES OF EACH NODES TO ARRAY NCSX()

*VGET,NCSY(1),NODE,1,LOC,Y,,,0        ! STORE Y COORDINATES OF EACH NODES TO ARRAY NCSY()

*VGET,NCSZ(1),NODE,1,LOC,Z,,,0        ! STORE Z COORDINATES OF EACH NODES TO ARRAY NCSZ()

*DO,ELEMT,1,ECOUNT,1                  ! START TO FILL ARRAY ET() FOR ELEMENT AND ASSOCIATED NODE NOs DATA

*DO,ELN,1,8,1

*GET,ELND,ELEM,ELEMT,NODE,ELN

*VFILL,ET(ELN,ELEMT),DATA,ELND

*ENDDO

*ENDDO                                ! END TO FILL ARRAY ET() FOR ELEMENT AND ASSOCIATED NODE NOS DATA

VSEL,S,MAT,,1

NSLV,S,1

TREF,CD(38,1)

BFUNIF,TEMP,CD(38,1)                  ! SET INITIAL MIXING TEMPERATURE (K)

NSEL,ALL

ITIME=CD(37,1)

*IF,ITIME,LE,0,THEN

ITIME=0
```

```
*ELSE
ITIME=ITIME
*ENDIF
*DO,J,1,NLS,1
*DO,I,1,ECOUNT,1
*IF,MI(I),EQ,1,THEN
ITLEN=CD(34,1)
*IF,J,NE,1,THEN                                  ! START SYSTEM TIME COMPUTATION
TIME1=ND(134,I,J-1)
*IF,TIME1,LE,ITLEN,THEN
TSMIN=CD(35,1)
TSTEP=TSMIN
*VFILL,ND(140,I,J),DATA,TSTEP
SLL=TSTEP
*VFILL,ND(48,I,J),DATA,SLL
*ELSE
TSMAX=CD(36,1)
TSTEP=TSMAX
*VFILL,ND(140,I,J),DATA,TSTEP
SLL=TSTEP
*VFILL,ND(48,I,J),DATA,SLL
*ENDIF
TSTEP=ND(140,I,J)
TIME1=ND(134,I,J-1)
TIME1=TIME1+TSTEP
*VFILL,ND(134,I,J),DATA,TIME1
*IF,I,EQ,1,THEN
*VFILL,TIME(J),DATA,TIME1
```

```
*ENDIF

TIME,TIME1

!TIME0=ND(138,I,J-1)

!*VFILL,ND(138,I,J),DATA,TIME0

*ENDIF                                          ! END SYSTEM TIME COMPUTATION

*IF,J,EQ,1,THEN

*DO,K,1,8,1

IC,ET(K,I),TEMP,CD(38,1)                        ! SET INITIAL CONDITIONS

*ENDDO

*VFILL,ND(1,I,J),DATA,CD(38,1)

*VFILL,ND(141,I,J),DATA,CD(38,1)

*ELSE

*DO,K,1,8,1                                     ! START READING NODAL TEMP OF 8 NODES ASSOCIATED WITH ELEMENT I

*GET,NTEMP,NODE,ET(K,I),TEMP

*VFILL,TNOD(K,I),DATA,NTEMP

*ENDDO                                          ! END READING NODAL TEMP OF 8 NODES ASSOCIATED WITH ELEMENT I

AVTEMP=(TNOD(1,I)+TNOD(2,I)+TNOD(3,I)+TNOD(4,I)+TNOD(5,I)+TNOD(6,I)+TNOD(7,I)+TNOD(8,I))/8

*VFILL,ND(1,I,J),DATA,AVTEMP

*VFILL,ND(141,I,J),DATA,AVTEMP

! COMPUTE AVERAGE TEMPERATURE FOR ELEMENT I

*ENDIF

!-------------------------------------START HEAT OF HYDRATION COMPUTATION----------------------

*USE,H100.MAC                                   ! START HEAT EVALUATION

*USE,H200.MAC

*USE,H500.MAC

*USE,H600.MAC
```

```
*USE,H900.MAC
*USE,H1000.MAC
*USE,H1200.MAC
*USE,H1500.MAC
*USE,H2000.MAC
*USE,H2300.MAC
*USE,H2400.MAC
*USE,H2600.MAC
*USE,H3000.MAC
*USE,H3500.MAC
*USE,H3600.MAC
*USE,H4000.MAC
*USE,H4100.MAC
*USE,H4200.MAC
*USE,H4600.MAC
*USE,H4800.MAC                          ! END HEAT EVALUATION
*IF,J,NE,1,THEN                        ! START COMPUTATION OF ACUMULATED HEAT
FRCSET=ND(36,I,J-1)
FRCSMN=ND(37,I,J-1)
CAOH2=ND(34,I,J-1)
*ELSE
FRCSET=ND(36,I,J)
FRCSMN=ND(37,I,J)
CAOH2=ND(34,I,J)
*ENDIF
RQCSET=ND(59,I,J)
FRCSET=FRCSET-RQCSET
*IF,FRCSET,LE,0,THEN
```

```
FRCSET=0
*ELSE
FRCSET=FRCSET
*ENDIF
*VFILL,ND(36,I,J),DATA,FRCSET
RQCSMN=ND(91,I,J)
FRCSMN=FRCSMN-RQCSMN
*IF,FRCSMN,LE,0,THEN
FRCSMN=0
*ELSE
FRCSMN=FRCSMN
*ENDIF
*VFILL,ND(37,I,J),DATA,FRCSMN
DCAOH2=ND(129,I,J)
CAOH2=CAOH2+DCAOH2
*VFILL,ND(34,I,J),DATA,CAOH2
*IF,J,NE,1,THEN
QGETA=ND(51,I,J)
QAETA=ND(38,I,J-1)
QAETA=QAETA+QGETA
*VFILL,ND(38,I,J),DATA,QAETA
QGETF=ND(56,I,J)
QAETF=ND(39,I,J-1)
QAETF=QAETF+QGETF
*VFILL,ND(39,I,J),DATA,QAETF
QGMNA=ND(89,I,J)
QAMNA=ND(40,I,J-1)
QAMNA=QAMNA+QGMNA
```

```
*VFILL,ND(40,I,J),DATA,QAMNA
QGMNF=ND(90,I,J)
QAMNF=ND(41,I,J-1)
QAMNF=QAMNF+QGMNF
*VFILL,ND(41,I,J),DATA,QAMNF
QG3A=ND(79,I,J)
QA3A=ND(42,I,J-1)
QA3A=QA3A+QG3A
*VFILL,ND(42,I,J),DATA,QA3A
QGAF=ND(85,I,J)
QAAF=ND(44,I,J-1)
QAAF=QAAF+QGAF
*VFILL,ND(44,I,J),DATA,QAAF
QG3S=ND(95,I,J)
QA3S=ND(43,I,J-1)
QA3S=QA3S+QG3S
*VFILL,ND(43,I,J),DATA,QA3S
QG2S=ND(101,I,J)
QA2S=ND(45,I,J-1)
QA2S=QA2S+QG2S
*VFILL,ND(45,I,J),DATA,QA2S
QGSG=ND(115,I,J)
QASG=ND(46,I,J-1)
QASG=QASG+QGSG
*VFILL,ND(46,I,J),DATA,QASG
QGFA=ND(124,I,J)
QAFA=ND(47,I,J-1)
QAFA=QAFA+QGFA
```

```
*VFILL,ND(47,I,J),DATA,QAFA
*ELSE
QGETA=ND(51,I,J)
QAETA=ND(38,I,J)
QAETA=QAETA+QGETA
*VFILL,ND(38,I,J),DATA,QAETA
QGETF=ND(56,I,J)
QAETF=ND(39,I,J)
QAETF=QAETF+QGETF
*VFILL,ND(39,I,J),DATA,QAETF
QGMNA=ND(89,I,J)
QAMNA=ND(40,I,J)
QAMNA=QAMNA+QGMNA
*VFILL,ND(40,I,J),DATA,QAMNA
QGMNF=ND(90,I,J)
QAMNF=ND(41,I,J)
QAMNF=QAMNF+QGMNF
*VFILL,ND(41,I,J),DATA,QAMNF
QG3A=ND(79,I,J)
QA3A=ND(42,I,J)
QA3A=QA3A+QG3A
*VFILL,ND(42,I,J),DATA,QA3A
QGAF=ND(85,I,J)
QAAF=ND(44,I,J)
QAAF=QAAF+QGAF
*VFILL,ND(44,I,J),DATA,QAAF
QG3S=ND(95,I,J)
QA3S=ND(43,I,J)
```

```
QA3S=QA3S+QG3S
*VFILL,ND(43,I,J),DATA,QA3S
QG2S=ND(101,I,J)
QA2S=ND(45,I,J)
QA2S=QA2S+QG2S
*VFILL,ND(45,I,J),DATA,QA2S
QGSG=ND(115,I,J)
QASG=ND(46,I,J)
QASG=QASG+QGSG
*VFILL,ND(46,I,J),DATA,QASG
QGFA=ND(124,I,J)
QAFA=ND(47,I,J)
QAFA=QAFA+QGFA
*VFILL,ND(47,I,J),DATA,QAFA
*ENDIF                          ! END COMPUTATION OF ACCUMULATED HEAT
DHTETA=ND(53,I,J)               ! START COMPUTATION OF HEAT OF HYDRATION RATE
DHTETF=ND(58,I,J)
HTETRG=DHTETA+DHTETF
*VFILL,ND(130,I,J),DATA,HTETRG
DHT3A=ND(137,I,J)
DHT3S=ND(98,I,J)
DHTAF=ND(88,I,J)
DHT2S=ND(104,I,J)
RCSMN=ND(92,I,J)
HTCL=DHT3A*RCSMN+DHT3S+DHTAF*RCSMN+DHT2S
HT=HTETRG+HTCL+DHTSG+DHTFA
*VFILL,ND(131,I,J),DATA,HT
SLL=ND(48,I,J)
```

```
HT=ND(131,I,J)

QGEN=HT*SLL*24

*VFILL,ND(132,I,J),DATA,QGEN

WC=CD(1,1)

HT=ND(131,I,J)

QR=HT*WC*24

*VFILL,ND(133,I,J),DATA,QR

QR=ND(133,I,J)

QRELEM=QR                    ! END COMPUTATION OF HEAT OF HYDRATION RATE

BFE,I,HGEN,,QRELEM           ! APPLYING HEAT GENERATION RATE FOR CONCRETE ELEMENT

*IF,J,EQ,1,THEN              ! START COMPUTING DEGREE OF HYDRATION [DOH]

QTOT=ND(132,I,J)*CD(1,1)

*ELSE

QTOT=ND(143,I,J-1)+ND(132,I,J)*CD(1,1)

*ENDIF

*VFILL,ND(143,I,J),DATA,QTOT

DOH=ND(143,I,J)/CD(39,1)

*VFILL,ND(142,I,J),DATA,DOH          ! END COMPUTING DEGREE OF HYDRATION

!----------------------------END HEAT OF HYDRATION COMPUTATION--------------------------------

!--------------------------START COMPUTATION OF ETC OF CONCRETE-----------------------------

*USE,ETC.MAC

*IF,I,EQ,1,THEN

KXYZ1=ND(158,I,J)

*VFILL,KXYZ(1,J),DATA,KXYZ1

TAVG1=ND(141,I,J)

*VFILL,KXYZ(2,J),DATA,TAVG1
```

```
NUM=1
*VFILL,KXYZ(3,J),DATA,NUM
*ELSE
KXY1Z=KXYZ(1,J)+ND(158,I,J)
*VFILL,KXYZ(1,J),DATA,KXY1Z
TAVG1=TAVG1+ND(141,I,J)
*VFILL,KXYZ(2,J),DATA,TAVG1
NUM=KXYZ(3,J)+1
*VFILL,KXYZ(3,J),DATA,NUM
*ENDIF
!-----------------------------------END COMPUTATION OF ETC OF CONCRETE----------------------
*ELSEIF,MI(I),EQ,2,THEN
*USE,SETINI.MAC
*ELSEIF,MI(I),EQ,3,THEN
*USE,SETINI.MAC
*ELSEIF,MI(I),EQ,4,THEN
*USE,SETINI.MAC
*ELSEIF,MI(I),EQ,5,THEN
*USE,SETINI.MAC
*ENDIF
*ENDDO                                          ! END TIME COMPUTATION
!-------------------------START SETTING THERMAL PROPERTIES OF CONCRETE-------------------
!-------------------START COMPUTING SPECIFIC HEAT CAPACITY OF CONCRETE---------------
*IF,J,EQ,1,THEN
*USE,SHC.MAC
MPTEMP,1,293,383
MP,C,1,CD(74,1)
MP,DENS,1,CD(50,1)                              ! DENSITY OF CONCRETE [MAT 1] [kg/m3]
```

```
!-------------------END COMPUTING SPECIFIC HEAT CAPACITY OF CONCRETE------------------
ETC1=ND(158,1,J)*0.8
*VFILL,ETCI(1,1),DATA,ETC1
ETC2=ND(158,1,J)*1.5
*VFILL,ETCI(2,1),DATA,ETC2
TAVG=KXYZ(2,J)/KXYZ(3,J)
*VFILL,ETCI(3,1),DATA,0.7*TAVG
MPTEMP,1,TAVG*0.8,TAVG*1.5
MPDATA,KXX,1,1,ETC1,ETC2
MPDATA,KYY,1,1,ETC1,ETC2
MPDATA,KZZ,1,1,ETC1,ETC2
*ENDIF
!---------------------------------------START SETTING ETC OF CONCRETE---------------------------------
KAVG=KXYZ(1,J)/KXYZ(3,J)
TAVG=KXYZ(2,J)/KXYZ(3,J)
K1=ETCI(1,1)
K2=ETCI(2,1)
T1=TAVG-(KAVG-K1)*ETCI(3,1)/(K2-K1)
T2=TAVG+(K2-KAVG)*ETCI(3,1)/(K2-K1)
MPTEMP,1,T1,T2
!-------------------------END SETTING THERMAL PROPERTIES OF CONCRETE----------------------
!------------------------START SETTING THERMAL BOUNDARY CONDITIONS----------------------
*USE,BOUND.MAC
!-------------------------END SETTING THERMAL BOUNDARY CONDITIONS-----------------------
SOLVE
*ENDDO
*MWRITE,ND,ND,TXT,,KIJ
(50000F15.4)                    ! WRITING PARAMETER ND DATA TO A TEXT FILE ND
```

```
!
*MWRITE,TATS,TATS,TXT,,IJK
(50000F15.4)                    ! WRITING PARAMETER TATS DATA TO A TEXT FILE TATS
*MWRITE,TIME,TIME,TXT,,KIJ
(50000F15.4)
FINISH                          ! EXIT SOLUTION PROCESSOR
```

APPENDIX D : APDL Codes of Subroutine to Estimate Heat of Hydration

H100.MAC

```
!--------------------POWDER FINENESS FACTOR ON THE RATE OF HYDRATION------------------
BLN=CD(8,1)
RBLN=BLN/3380
*VFILL,ND(2,I,J),DATA,RBLN
RBLN3A=RBLN
*VFILL,ND(3,I,J),DATA,RBLN3A
RBLNAF=RBLN
*VFILL,ND(4,I,J),DATA,RBLNAF
RBLN3S=RBLN
*VFILL,ND(5,I,J),DATA,RBLN3S
RBLN2S=RBLN
*VFILL,ND(6,I,J),DATA,RBLN2S
BLNSG=CD(10,1)
RBLNSG=BLNSG/4330
*VFILL,ND(7,I,J),DATA,RBLNSG
BLNFA=CD(14,1)
RBLNFA=BLNFA/3280
*VFILL,ND(8,I,J),DATA,RBLNFA
BLNLS=CD(18,1)
RBLNLS=BLNLS/7000
*VFILL,ND(9,I,J),DATA,RBLNLS
QSGMX=CD(23,1)
RSGMX=QSGMX/110.0
*VFILL,ND(10,I,J),DATA,RSGMX
QFAMX=CD(26,1)
```

```
RFAMX=QFAMX/50.0
*VFILL,ND(11,I,J),DATA,RFAMX
*IF,J,NE,1,THEN
QA3S=ND(43,I,J-1)
QA2S=ND(45,I,J-1)
*ELSE
QA3S=ND(43,I,J)
QA2S=ND(45,I,J)
*ENDIF
QLV3S=(QA3S/120)*100
*VFILL,ND(12,I,J),DATA,QLV3S
QLV2S=(QA2S/62)*100
*VFILL,ND(13,I,J),DATA,QLV2S
P3A=CD(2,1)
P4AF=CD(4,1)
PPC=CD(7,1)
PSG=CD(9,1)
PFA=CD(13,1)
QSPDED=(0.080*P3A+0.020*P4AF)/100*PPC*RBLN+0.005*PSG*RBLNSG+0.025*PFA*RBLN
FA
QSP=CD(20,1)
QSPAD=CD(21,1)
CHARSP=CD(22,1)
!
ESP=QSP*CHARSP-QSPDED
*VFILL,ND(15,I,J),DATA,ESP
*IF,ESP,LT,0.0,THEN
ESP=0.0
```

```
*VFILL,ND(15,I,J),DATA,ESP
QSPDED=QSP*CHARSP
*ENDIF
ESP=ND(15,I,J)
ESP=ESP+QSPAD*CHARSP+0.020*PFA*RBLNFA
*IF,ESP,LT,0.0,THEN
ESP=0.0
*ENDIF
*VFILL,ND(14,I,J),DATA,QSPDED
*VFILL,ND(15,I,J),DATA,ESP
P2S=CD(5,1)
PLS=CD(17,1)
SUP=(0.020*P3S+0.010*P2S)/100*PPC*RBLN+0.005*PSG*RBLNSG+0.150*PLS*RBLNLS
*VFILL,ND(16,I,J),DATA,SUP
ESP=ND(15,I,J)
SUP=ND(16,I,J)
RSP=ESP/SUP
*VFILL,ND(17,I,J),DATA,RSP
P3S=CD(3,1)
RFL=1-EXP(-5000.0*((P3S+P2S)/100*PPC/100)**10.0)
*VFILL,ND(18,I,J),DATA,RFL
RCMAL=(1-(EXP(-0.48*(P3S/P2S)**1.4))*RFL)*(1.0+0.4*RFL)+0.1*RFL
*VFILL,ND(19,I,J),DATA,RCMAL
!
RCM3A=1.0
*VFILL,ND(20,I,J),DATA,RCM3A
RCMAF=1.0
*VFILL,ND(21,I,J),DATA,RCMAF
```

```
RCM3S=RCMAL
*VFILL,ND(22,I,J),DATA,RCM3S
RCM2S=RCMAL
*VFILL,ND(23,I,J),DATA,RCM2S
RCMSG=1.0
*VFILL,ND(24,I,J),DATA,RCMSG
RCMFA=1.0
*VFILL,ND(25,I,J),DATA,RCMFA
IDED=0
*VFILL,ND(26,I,J),DATA,IDED
IEFW=0
*VFILL,ND(27,I,J),DATA,IEFW
RBG3A=1.0
*VFILL,ND(28,I,J),DATA,RBG3A
RBGAF=1.0
*VFILL,ND(29,I,J),DATA,RBGAF
RBG3S=1.0
*VFILL,ND(30,I,J),DATA,RBG3S
RBG2S=1.0
*VFILL,ND(31,I,J),DATA,RBG2S
RBGSG=1.0
*VFILL,ND(32,I,J),DATA,RBGSG
RBGFA=1.0
*VFILL,ND(33,I,J),DATA,RBGFA
CAOH2=0.0
*VFILL,ND(34,I,J),DATA,CAOH2
*IF,J,NE,1,THEN
*RETURN,1
```

```
*ENDIF
PPCS2H=CD(6,1)
SGCS2H=CD(11,1)
FACS2H=CD(15,1)
CS2H=PPCS2H*PPC/100+SGCS2H*PSG/100+FACS2H*PFA/100
*VFILL,ND(35,I,J),DATA,CS2H
FRCSET=CS2H
*VFILL,ND(36,I,J),DATA,FRCSET
FRCSMN=CS2H
*VFILL,ND(37,I,J),DATA,FRCSMN
!-------------------INITIALIZATION OF HEAT GENERATION ACCUMULATOR----------------------
QAETA=0
*VFILL,ND(38,I,J),DATA,QAETA
QAETF=0
*VFILL,ND(39,I,J),DATA,QAETF
QAMNA=0
*VFILL,ND(40,I,J),DATA,QAMNA
QAMNF=0
*VFILL,ND(41,I,J),DATA,QAMNF
QA3A=0
*VFILL,ND(42,I,J),DATA,QA3A
QA3S=0
*VFILL,ND(43,I,J),DATA,QA3S
QAAF=0
*VFILL,ND(44,I,J),DATA,QAAF
QA2S=0
*VFILL,ND(45,I,J),DATA,QA2S
QASG=0
```

```
*VFILL,ND(46,I,J),DATA,QASG
QAFA=0
*VFILL,ND(47,I,J),DATA,QAFA
IDED=1
*VFILL,ND(26,I,J),DATA,IDED
SLLDED=CD(31,1)
SLL=SLLDED
*VFILL,ND(48,I,J),DATA,SLL
/EOF
```

H200.MAC

```
!-----------------------------------------------ETTRINGITE MODEL-----------------------------------------
!----------------------------------C3A ETTRIGITE (GYPSUM-2-HYDRATE)-------------------------------
BTMETA=293.0
ZETA=-6500
*IF,J,NE,1,THEN
QAETA=ND(38,I,J-1)
*ELSE
QAETA=ND(38,I,J)
*ENDIF
TEMETA=ND(1,I,J)
*IF,QAETA,LT,3.94,THEN
HSETA=((20.00-80.00)/(3.94-0.0))*(QAETA-0.0)+80.00
*ELSEIF,QAETA,LT,31.52,THEN
HSETA=((8.00-20.00)/(31.52-3.94))*(QAETA-3.94)+20.00
*ELSEIF,QAETA,LT,78.8,THEN
HSETA=((4.00-8.00)/(78.8-31.52))*(QAETA-31.52)+8.00
*ELSEIF,QAETA,LT,197.0,THEN
```

```
HSETA=((2.00-4.00)/(197.0-78.8))*(QAETA-78.8)+4.00
*ELSEIF,QAETA,LT,394.0,THEN
HSETA=((0.00-2.00)/(394.0-197.0))*(QAETA-197.0)+2.00
*ELSE
HSETA=0.0
*ENDIF
*IF,HSETA,LT,0.0,THEN
HSETA=0.0
*ENDIF
*VFILL,ND(49,I,J),DATA,HSETA
RBLN3A=ND(3,I,J)
HTETA=HSETA*RBLN3A*EXP(ZETA*(1.0/(TEMETA)-1.0/(BTMETA)))
*VFILL,ND(50,I,J),DATA,HTETA
SLL=ND(48,I,J)
QGETA=HTETA*SLL*24
*VFILL,ND(51,I,J),DATA,QGETA
QETAAD=QAETA+QGETA
*VFILL,ND(52,I,J),DATA,QETAAD
*IF,QGETA,LE,0.0,THEN
*RETURN,1
*ENDIF
*IF,QETAAD,GT,394.0,THEN
RRETA=(394.0-QAETA)/QGETA
*VFILL,ND(81,I,J),DATA,RRETA
HTETA=RRETA*HTETA
QGETA=RRETA*QGETA
*VFILL,ND(50,I,J),DATA,HTETA
*VFILL,ND(51,I,J),DATA,QGETA
```

```
*ENDIF
/EOF
-----------------------------------------------------------------------------------------------------------------------
H500.MAC
P3A=CD(2,1)
PPC=CD(7,1)
HTETA=ND(50,I,J)
DHTETA=HTETA*P3A/100*PPC/100
*VFILL,ND(53,I,J),DATA,DHTETA
!------------------------------C4AF ETTRINGITE(GYPSUM-2-HYDRATE)-------------------------------
BTMETF=293.0
ZETF=-4000
*IF,J,NE,1,THEN
QAETF=ND(39,I,J-1)
*ELSE
QAETF=ND(39,I,J)
*ENDIF
TEMETF=ND(1,I,J)
*IF,QAETF,LT,1.0,THEN
HSETF=((3.384-13.54)/(1.0-0.0))*(QAETF-0.0)+13.54
*ELSEIF,QAETF,LT,8.0,THEN
HSETF=((1.354-3.384)/(8.0-1.0))*(QAETF-1.0)+3.384
*ELSEIF,QAETF,LT,20.0,THEN
HSETF=((0.677-1.354)/(20.0-8.0))*(QAETF-8.0)+1.354
*ELSEIF,QAETF,LT,50.0,THEN
HSETF=((0.338-0.677)/(50.0-20.0))*(QAETF-20.0)+0.677
*ELSEIF,QAETF,LT,100.0,THEN
HSETF=((0.000-0.338)/(100.0-50.0))*(QAETF-50.0)+0.338
```

```
*ELSE
HSETF=0.0
*ENDIF
*IF,HSETF,LT,0.0,THEN
HSETF=0.0
*ENDIF
*VFILL,ND(54,I,J),DATA,HSETF
RBLNAF=ND(4,I,J)
HTETF=HSETF*RBLNAF*EXP(ZETF*(1.0/(TEMETF)-1.0/(BTMETF)))
*VFILL,ND(55,I,J),DATA,HTETF
SLL=ND(48,I,J)
QGETF=HTETF*SLL*24
*VFILL,ND(56,I,J),DATA,QGETF
QETFAD=QAETF+QGETF
*VFILL,ND(57,I,J),DATA,QETFAD
*IF,QGETF,LE,0.0,THEN
*RETURN,1
*ENDIF
*IF,QETFAD,GT,100.0,THEN
QGETF=ND(56,I,J)
RRETF=(100.0-QAETF)/QGETF
*VFILL,ND(82,I,J),DATA,RRETF
HTETF=RRETF*HTETF
QGETF=RRETF*QGETF
*VFILL,ND(55,I,J),DATA,HTETF
*VFILL,ND(56,I,J),DATA,QGETF
*ENDIF
/EOF
```

```
---------------------------------------------------------------------------------------------------------------------

H600.MAC

P4AF=CD(4,1)

PPC=CD(7,1)

HTETF=ND(55,I,J)

DHTETF=HTETF*P4AF/100*PPC/100

*VFILL,ND(58,I,J),DATA,DHTETF

!-------------------------------------------------TOTAL ETRINGITE-----------------------------------------------

QGETA=ND(51,I,J)

RQETA=QGETA/394.0*P3A*PPC/100/270.2*(172.182*3)

*VFILL,ND(118,I,J),DATA,RQETA

QGETF=ND(56,I,J)

RQETF=QGETF/100.0*P4AF*PPC/100/(485.92/2)*(172.182*3)

*VFILL,ND(135,I,J),DATA,RQETF

RQETA=ND(118,I,J)

RQETF=ND(135,I,J)

RQCSET=RQETA+RQETF

*VFILL,ND(59,I,J),DATA,RQCSET

RQCSET=ND(59,I,J)

*IF,RQCSET,LE,0,THEN

RCSET=0.0

*VFILL,ND(60,I,J),DATA,RCSET

*RETURN,1

*ENDIF

*IF,J,NE,1,THEN

FRCSET=ND(36,I,J-1)

*ELSE

FRCSET=ND(36,I,J)
```

```
*ENDIF
RQCSET=ND(59,I,J)
RCSET=FRCSET/RQCSET
*IF,RCSET,GE,1.0,THEN
RCSET=1.0
*ENDIF
*IF,RCSET,LE,0.0,THEN
RCSET=0.0
*ENDIF
*VFILL,ND(60,I,J),DATA,RCSET
/EOF
```

```
H900.MAC
QGETA=ND(51,I,J)
RCSET=ND(60,I,J)
QGETA=QGETA*RCSET
*VFILL,ND(51,I,J),DATA,QGETA
QGETF=ND(56,I,J)
QGETF=QGETF*RCSET
*VFILL,ND(56,I,J),DATA,QGETF
DHTETF=ND(58,I,J)
DHTETF=DHTETF*RCSET
*VFILL,ND(58,I,J),DATA,DHTETF
DHTETA=ND(53,I,J)
DHTETA=DHTETA*RCSET
*VFILL,ND(53,I,J),DATA,DHTETA
RQCSET=ND(59,I,J)
RQCSET=RQCSET*RCSET
```

```
*VFILL,ND(59,I,J),DATA,RQCSET
/EOF
```

H1100.MAC

```
!-----------------------------------------HYDRATION HEAT MODEL-----------------------------------
*IF,J,NE,1,THEN
QAMNA=ND(40,I,J-1)
QAMNF=ND(41,I,J-1)
QA3A=ND(42,I,J-1)
QAAF=ND(44,I,J-1)
QA3S=ND(43,I,J-1)
QA2S=ND(45,I,J-1)
QASG=ND(46,I,J-1)
QAFA=ND(47,I,J-1)
*ELSE
QAMNA=ND(40,I,J)
QAMNF=ND(41,I,J)
QA3A=ND(42,I,J)
QAAF=ND(44,I,J)
QA3S=ND(43,I,J)
QA2S=ND(45,I,J)
QASG=ND(46,I,J)
QAFA=ND(47,I,J)
*ENDIF
P3A=CD(2,1)
PPC=CD(7,1)
P4AF=CD(4,1)
P3S=CD(3,1)
```

```
P2S=CD(5,1)
QSGMX=CD(23,1)
RSGMX=ND(10,I,J)
PSG=CD(9,1)
RSGW1=CD(24,1)
QFAMX=CD(26,1)
RFAMX=ND(11,I,J)
PFA=CD(13,1)
RFAW1=CD(27,1)
SWMNA=QAMNA/207*P3A/100*PPC*(0.6668+0.15)
SWMNF=QAMNF/100*P4AF/100*PPC*(0.7414+0.15)
SW3A=(QA3A-QAMNA)/207*P3A/100*PPC*(0.4001+0.15)
SWAF=(QAAF-QAMNF)/100*P4AF/100*PPC*(0.3707+0.15)
SW3S=QA3S/120*P3S/100*PPC*(0.2367+0.15)
SW2S=QA2S/62*P2S/100*PPC*(0.2092+0.15)
SWSG=QASG/(QSGMX/RSGMX)*PSG*(RSGW1+0.15)
SWFA=QAFA/(QFAMX/RFAMX)*PFA*(RFAW1+0.15)
WP=CD(19,1)
FREEW=WP-SWMNA-SWMNF-SW3A-SWAF-SW3S-SW2S-SWSG-SWFA
*VFILL,ND(61,I,J),DATA,FREEW
PLS=CD(17,1)
FREEWO=FREEW/((PPC+PSG+PFA)/(PPC+PSG+PFA+PLS))
*VFILL,ND(62,I,J),DATA,FREEWO
!------COMPUTING THICKNESS OF CEMENT HYDRATE CLUSTER AROUND POWDERS-----
TEI3A=100-QA3A/207*100
*IF,TEI3A,LT,0,THEN
TEI3A=0
*ENDIF
```

```
TEIAF=100-QAAF/100*100
*IF,TEIAF,LT,0,THEN
TEIAF=0
*ENDIF
TEI3S=100-QA3S/120*100
*IF,TEI3S,LT,0,THEN
TEI3S=0
*ENDIF
TEI2S=100-QA2S/62*100
*IF,TEI2S,LT,0,THEN
TEI2S=0
*ENDIF
TEISG=100-QASG/(QSGMX/RSGMX)*100
*IF,TEISG,LT,0,THEN
TEISG=0
*ENDIF
TEIFA=100-QAFA/(QFAMX/RFAMX)*100
*IF,TEIFA,LT,0,THEN
TEIFA=0
*ENDIF
THCK3A=(100-(10000*TEI3A)**0.333333)
THCKAF=(100-(10000*TEIAF)**0.333333)
THCK3S=(100-(10000*TEI3S)**0.333333)
THCK2S=(100-(10000*TEI2S)**0.333333)
THCKSG=(100-(10000*TEISG)**0.333333)
THCKFA=(100-(10000*TEIFA)**0.333333)
*IF,THCK3A,LT,1.0,THEN
THCK3A=1.0
```

```
*ENDIF
*VFILL,ND(64,I,J),DATA,THCK3A
*IF,THCKAF,LT,1.0,THEN
THCKAF=1.0
*ENDIF
*VFILL,ND(65,I,J),DATA,THCKAF
*IF,THCK3S,LT,1.0,THEN
THCK3S=1.0
*ENDIF
*VFILL,ND(66,I,J),DATA,THCK3S
*IF,THCK2S,LT,1.0,THEN
THCK2S=1.0
*ENDIF
*VFILL,ND(67,I,J),DATA,THCK2S
*IF,THCKSG,LT,1.0,THEN
THCKSG=1.0
*ENDIF
*VFILL,ND(68,I,J),DATA,THCKSG
*IF,THCKFA,LT,1.0,THEN
THCKFA=1.0
*ENDIF
*VFILL,ND(69,I,J),DATA,THCKFA
/EOF
```

```
H1200.MAC
*IF,J,NE,1,THEN
IEFW=ND(27,I,J-1)
FREEWO=ND(62,I,J-1)
```

```
FREEWN=ND(128,I,J-1)
*ELSE
IEFW=ND(27,I,J)
FREEWO=ND(62,I,J)
FREEWN=ND(128,I,J)
*ENDIF
*IF,IEFW,EQ,0,THEN
FRW=FREEWO
*VFILL,ND(70,I,J),DATA,FRW
*ELSE
FRW=FREEWN
*VFILL,ND(70,I,J),DATA,FRW
*ENDIF
RBLN3A=ND(3,I,J)
RBLNAF=ND(4,I,J)
RBLN3S=ND(5,I,J)
RBLN2S=ND(6,I,J)
RBLNSG=ND(7,I,J)
RBLNFA=ND(8,I,J)
ALPHA=CD(32,1)
THCK3A=ND(64,I,J)
THCKAF=ND(65,I,J)
THCK3S=ND(66,I,J)
THCK2S=ND(67,I,J)
THCKSG=ND(68,I,J)
THCKFA=ND(69,I,J)
FRW=ND(70,I,J)
PI3A=FRW/(THCK3A**ALPHA)/RBLN3A**0.5
```

```
PIAF=FRW/(THCKAF**ALPHA)/RBLNAF**0.5
PI3S=FRW/(THCK3S**ALPHA)/RBLN3S**0.5
PI2S=FRW/(THCK2S**ALPHA)/RBLN2S**0.5
PISG=FRW/(THCKSG**ALPHA)/RBLNSG**0.5
PIFA=FRW/(THCKFA**ALPHA)/RBLNFA**0.5
FI3A=1-EXP(-5.0*PI3A**2.4)
*IF,PI3A,LT,0.0,THEN
FI3A=0.0
*ENDIF
*VFILL,ND(71,I,J),DATA,FI3A
FIAF=1-EXP(-5.0*PIAF**2.4)
*IF,PIAF,LT,0.0,THEN
FIAF=0.0
*ENDIF
*VFILL,ND(72,I,J),DATA,FIAF
FI3S=1-EXP(-5.0*PI3S**2.4)
*IF,PI3S,LT,0.0,THEN
FI3S=0.0
*ENDIF
*VFILL,ND(73,I,J),DATA,FI3S
FI2S=1-EXP(-5.0*PI2S**2.4)
*IF,PI2S,LT,0.0,THEN
FI2S=0.0
*ENDIF
*VFILL,ND(74,I,J),DATA,FI2S
FISG=1-EXP(-5.0*PISG**2.4)
*IF,PISG,LT,0.0,THEN
FISG=0.0
```

```
*ENDIF
*VFILL,ND(75,I,J),DATA,FISG
FIFA=1-EXP(-5.0*PIFA**2.4)
*IF,PIFA,LT,0.0,THEN
FIFA=0.0
*ENDIF
*VFILL,ND(76,I,J),DATA,FIFA
!----------C3A (MONOSULFATE & HYDRATION)----------
BTM3A=293.0
ZC3A=-6500
*IF,J,NE,1,THEN
QA3A=ND(42,I,J-1)
*ELSE
QA3A=ND(42,I,J)
*ENDIF
TEM3A=ND(1,I,J)
*IF,QA3A,LT,2.070,THEN
HS3A=1.3800
*ELSEIF,QA3A,LT,6.21,THEN
HS3A=((5.0000-1.3800)/(6.21-2.070))*(QA3A-2.070)+1.3800
*ELSEIF,QA3A,LT,16.56,THEN
HS3A=5.0000
*ELSEIF,QA3A,LT,41.40,THEN
HS3A=((3.105-5.0000)/(41.40-16.56))*(QA3A-16.56)+5.0000
*ELSEIF,QA3A,LT,103.5,THEN
HS3A=((1.656-3.105)/(103.5-41.40))*(QA3A-41.40)+3.105
*ELSEIF,QA3A,LT,207.0,THEN
HS3A=((0.0-1.656)/(207.0-103.5))*(QA3A-103.5)+1.656
```

```
*ELSE
HS3A=0.0
*ENDIF
*IF,HS3A,LT,0.0,THEN
HS3A=0.0
*ENDIF
RBLN3A=ND(3,I,J)
HT3A=HS3A*RBLN3A*EXP(ZC3A*(1.0/(TEM3A)-1.0/(BTM3A)))
*VFILL,ND(77,I,J),DATA,HT3A
RSP=ND(17,I,J)
*IF,QA3A,LT,2.07,THEN
RBG3A=EXP(-2.0*RSP)
*VFILL,ND(28,I,J),DATA,RBG3A
*ENDIF
*IF,J,NE,1,THEN
FRCSMN=ND(37,I,J-1)
*ELSE
FRCSMN=ND(37,I,J)
*ENDIF
*IF,FRCSMN,GT,0.0,THEN
RCM3A=1.0
*VFILL,ND(20,I,J),DATA,RCM3A
*ENDIF
RCM3A=ND(20,I,J)
*IF,RCM3A,GT,1.0,THEN
*RETURN,1
*ENDIF
FI3A=ND(71,I,J)
```

```
*IF,RCM3A,LT,FI3A,THEN
FI3A=1.0
*VFILL,ND(71,I,J),DATA,FI3A
*ELSE
RCM3A=1.0
*VFILL,ND(20,I,J),DATA,RCM3A
*ENDIF
/EOF
```

```
H1500.MAC
FI3A=ND(71,I,J)
RCM3A=ND(20,I,J)
RDCE3A=FI3A*RCM3A
*VFILL,ND(78,I,J),DATA,RDCE3A
HT3A=ND(77,I,J)
RBG3A=ND(28,I,J)
SLL=ND(48,I,J)
RCSET=ND(60,I,J)
RDCE3A=ND(78,I,J)
QG3A=HT3A*(1-RCSET)*RDCE3A*RBG3A*SLL*24
*VFILL,ND(79,I,J),DATA,QG3A
*IF,J,NE,1,THEN
QA3A=ND(42,I,J-1)
*ELSE
QA3A=ND(42,I,J)
*ENDIF
Q3AD=QA3A+QG3A
*VFILL,ND(80,I,J),DATA,Q3AD
```

```
*IF,QG3A,LE,0.0,THEN
*RETURN,1
*ENDIF
*IF,Q3AD,GT,207,THEN
HT3A=ND(77,I,J)
QG3A=ND(79,I,J)
RR3A=(207-QA3A)/QG3A
*VFILL,ND(136,I,J),DATA,RR3A
HT3A=RR3A*HT3A
*VFILL,ND(77,I,J),DATA,HT3A
QG3A=RR3A*QG3A
*VFILL,ND(79,I,J),DATA,QG3A
*ENDIF
/EOF
-----------------------------------------------------------------------------------------------------------------------
H2000.MAC
P3A=CD(2,1)
HT3A=ND(77,I,J)
RCSET=ND(60,I,J)
RDCE3A=ND(78,I,J)
RBG3A=ND(28,I,J)
PPC=CD(7,1)
DHT3A=P3A/100*(HT3A*(1-RCSET)*RDCE3A*RBG3A)*PPC/100
*VFILL,ND(137,I,J),DATA,DHT3A
!--------------------------------------C4AF (MONOSULFATE & HYDRATION)-----------------------------
BTMAF=293.0
ZC4AF=-4000
*IF,J,NE,1,THEN
```

```
QAAF=ND(44,I,J-1)
*ELSE
QAAF=ND(44,I,J)
*ENDIF
TEMAF=ND(1,I,J)
*IF,QAAF,LT,1.0,THEN
HSAF=((0.6667-0.6667)/(1.0-0.0))*(QAAF-0.0)+0.6667
*ELSEIF,QAAF,LT,3.0,THEN
HSAF=((1.610-0.6667)/(3.0-1.0))*(QAAF-1.0)+0.6667
*ELSEIF,QAAF,LT,8.0,THEN
HSAF=((1.610-1.610)/(8.0-3.0))*(QAAF-3.0)+1.610
*ELSEIF,QAAF,LT,20.0,THEN
HSAF=((1.0-1.610)/(20.0-8.0))*(QAAF-8.0)+1.610
*ELSEIF,QAAF,LT,50.0,THEN
HSAF=((0.533-1.0)/(50.0-20.0))*(QAAF-20.0)+1.0
*ELSEIF,QAAF,LT,100.0,THEN
HSAF=((0.0-0.533)/(100.0-50.0))*(QAAF-50.0)+0.533
*ELSE
HSAF=0.0
*ENDIF
*IF,HSAF,LT,0.0,THEN
HSAF=0.0
*ENDIF
RBLNAF=ND(4,I,J)
HTAF=HSAF*RBLNAF*EXP(ZC4AF*(1.0/(TEMAF)-1.0/(BTMAF)))
*VFILL,ND(83,I,J),DATA,HTAF
RSP=ND(17,I,J)
*IF,QAAF,LT,1.0,THEN
```

```
RBGAF=EXP(-2.0*RSP)
*VFILL,ND(29,I,J),DATA,RBGAF
*ENDIF
*IF,J,NE,1,THEN
FRCSMN=ND(37,I,J-1)
*ELSE
FRCSMN=ND(37,I,J)
*ENDIF
*IF,FRCSMN,GT,0.0,THEN
RCMAF=1.0
*VFILL,ND(21,I,J),DATA,RCMAF
*ENDIF
RCMAF=ND(21,I,J)
*IF,RCMAF,GT,1.0,THEN
*RETURN,1
*ENDIF
FIAF=ND(72,I,J)
*IF,RCMAF,LT,FIAF,THEN
FIAF=1.0
*VFILL,ND(72,I,J),DATA,FIAF
*ELSE
RCMAF=1.0
*VFILL,ND(21,I,J),DATA,RCMAF
*ENDIF
/EOF
```

H2300.MAC

```
FIAF=ND(72,I,J)
```

```
RCMAF=ND(21,I,J)
RDCEAF=FIAF*RCMAF
*VFILL,ND(84,I,J),DATA,RDCEAF
HTAF=ND(83,I,J)
RCSET=ND(60,I,J)
RDCEAF=ND(84,I,J)
RBGAF=ND(29,I,J)
SLL=ND(48,I,J)
QGAF=HTAF*(1-RCSET)*RDCEAF*RBGAF*SLL*24
*VFILL,ND(85,I,J),DATA,QGAF
*IF,J,NE,1,THEN
QAAF=ND(44,I,J-1)
*ELSE
QAAF=ND(44,I,J)
*ENDIF
QAFD=QAAF+QGAF
*VFILL,ND(86,I,J),DATA,QAFD
*IF,QGAF,LE,0.0,THEN
*RETURN,1
*ENDIF
*IF,QAFD,GT,100,THEN
HTAF=ND(83,I,J)
QGAF=ND(85,I,J)
RRAF=(100-QAAF)/QGAF
*VFILL,ND(87,I,J),DATA,RRAF
HTAF=RRAF*HTAF
*VFILL,ND(83,I,J),DATA,HTAF
QGAF=RRAF*QGAF
```

```
*VFILL,ND(85,I,J),DATA,QGAF
*ENDIF
/EOF
```

```
H2400.MAC
P4AF=CD(4,1)
HTAF=ND(83,I,J)
RCSET=ND(60,I,J)
RDCEAF=ND(84,I,J)
RBGAF=ND(29,I,J)
PPC=CD(7,1)
DHTAF=P4AF/100*(HTAF*(1-RCSET)*RDCEAF*RBGAF)*PPC/100
*VFILL,ND(88,I,J),DATA,DHTAF
!----------TOTAL MONOSUFATE & HYDRATION----------
QG3A=ND(79,I,J)
QGAF=ND(85,I,J)
RH3AMN=CD(29,1)
RHAFMN=CD(30,1)
QGMNA=QG3A/RH3AMN
QGMNF=QGAF/RHAFMN
*VFILL,ND(89,I,J),DATA,QGMNA
*VFILL,ND(90,I,J),DATA,QGMNF
P3A=CD(2,1)
RQMNA=QGMNA/207*P3A*PPC/100/270.2*172.182
RQMNF=QGMNF/100*P4AF*PPC/100/242.99*172.182
RQCSMN=RQMNA+RQMNF
*VFILL,ND(91,I,J),DATA,RQCSMN
*IF,RQCSMN,LE,0.0,THEN
```

```
RCSMN=0.0
*VFILL,ND(92,I,J),DATA,RCSMN
*RETURN,1
*ENDIF
*IF,J,NE,1,THEN
FRCSMN=ND(37,I,J-1)
*ELSE
FRCSMN=ND(37,I,J)
*ENDIF
RQCSMN=ND(91,I,J)
RCSMN=FRCSMN/RQCSMN
*VFILL,ND(92,I,J),DATA,RCSMN
*IF,RCSMN,GT,1.0,THEN
RCSMN=1.0
*VFILL,ND(92,I,J),DATA,RCSMN
*ENDIF
*IF,RCSMN,LT,0.0,THEN
RCSMN=0.0
*VFILL,ND(92,I,J),DATA,RCSMN
*ENDIF
/EOF
```

```
H2600.MAC
QGMNA=ND(89,I,J)
QGMNF=ND(90,I,J)
RCSMN=ND(92,I,J)
QG3A=ND(79,I,J)
RH3AMN=CD(29,1)
```

```
RHAFMN=CD(30,1)

QGAF=ND(85,I,J)

RQCSMN=ND(91,I,J)

QGMNA=QGMNA*RCSMN

*VFILL,ND(89,I,J),DATA,QGMNA

QGMNF=QGMNF*RCSMN

*VFILL,ND(90,I,J),DATA,QGMNF

QG3A=QG3A*(RCSMN/RH3AMN+(1-RCSMN))

*VFILL,ND(79,I,J),DATA,QG3A

QGAF=QGAF*(RCSMN/RHAFMN+(1-RCSMN))

*VFILL,ND(85,I,J),DATA,QGAF

RQCSMN=RQCSMN*RCSMN

*VFILL,ND(91,I,J),DATA,RQCSMN

/EOF

-----------------------------------------------------------------------------------------------------------------------

H3000.MAC

!--------------------------------------------------C3S-----------------------------------------------------------

BTM3S=293.0

TEM3S=ND(1,I,J)

*IF,J,NE,1,THEN

QA3S=ND(43,I,J-1)

*ELSE

QA3S=ND(43,I,J)

*ENDIF

*IF,QA3S,LT,1.2,THEN

HS3S=0.8

*ELSEIF,QA3S,LT,7.5,THEN

HS3S=((3.0-0.8)/(7.5-1.2))*(QA3S-1.2)+0.8
```

```
*ELSEIF,QA3S,LT,18.0,THEN
HS3S=3.0
*ELSEIF,QA3S,LT,30.0,THEN
HS3S=((1.5-3.0)/(30.0-18.0))*(QA3S-18.0)+3.0
*ELSEIF,QA3S,LT,60.0,THEN
HS3S=((0.8-1.5)/(60.0-30.0))*(QA3S-30.0)+1.5
*ELSEIF,QA3S,LT,120.0,THEN
HS3S=((0.0-0.8)/(120.0-60.00))*(QA3S-60.00)+0.8
*ELSE
HS3S=0.0
*ENDIF
*IF,HS3S,LT,0.0,THEN
HS3S=0.0
*ENDIF
*VFILL,ND(63,I,J),DATA,HS3S
*IF,QA3S,LT,1.2,THEN
ZC3S=-5000
*ELSEIF,QA3S,LT,7.5,THEN
ZC3S=((-6000+5000)/(7.5-1.2))*(QA3S-1.2)-5000
*ELSEIF,QA3S,LT,18.0,THEN
ZC3S=((-6000+6000)/(18.0-7.5))*(QA3S-7.5)-6000
*ELSEIF,QA3S,LT,30.0,THEN
ZC3S=((-5000+6000)/(30.0-18.0))*(QA3S-18.0)-6000
*ELSE
ZC3S=-5000
*ENDIF
QLV3S=ND(12,I,J)
*IF,QLV3S,LT,15.0,THEN
```

```
RBLN3S=1.0
*VFILL,ND(5,I,J),DATA,RBLN3S
*ELSEIF,QLV3S,LE,25.0,THEN
RBLN3S=((RBLN3S-1.0)/(25.0-15.0))*(QLV3S-15.0)+1.0
*VFILL,ND(5,I,J),DATA,RBLN3S
*ENDIF
RBLN3S=ND(5,I,J)
HS3S=ND(63,I,J)
HT3S=HS3S*RBLN3S*EXP(ZC3S*(1.0/(TEM3S)-1.0/(BTM3S)))
*VFILL,ND(93,I,J),DATA,HT3S
RSP=ND(17,I,J)
*IF,QA3S,LT,1.20,THEN
RBG3S=EXP(-2.0*RSP)
*VFILL,ND(30,I,J),DATA,RBG3S
*ENDIF
RCM3S=ND(22,I,J)
QLV3S=ND(12,I,J)
*IF,QLV3S,LT,15.0,THEN
RCM3S=1.0
*VFILL,ND(22,I,J),DATA,RCM3S
*ELSEIF,QLV3S,LT,25.0,THEN
RCM3S=((RCM3S-1.0)/(25.0-15.0))*(QLV3S-15.0)+1.0
*VFILL,ND(22,I,J),DATA,RCM3S
*ENDIF
*IF,RCM3S,GT,1.0,THEN
*RETURN,1
*ENDIF
FI3S=ND(73,I,J)
```

```
RCM3S=ND(22,I,J)
*IF,RCM3S,LT,FI3S,THEN
FI3S=1.0
*VFILL,ND(73,I,J),DATA,FI3S
*ELSE
RCM3S=1.0
*VFILL,ND(22,I,J),DATA,RCM3S
*ENDIF
/EOF
```

```
H3500.MAC
FI3S=ND(73,I,J)
RCM3S=ND(22,I,J)
RDCE3S=FI3S*RCM3S
*VFILL,ND(94,I,J),DATA,RDCE3S
HT3S=ND(93,I,J)
RDCE3S=ND(94,I,J)
RBG3S=ND(30,I,J)
SLL=ND(48,I,J)
QG3S=HT3S*RDCE3S*RBG3S*SLL*24
*VFILL,ND(95,I,J),DATA,QG3S
*IF,J,NE,1,THEN
QA3S=ND(43,I,J-1)
*ELSE
QA3S=ND(43,I,J)
*ENDIF
Q3SD=QA3S+QG3S
*VFILL,ND(96,I,J),DATA,Q3SD
```

```
*IF,QG3S,LE,0.0,THEN
*RETURN,1
*ENDIF
*IF,Q3SD,GT,120,THEN
RR3S=(120-QA3S)/QG3S
HT3S=RR3S*HT3S
QG3S=RR3S*QG3S
*VFILL,ND(97,I,J),DATA,RR3S
*VFILL,ND(93,I,J),DATA,HT3S
*VFILL,ND(95,I,J),DATA,QG3S
*ENDIF
/EOF
```

```
H3600.MAC
P3S=CD(3,1)
HT3S=ND(93,I,J)
RDCE3S=ND(94,I,J)
RBG3S=ND(30,I,J)
PPC=CD(7,1)
DHT3S=P3S/100*(HT3S*RDCE3S*RBG3S)*PPC/100
*VFILL,ND(98,I,J),DATA,DHT3S
!----------C2S----------
BTM2S=293.0
TEM2S=ND(1,I,J)
*IF,J,NE,1,THEN
QA2S=ND(45,I,J-1)
*ELSE
QA2S=ND(45,I,J)
```

```
*ENDIF
*IF,QA2S,LT,0.62,THEN
HS2S=((0.4133-0.4133)/(0.62-0.0))*(QA2S-0.0)+0.4133
*ELSEIF,QA2S,LT,4.65,THEN
HS2S=((0.861-0.4133)/(4.65-0.62))*(QA2S-0.62)+0.4133
*ELSEIF,QA2S,LT,11.2,THEN
HS2S=((0.861-0.861)/(11.2-4.65))*(QA2S-4.65)+0.861
*ELSEIF,QA2S,LT,18.6,THEN
HS2S=((0.3513-0.861)/(18.6-11.2))*(QA2S-11.2)+0.861
*ELSEIF,QA2S,LT,31.0,THEN
HS2S=((0.2067-0.3513)/(31.0-18.6))*(QA2S-18.6)+0.3513
*ELSEIF,QA2S,LT,62.0,THEN
HS2S=((0.0-0.2067)/(62.0-31.0))*(QA2S-31.0)+0.2067
*ELSE
HS2S=0.0
*ENDIF
*IF,HS2S,LT,0.0,THEN
HS2S=0.0
*ENDIF
*VFILL,ND(139,I,J),DATA,HS2S
*IF,QA2S,LT,0.62,THEN
ZC2S=((-2500+2500)/(0.62-0.0))*(QA2S-0.0)-2500
*ELSEIF,QA2S,LT,4.65,THEN
ZC2S=((-5000+2500)/(4.65-0.62))*(QA2S-0.62)-2500
*ELSEIF,QA2S,LT,11.2,THEN
ZC2S=((-5000+5000)/(11.2-4.65))*(QA2S-4.65)-5000
*ELSEIF,QA2S,LT,18.6,THEN
ZC2S=((-2500+5000)/(18.6-11.2))*(QA2S-11.2)-5000
```

```
*ELSE
ZC2S=-2500
*ENDIF
QLV2S=ND(13,I,J)
RBLN2S=ND(6,I,J)
*IF,QLV2S,LT,18.0,THEN
RBLN2S=1.0
*ELSEIF,QLV2S,LT,30.0,THEN
RBLN2S=((RBLN2S-1.0)/(30.0-18.0))*(QLV2S-18.0)+1.0
*ENDIF
*VFILL,ND(6,I,J),DATA,RBLN2S
RBLN2S=ND(6,I,J)
HT2S=HS2S*RBLN2S*EXP(ZC2S*(1.0/(TEM2S)-1.0/(BTM2S)))
*VFILL,ND(99,I,J),DATA,HT2S
RSP=ND(17,I,J)
*IF,QA2S,LT,0.62,THEN
RBG2S=EXP(-2.0*RSP)
*VFILL,ND(31,I,J),DATA,RBG2S
*ENDIF
!
RCM2S=ND(23,I,J)
*IF,QLV2S,LT,18.0,THEN
RCM2S=1.0
*ELSEIF,QLV2S,LT,30.0,THEN
RCM2S=((RCM2S-1.0)/(30.0-18.0))*(QLV2S-18.0)+1.0
*ENDIF
*VFILL,ND(23,I,J),DATA,RCM2S
*IF,RCM2S,GT,1.0,THEN
```

```
*RETURN,1
*ENDIF
FI2S=ND(74,I,J)
RCM2S=ND(23,I,J)
*IF,RCM2S,LT,FI2S,THEN
FI2S=1.0
*VFILL,ND(74,I,J),DATA,FI2S
*ELSE
RCM2S=1.0
*VFILL,ND(23,I,J),DATA,RCM2S
*ENDIF
/EOF
```

```
H4000.MAC
FI2S=ND(74,I,J)
RCM2S=ND(23,I,J)
RDCE2S=FI2S*RCM2S
*VFILL,ND(100,I,J),DATA,RDCE2S
HT2S=ND(99,I,J)
RDCE2S=ND(100,I,J)
RBG2S=ND(31,I,J)
SLL=ND(48,I,J)
QG2S=HT2S*RDCE2S*RBG2S*SLL*24
*VFILL,ND(101,I,J),DATA,QG2S
*IF,J,NE,1,THEN
QA2S=ND(45,I,J-1)
*ELSE
QA2S=ND(45,I,J)
```

```
*ENDIF
Q2SD=QA2S+QG2S
*VFILL,ND(102,I,J),DATA,Q2SD
*IF,QG2S,LE,0.0,THEN
*RETURN,1
*ENDIF
*IF,Q2SD,GT,62,THEN
RR2S=(62-QA2S)/QG2S
HT2S=RR2S*HT2S
QG2S=RR2S*QG2S
*VFILL,ND(103,I,J),DATA,RR2S
*VFILL,ND(99,I,J),DATA,HT2S
*VFILL,ND(101,I,J),DATA,QG2S
*ENDIF
/EOF
-------------------------------------------------------------------------------------------------------------------------
H4100.MAC
P2S=CD(5,1)
HT2S=ND(99,I,J)
RDCE2S=ND(100,I,J)
RBG2S=ND(31,I,J)
PPC=CD(7,1)
DHT2S=P2S/100*(HT2S*RDCE2S*RBG2S)*PPC/100
*VFILL,ND(104,I,J),DATA,DHT2S
!-----------------------------------------------SLAG-------------------------------------------------------
BTMSG=293.0
ZSG=-4500
TEMSG=ND(1,I,J)
```

```
*IF,J,NE,1,THEN
QASG=ND(46,I,J-1)
*ELSE
QASG=ND(46,I,J)
*ENDIF
*IF,QASG,LT,1.10,THEN
HSSG=((0.733-0.733)/(1.10-0.0))*(QASG-0.0)+0.733
*ELSEIF,QASG,LT,6.875,THEN
HSSG=((2.750-0.733)/(6.875-1.1))*(QASG-1.1)+0.733
*ELSEIF,QASG,LT,16.5,THEN
HSSG=((2.750-2.750)/(16.5-6.875))*(QASG-6.875)+2.750
*ELSEIF,QASG,LT,27.5,THEN
HSSG=((0.4125-2.75)/(27.5-16.5))*(QASG-16.5)+2.75
*ELSEIF,QASG,LT,55.0,THEN
HSSG=((0.220-0.4125)/(55.0-27.5))*(QASG-27.5)+0.4125
*ELSEIF,QASG,LT,110.0,THEN
HSSG=((0.0-0.220)/(110.0-55.0))*(QASG-55.0)+0.220
*ELSE
HSSG=0.0
*ENDIF
*IF,HSSG,LT,0.0,THEN
HSSG=0.0
*ENDIF
QSGMX=CD(23,1)
RSGMX=ND(10,I,J)
QLVSG=(QASG/(QSGMX/RSGMX))*100
*VFILL,ND(105,I,J),DATA,QLVSG
RBLNSG=ND(7,I,J)
```

```
QLVSG=ND(105,I,J)
*IF,QLVSG,LT,15.0,THEN
RBLNSG=1.0
*ELSEIF,QLVSG,LT,25.0,THEN
RBLNSG=((RBLNSG-1.0)/(25.0-15.0))*(QLVSG-15.0)+1.0
*ENDIF
*VFILL,ND(7,I,J),DATA,RBLNSG
HTSG=HSSG*RBLNSG*EXP(ZSG*(1.0/(TEMSG)-1.0/(BTMSG)))
*VFILL,ND(106,I,J),DATA,HTSG
RSP=ND(17,I,J)
*IF,QASG,LT,1.1,THEN
RBGSG=EXP(-2.0*RSP)
*VFILL,ND(32,I,J),DATA,RBGSG
*ENDIF
!-----------------------------------------------FLY ASH-----------------------------------------------------------
BTMFA=293.0
ZFA=-8000
TEMFA=ND(1,I,J)
*IF,J,NE,1,THEN
QAFA=ND(47,I,J-1)
*ELSE
QAFA=ND(47,I,J)
*ENDIF
*IF,QAFA,LT,0.50,THEN
HSFA=((0.005-0.005)/(0.50-0.0))*(QAFA-0.0)+0.005
*ELSEIF,QAFA,LT,2.50,THEN
HSFA=((0.0625-0.005)/(2.50-0.5))*(QAFA-0.5)+0.005
*ELSEIF,QAFA,LT,9.00,THEN
```

```
HSFA=((0.0625-0.0625)/(9.00-2.5))*(QAFA-2.5)+0.0625
*ELSEIF,QAFA,LT,15.0,THEN
HSFA=((0.04688-0.0625)/(15.0-9.00))*(QAFA-9.00)+0.0625
*ELSEIF,QAFA,LT,25.0,THEN
HSFA=((0.02188-0.04688)/(25.0-15.0))*(QAFA-15.0)+0.04688
*ELSEIF,QAFA,LT,42.50,THEN
HSFA=((0.00531-0.02188)/(42.5-25.0))*(QAFA-25.0)+0.02188
*ELSEIF,QAFA,LT,50.0,THEN
HSFA=((0.0-0.00531)/(ARG4-42.5))*(QAFA-42.5)+0.00531
*ELSE
HSFA=0.0
*ENDIF
*IF,HSFA,LT,0.0,THEN
HSFA=0.0
*ENDIF
RBLNFA=ND(8,I,J)
HTFA=HSFA*RBLNFA*EXP(ZFA*(1.0/(TEMFA)-1.0/(BTMFA)))
*VFILL,ND(107,I,J),DATA,HTFA
RSP=ND(17,I,J)
*IF,QAFA,LT,1.5,THEN
RBGFA=EXP(-0.0*RSP)
*VFILL,ND(33,I,J),DATA,RBGFA
*ENDIF
/EOF
-----------------------------------------------------------------------------------------------------------------------
H4200.MAC
!-----------------------------------------------SLAG & FLY ASH-----------------------------------------------
HTSG=ND(106,I,J)
```

```
RBGSG=ND(32,I,J)
QSGMX=CD(23,1)
RSGMX=ND(10,I,J)
PSG=CD(9,1)
RSGCA=CD(25,1)
HTFA=ND(107,I,J)
RBGFA=ND(33,I,J)
QFAMX=CD(26,1)
RFAMX=ND(11,I,J)
PFA=CD(13,1)
RFACA=CD(28,1)
SLL=ND(48,I,J)
RQCASG=((HTSG*RBGSG*SLL*24)/(QSGMX/RSGMX)*PSG)*RSGCA
*VFILL,ND(108,I,J),DATA,RQCASG
RQCAFA=((HTFA*RBGFA*SLL*24)/(QFAMX/RFAMX)*PFA)*RFACA
*VFILL,ND(109,I,J),DATA,RQCAFA
RQCAOH=RQCASG+RQCAFA
*VFILL,ND(110,I,J),DATA,RQCAOH
*IF,J,NE,1,THEN
CAOH2=ND(34,I,J-1)
*ELSE
CAOH2=ND(34,I,J)
*ENDIF
RQCAOH=ND(110,I,J)
*IF,RQCAOH,GT,0.0,THEN
RCOH=CAOH2/RQCAOH
*ELSE
RCOH=10.0
```

```
*ENDIF
*IF,RCOH,LT,0.0,THEN
RCOH=0.0
*ENDIF
*VFILL,ND(111,I,J),DATA,RCOH
!-----------------------------------------------------SLAG-----------------------------------------------------
RCOH=ND(111,I,J)
RSGCA=CD(25,1)
RCOHSG=RCOH
RSGCAV=RSGCA
*VFILL,ND(112,I,J),DATA,RSGCAV
RSGRED=1-EXP(-2.0*RCOHSG**5.0)
RQCASG=ND(108,I,J)
*IF,RQCASG,EQ,0.0,THEN
RSGRED=1.0
*ENDIF
*VFILL,ND(113,I,J),DATA,RSGRED
FISG=ND(75,I,J)
*IF,RSGRED,LT,FISG,THEN
RDSG=RSGRED
*ELSE
RDSG=FISG
*ENDIF
*VFILL,ND(114,I,J),DATA,RDSG
*IF,RDSG,LT,RBGSG,THEN
RBGSG=1.0
*VFILL,ND(32,I,J),DATA,RBGSG
*ELSE
```

```
RDSG=1.0
*VFILL,ND(114,I,J),DATA,RDSG
*ENDIF
QGSG=HTSG*RDSG*RBGSG*SLL*24
*VFILL,ND(115,I,J),DATA,QGSG
*IF,J,NE,1,THEN
QASG=ND(46,I,J-1)
*ELSE
QASG=ND(46,I,J)
*ENDIF
QSGD=QASG+QGSG
*VFILL,ND(116,I,J),DATA,QSGD
*IF,QGSG,LE,0.0,THEN
*RETURN,1
*ENDIF
*IF,QSGD,GT,QSGMX,THEN
RRSG=(QSGMX-QASG)/QGSG
HTSG=RRSG*HTSG
QGSG=RRSG*QGSG
*VFILL,ND(117,I,J),DATA,RRSG
*VFILL,ND(106,I,J),DATA,HTSG
*VFILL,ND(115,I,J),DATA,QGSG
*ENDIF
/EOF
```

```
H4600.MAC
HTSG=ND(106,I,J)
RSGMX=ND(10,I,J)
```

```
RDSG=ND(114,I,J)
RBGSG=ND(32,I,J)
PSG=CD(9,1)
DHTSG=(HTSG*RSGMX)*RDSG*RBGSG*PSG/100
*VFILL,ND(119,I,J),DATA,DHTSG
*IF,PSG,EQ,0.0,THEN
QGSG=0.0
*VFILL,ND(115,I,J),DATA,QGSG
*ENDIF
!-----------------------------------------------------FLY ASH-----------------------------------------------------
RCOH=ND(111,I,J)
RCOHFA=RCOH
*VFILL,ND(120,I,J),DATA,RCOHFA
RFACA=CD(28,1)
RFACAV=RFACA
*VFILL,ND(121,I,J),DATA,RFACAV
RFARED=1-EXP(-2.0*RCOHFA**5.0)
*VFILL,ND(122,I,J),DATA,RFARED
*IF,RQCAFA,EQ,0.0,THEN
RFARED=1.0
*VFILL,ND(122,I,J),DATA,RFARED
*ENDIF
FIFA=ND(76,I,J)
*IF,RFARED,LT,FIFA,THEN
RDFA=RFARED
*ELSE
RDFA=FIFA
*ENDIF
```

```
*VFILL,ND(123,I,J),DATA,RDFA
RBGFA=ND(33,I,J)
*IF,RDFA,LT,RBGFA,THEN
RBGFA=1.0
*VFILL,ND(33,I,J),DATA,RBGFA
*ELSE
RDFA=1.0
*VFILL,ND(123,I,J),DATA,RDFA
*ENDIF
SLL=ND(48,I,J)
HTFA=ND(107,I,J)
RDFA=ND(123,I,J)
RBGFA=ND(33,I,J)
QGFA=HTFA*RDFA*RBGFA*SLL*24
*VFILL,ND(124,I,J),DATA,QGFA
RFAMX=ND(11,I,J)
PFA=CD(13,1)
DHTFA=(HTFA*RFAMX)*RDFA*RBGFA*PFA/100
*VFILL,ND(125,I,J),DATA,DHTFA
*IF,PFA,EQ,0.0,THEN
QGFA=0.0
*VFILL,ND(124,I,J),DATA,QGFA
*ENDIF
!-----------------------------------------------EFFECTIVE WATER-----------------------------------------------
IEFW=ND(27,I,J)
*IF,IEFW,EQ,1.0,THEN
*RETURN,1
*ENDIF
```

```
RSGRED=ND(113,I,J)
FISG=ND(75,I,J)
*IF,RSGRED,GE,FISG,THEN
RSGEFW=1.0
*ELSEIF,FISG,GT,0.0,THEN
RSGEFW=RSGRED/FISG
*ELSE
RSGEFW=1.0
*ENDIF
*IF,RSGEFW,LT,0.0,THEN
RSGEFW=0.0
*ENDIF
*VFILL,ND(126,I,J),DATA,RSGEFW
RFARED=ND(122,I,J)
FIFA=ND(76,I,J)
*IF,RFARED,GE,FIFA,THEN
RFAEFW=1.0
*ELSEIF,FIFA,GT,0.0,THEN
RFAEFW=RFARED/FIFA
*ELSE
RFAEFW=1.0
*ENDIF
*IF,RFAEFW,LT,0.0,THEN
RFAEFW=0.0
*ENDIF
*VFILL,ND(127,I,J),DATA,RFAEFW
FREEW=ND(61,I,J)
PPC=CD(7,1)
```

```
RSGEFW=ND(126,I,J)

PSG=CD(9,1)

RFAEFW=ND(127,I,J)

PFA=CD(13,1)

PPC=CD(7,1)

PLS=CD(17,1)

FREEWN=FREEW/((PPC+RSGEFW*PSG+RFAEFW*PFA)/(PPC+PSG+PFA+PLS))

*VFILL,ND(128,I,J),DATA,FREEWN

IEFW=1

*VFILL,ND(27,I,J),DATA,IEFW

*USE,H1200.MAC

*USE,H1500.MAC

*USE,H2000.MAC

*USE,H2300.MAC

*USE,H2400.MAC

*USE,H2600.MAC

*USE,H3000.MAC

*USE,H3500.MAC

*USE,H3600.MAC

*USE,H4000.MAC

*USE,H4100.MAC

*USE,H4200.MAC

*USE,H4600.MAC

/EOF
```

```
H4800.MAC

!-----------------------CALCULATION OF CALCIUM HYDRO-OXIDE LEFT----------------------

QG3S=ND(95,I,J)
```

```
P3S=CD(3,1)

PPC=CD(7,1)

QG2S=ND(101,I,J)

P2S=CD(5,1)

QGAF=ND(85,I,J)

RCSMN=ND(92,I,J)

P4AF=CD(4,1)

QGSG=ND(115,I,J)

QSGMX=CD(23,1)

RSGMX=ND(10,I,J)

PSG=CD(9,1)

RSGCAV=ND(112,I,J)

QGFA=ND(124,I,J)

QFAMX=CD(26,1)

RFAMX=ND(11,I,J)

PFA=CD(13,1)

RFACAV=ND(121,I,J)

DCA3S=QG3S/120*P3S/100*PPC*0.4868

DCA2S=QG2S/62*P2S/100*PPC*0.2151

DCAAF=QGAF*(1-RCSMN)/100*P4AF/100*PPC*0.3049

DCASG=QGSG/(QSGMX/RSGMX)*PSG*RSGCAV

DCAFA=QGFA/(QFAMX/RFAMX)*PFA*RFACAV

DCAOH2=DCA3S+DCA2S-DCAAF-DCASG-DCAFA

*VFILL,ND(129,I,J),DATA,DCAOH2

!----------TOTAL HEAT GENERATION----------

IDED=ND(26,I,J)

*IF,IDED,NE,1.0,THEN

*RETURN,1
```

```
*ENDIF
QGETA=ND(51,I,J)
QAETA=QGETA
*VFILL,ND(38,I,J),DATA,QAETA
QGETF=ND(56,I,J)
QAETF=QGETF
*VFILL,ND(39,I,J),DATA,QAETF
QGMNA=ND(89,I,J)
QAMNA=QGMNA
*VFILL,ND(40,I,J),DATA,QAMNA
QGMNF=ND(90,I,J)
QAMNF=QGMNF
*VFILL,ND(41,I,J),DATA,QAMNF
QG3A=ND(79,I,J)
QA3A=QG3A
*VFILL,ND(42,I,J),DATA,QA3A
QGAF=ND(85,I,J)
QAAF=QGAF
*VFILL,ND(44,I,J),DATA,QAAF
QG3S=ND(95,I,J)
QA3S=QG3S
*VFILL,ND(43,I,J),DATA,QA3S
QG2S=ND(101,I,J)
QA2S=QG2S
*VFILL,ND(45,I,J),DATA,QA2S
QGSG=ND(115,I,J)
QASG=QGSG
*VFILL,ND(46,I,J),DATA,QASG
```

```
QGFA=ND(124,I,J)
QAFA=QGFA
*VFILL,ND(47,I,J),DATA,QAFA
IDED=0
*VFILL,ND(26,I,J),DATA,IDED
TSTEP=CD(35,1)
*VFILL,ND(140,I,J),DATA,TSTEP
SLLDED=CD(31,1)
SLL=TSTEP
*VFILL,ND(48,I,J),DATA,SLL
ITIME=CD(37,1)
TIME1=ITIME
*VFILL,ND(134,I,J),DATA,TIME1
*VFILL,TIME(J),DATA,TIME1
TIME,TIME1
FRCSET=ND(36,I,J)
RQCSET=ND(59,I,J)
FRCSET=FRCSET-RQCSET
*VFILL,ND(36,I,J),DATA,FRCSET
FRCSMN=ND(37,I,J)
RQCSMN=ND(91,I,J)
FRCSMN=FRCSMN-RQCSMN
*VFILL,ND(37,I,J),DATA,FRCSMN
*USE,H200.MAC
*USE,H500.MAC
*USE,H600.MAC
*USE,H900.MAC
*USE,H1000.MAC
```

*USE,H1200.MAC

*USE,H1500.MAC

*USE,H2000.MAC

*USE,H2300.MAC

*USE,H2400.MAC

*USE,H2600.MAC

*USE,H3000.MAC

*USE,H3500.MAC

*USE,H3600.MAC

*USE,H4000.MAC

*USE,H4100.MAC

*USE,H4200.MAC

*USE,H4600.MAC

*USE,H4800.MAC

/EOF

APPENDIX E : APDL Codes of Subroutine to Set Specific Heat Capacity of Concrete

```
MFC3A=CD(2,1)/CD(7,1)
MFC3S=CD(3,1)/CD(7,1)
MFC2S=CD(5,1)/CD(7,1)
MFC4AF=CD(4,1)/CD(7,1)
MFCS2H=CD(6,1)/CD(7,1)
CC1=MFC3A*0.1837+MFC3S*0.1857+MFC2S*0.1870
CC2=MFC4AF*0.1733+MFCS2H*0.7522
CC=CC1+CC2              ! SPECIFIC HEAT CAPACITY OF CEMENT POWDER
MC=CD(1,1)
MW=CD(1,1)*CD(19,1)/100
MS=CD(46,1)
MA=CD(49,1)
MTOT=MC+MW+MS+MA
*VFILL,CD(50,1),DATA,MTOT
MFC=MC/MTOT
MFW=MW/MTOT
MFS=MS/MTOT
MFA=MA/MTOT
C=MFC*CC+MFW*CD(42,1)+MFS*CD(44,1)+MFA*CD(47,1)
*VFILL,CD(74,1),DATA,C
```

APPENDIX F : APDL Codes of Subroutine to Set Thermal Conductivity of Concrete

```
!----------------------------START COMPUTATION OF ETC OF CEMENT PASTE----------------------
DOH=ND(142,I,J)
TAVG=ND(141,I,J)
CAVG=TAVG-273
PSV1=0.7073034146-2.703615165*10**(-2)*CAVG
PSV2=4.36088211*10**(-3)*CAVG**2
PSV3=-4.662575642*10**(-5)*CAVG**3
PSV4=1.034693708*10**(-6)*CAVG**4
PSV=PSV1+PSV2+PSV3+PSV4
PS0=101.325              ! ATMOSPHERIC PRESSURE IN KPa
RH=0.95                  ! RELATIVE HUMIDITY IN PORES
XV=RH*PSV/PS0
KW1=-5.82187*10**(-1)+6.3613*10**(-3)*TAVG     ! THERMAL CONDUCTIVITY OF WATER
KW2=-7.9715*10**(-6)*TAVG**2
KW=(KW1+KW2)*86400/4185.8
*VFILL,ND(151,I,J),DATA,KW
KA1=-2.276501*10**(-3)+1.2598485*10**(-4)*TAVG    ! THERMAL CONDUCTIVITY OF AIR
KA2=-1.4815235*10**(-7)*TAVG**2
KA3=1.73550646*10**(-10)*TAVG**3
KA4=-1.066657*10**(-13)*TAVG**4
KA5=2.47663035*10**(-17)*TAVG**5
KA=(KA1+KA2+KA3+KA4+KA5)*86400/4185.8
*VFILL,ND(153,I,J),DATA,KA
KV1=1.48436432*10**(-2)-3.52786713*10**(-5)*TAVG! THERMAL CONDUCTIVITY OF VAPOR
KV2=1.663336663*10**(-7)*TAVG**2
```

```
KV=(KV1+KV2)*86400/4185.8
*VFILL,ND(152,I,J),DATA,KV
KG=(KA+XV*(0.8536*KV-KA))/(1-0.1464*XV)
! THERMAL CONUDCITIVITY OF HUMID AIR
*VFILL,ND(154,I,J),DATA,KG
KS=CD(57,1)              ! THERMAL CONDUCTIVITY OF SOLID CEMENT PASTE
WP=CD(19,1)/100
PIEP=0.0575*DOH/(WP+0.32)
*VFILL,ND(149,I,J),DATA,PIEP
PITP=(WP-0.17*DOH)/(WP+0.32)
*VFILL,ND(144,I,J),DATA,PITP
VFW=CD(1,1)*ND(61,I,J)/(CD(43,1)*100)
PIFW=VFW/CD(59,1)
*VFILL,ND(150,I,J),DATA,PIFW
PICP=1-(PIEP+PIFW)
*VFILL,ND(147,I,J),DATA,PICP
K1=KW
K2=KG
K3=KS
V1=PIFW
V2=PIEP
V3=PICP
DIW=CD(64,1)+0.5*DOH**10*(3.0/(1-WP**2.7))**2.7
DIG=DIW
ETCPU1=K1*V1+K2*V2*DIG*K1/((DIG-1)*K1+K2)
ETCPU2=K3*V3*DIW*K1/((DIW-1)*K1+K3)
ETCPL1=V1+V2*DIG*K1/((DIG-1)*K1+K2)
ETCPL2=V3*DIW*K1/((DIW-1)*K1+K3)
```

```
ETCP=(ETCPU1+ETCPU2)/(ETCPL1+ETCPL2)
*VFILL,ND(148,I,J),DATA,ETCP         ! THERMAL CONDUCTIVITY OF CEMENT PASTE
!------------------------------END COMPUTATION OF ETC OF CEMENT PASTE-------------------------
!-------------------START COMPUTATION OF ETC OF CEMENT PASTE AND SAND---------------
VCP=CD(59,1)
*VFILL,ND(156,I,J),DATA,VCP
VSD=CD(46,1)/CD(45,1)
*VFILL,ND(157,I,J),DATA,VSD
V1=VCP/(VCP+VSD)
V2=VSD/(VCP+VSD)
K1=ETCP
K2=CD(55,1)
ETCPSD1=(3*V1-1)*K2+(3*V1-1)*K1
ETCPSD2=((3*V2-1)*K2+(3*V1-1)*K1)**2+8*K1*K2
ETCPSD=0.25*(ETCPSD1+ETCPSD2**(0.5))
*VFILL,ND(155,I,J),DATA,ETCPSD         ! THERMAL CONDUCTIVITY OF CEMENT PASTE
AND SAND
!----------------------END COMPUTATION OF ETC OF CEMENT PASTE AND SAND----------------
VAG=CD(49,1)/CD(48,1)
*VFILL,ND(159,I,J),DATA,VAG
V1=(VCP+VSD)/(VCP+VSD+VAG)
V2=VAG/(VCP+VSD+VAG)
K1=ETCPSD
K2=CD(56,1)*(5.9315*WP**2-3.0328*WP+1.41)
ETC1=(3*V1-1)*K2+(3*V1-1)*K1
ETC2=((3*V2-1)*K2+(3*V1-1)*K1)**2+8*K1*K2
ETC=0.25*(ETC1+ETC2**(0.5))
*VFILL,ND(158,I,J),DATA,ETC
```

!----------END EVALUATION OF THERMAL CONDUCTIVITY----------

APPENDIX G : APDL Codes of Subroutine to Set Ambient Temperature

```
TST=TIME(J)          ! TIME AT LOAD STEP
A0=-11.26924
A1=253.55898
A2=-570.22416
A3=604.58038
A4=-314.71029
A5=64.84901
TX=MOD(ABS(TST),1)
*IF,TX,LT,0.25,THEN
TX=1.0+TX
*ENDIF
TA1=A0+A1*TX+A2*TX**2+A3*TX**3          ! COMPUTE AMBIENT TEMPERATURE
TA2=A4*TX**4+A5*TX**5
TA=TA1+TA2+273
*VFILL,TATS(1,J),DATA,TA
```

APPENDIX H : APDL Codes of Program to Investigate Thermal Conductivity of Concrete

```
/TITLE, TEMPERATURE VARIATION DUE TO HEAT OF HYDRATION
*USE,CUBE.MAC
/CONFIG,NRES,1000
/SOLU                    ! ENTER SOLUTION PROCESSOR
ANTYPE,TRANS             ! DEFINE ANALYSIS TYPE AS TRANSIENT
SOLCONTROL,ON            ! ACTIVATE OPTIMIZED NONLINEAR SOLU DEFAULTS
CNVTOL,TEMP,0,0.005,2,0.01
!-----------------------------------------------START DATA INPUT-----------------------------------------------
TSTPS=30/(3600*24)       ! DURATION OF A TIME STEP
ITEMP=30.0+273           ! INITIAL TEMPERATURE (K)
OTEMP=40.0+273           ! OUTSIDE TEMPERATURE (K)
NLS=200                  ! NUMBER OF TIME STEPS
ETCCT=52.697             ! THERMAL CONDUCTIVITY CONCRETE (kcal/day/m/K)
CCT=0.32                 ! ASSUMED SPECIFIC HEAT CAPACITY OF CONCRETE (kcal/kg/K)
ETCST=1114.626           ! THERMAL CONDUCTIVITY OF STEEL MOULD (kcal/day/m/K)
CST=0.111                ! SPECIFIC HEAT CAPACITY OF STEEL MOULD (kcal/kg/K)
!-----------------------------------------------END DATE INPUT-------------------------------------------------
DELTIM,TSTPS,TSTPS,TSTPS,ON
NSEL,ALL
IC,ALL,TEMP,ITEMP   ! SET INITIAL MIXING TEMPERATURE
NSEL,ALL
ASEL,S,LOC,X,0
DA,ALL,TEMP,OTEMP           ! SET BOUNDARY TEMPERATURE
ASEL,ALL
ASEL,S,LOC,Y,0
```

```
DA,ALL,TEMP,OTEMP          ! SET BOUNDARY TEMPERATURE
ASEL,ALL
ASEL,S,LOC,Z,0
DA,ALL,TEMP,OTEMP          ! SET BOUNDARY TEMPERATURE
ASEL,ALL
ASEL,S,LOC,X,2*T+L
DA,ALL,TEMP,OTEMP          ! SET BOUNDARY TEMPERATURE
ASEL,ALL
ASEL,S,LOC,Y,T+H
DA,ALL,TEMP,OTEMP          ! SET BOUNDARY TEMPERATURE
ASEL,ALL
ASEL,S,LOC,Z,2*T+W
DA,ALL,TEMP,OTEMP          ! SET BOUNDARY TEMPERATURE
ASEL,ALL
*GET,NCOUNT,NODE,0,COUNT       ! RETRIEVE MAXIMUM NODE NUMBER
*DIM,NDT,ARRAY,2,NCOUNT,NLS    ! DEFINE 3D ARRAY ND() TO STORE PARAMETERS
MP,C,1,CCT             ! DEFINE SPECIFIC HEAT CAPACITY OF CONCRETE
MP,KXX,1,ETCCT         ! DEFINE THERMAL CONDUCTIVITY OF CONCRETE IN X DIRECTION
MP,KYY,1,ETCCT         ! DEFINE THERMAL CONDUCTIVITY OF CONCRETE IN Y DIRECTION
MP,KZZ,1,ETCCT         ! DEFINE THERMAL CONDUCTIVITY OF CONCRETE IN Z DIRECTION
MP,C,2,CST             ! DEFINE SPECIFIC HEAT CAPACITY OF STEEL
MP,KXX,2,ETCST         ! DEFINE THERMAL CONDUCTIVITY OF STEEL IN X DIRECTION
MP,KYY,2,ETCST         ! DEFINE THERMAL CONDUCTIVITY OF STEEL IN Y DIRECTION
MP,KZZ,2,ETCST         ! DEFINE THERMAL CONDUCTIVITY OF STEEL IN Z DIRECTION
*DO,J,1,NLS,1
```

```
*DO,I,1,NCOUNT,1
*IF,J,NE,1,THEN
TIME1=TSTPS*(J-1)
TIME1=TIME1+TSTPS
*ELSE
TIME1=TSTPS*J
*ENDIF
*VFILL,NDT(1,I,J),DATA,TIME1
*GET,NTEMP,NODE,I,TEMP          ! READING NODAL TEMPERATURE OF NODE I
*VFILL,NDT(2,I,J),DATA,NTEMP
*ENDDO
TIME,TIME1
SOLVE
*ENDDO
*MWRITE,NDT,NDT,TXT,,KIJ
(50000F15.4)
FINISH              ! EXIT SOLUTION PROCESSOR
```

APPENDIX I : Outputs of Thermal Conductivity Model

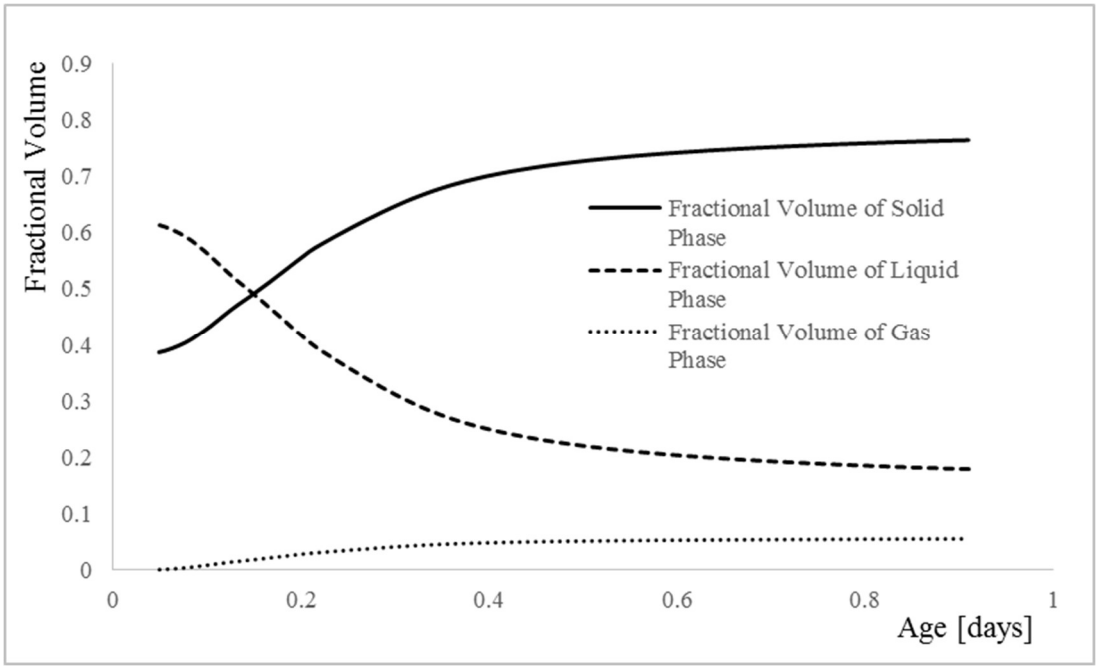

Figure I-1: Variation of Fractional Volumes of each components in Cement Paste for mix M-1 during initial stages

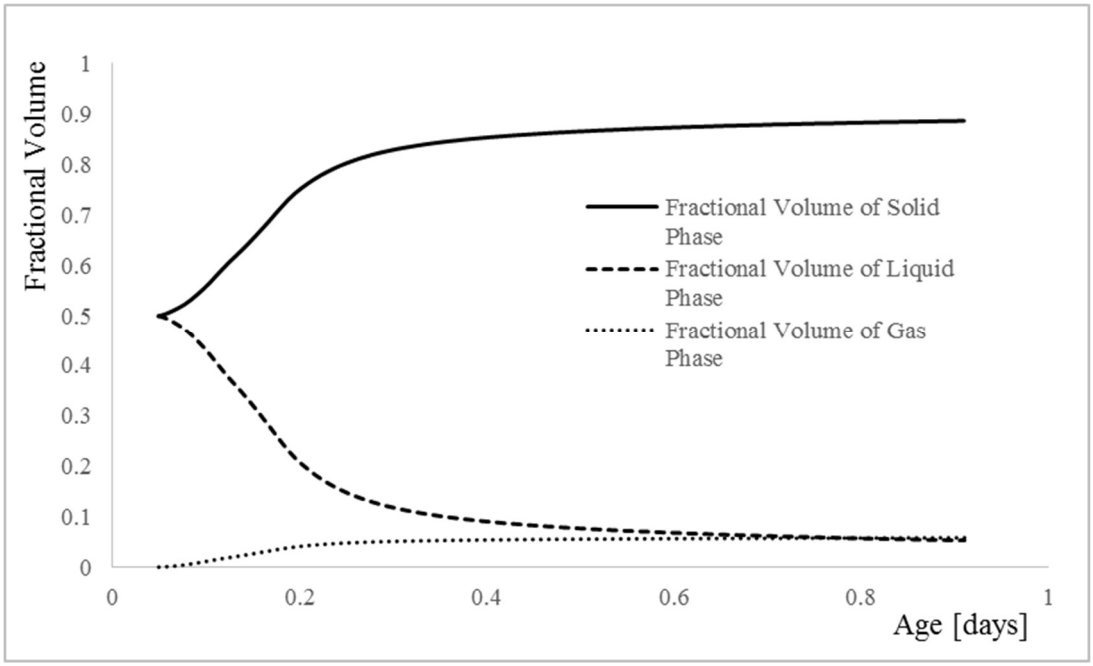

Figure I-2: Variation of Fractional Volumes of each components in Cement Paste for mix M-3 during initial stages

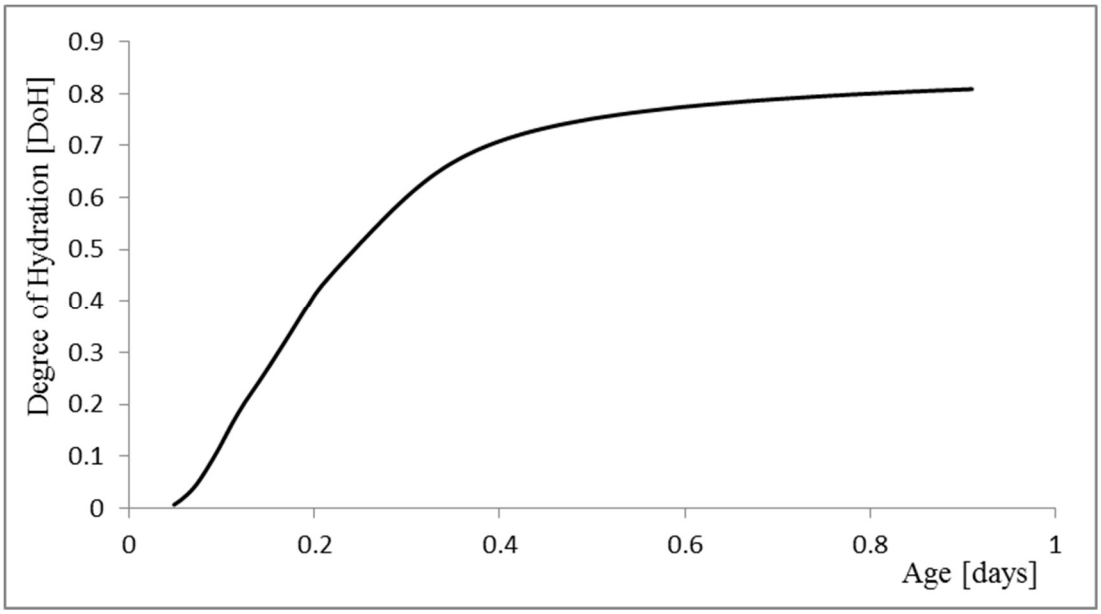

Figure I-3: Variation of Degrees of Hydration [DoH] for mix M-1 during initial stages

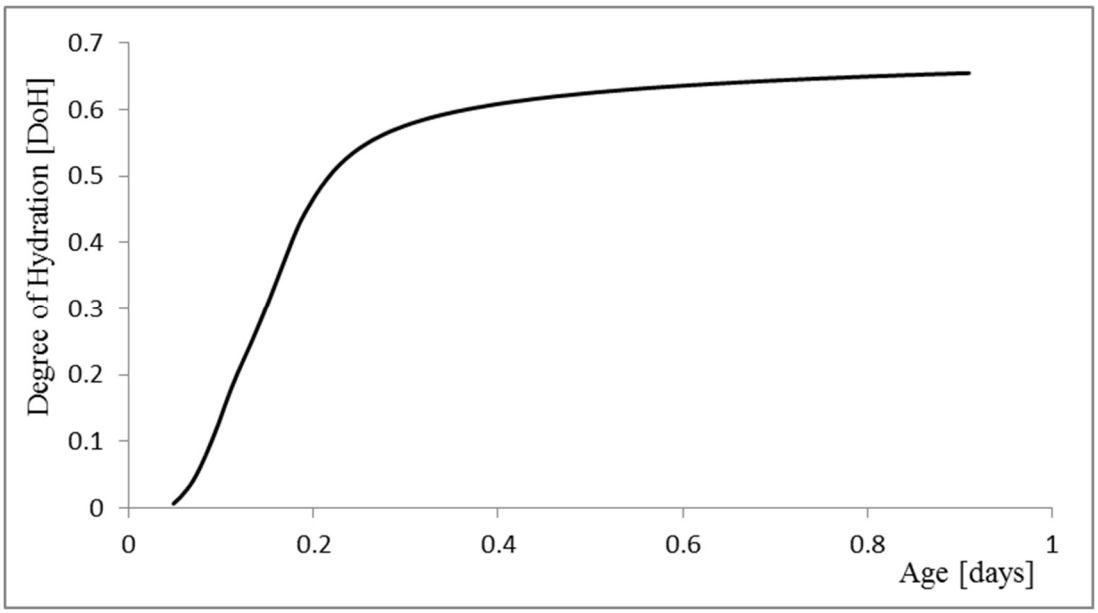

Figure I-4: Variation of Degrees of Hydration [DoH] for mix M-3 during initial stages

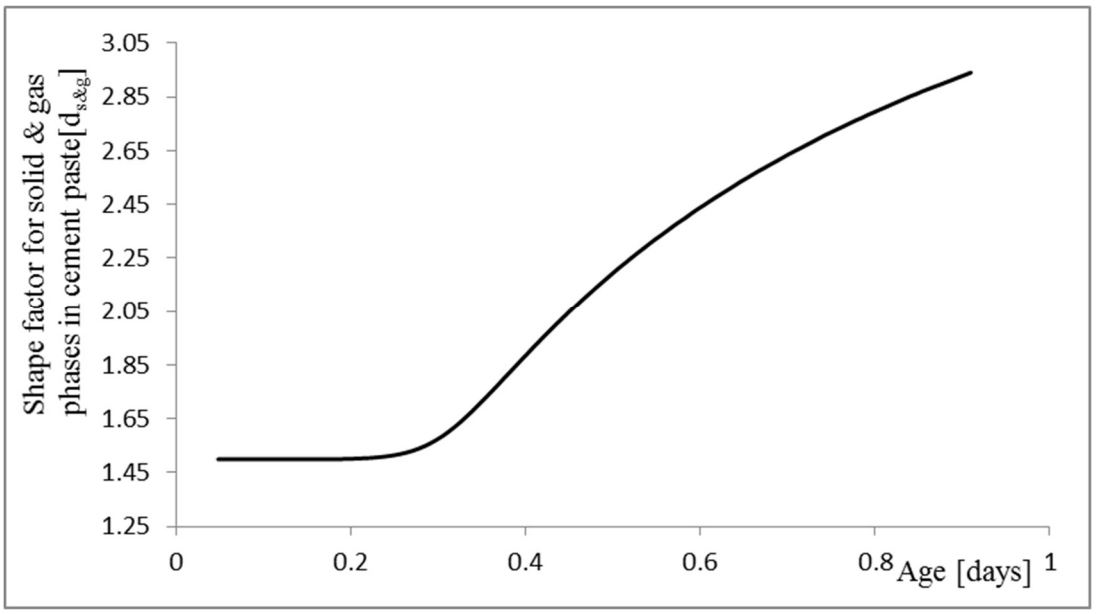

Figure I-5: Variation of shape factor for solid and gas phases in cement paste [$d_{s\&g}$] for mix M-1 during initial stages

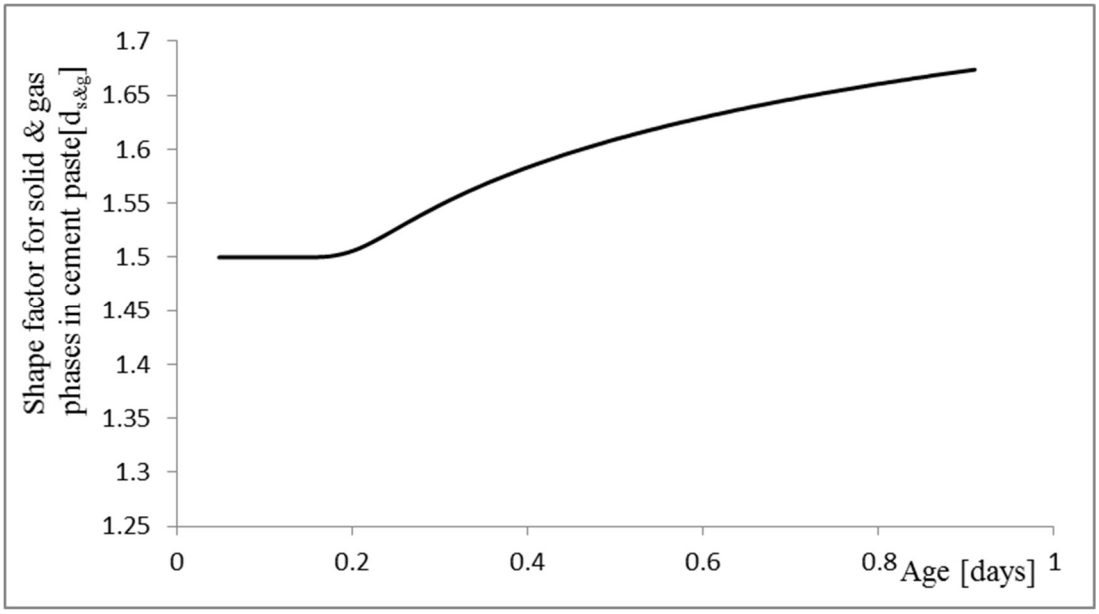

Figure I-6: Variation of shape factor for solid and gas phases in cement paste [$d_{s\&g}$] for mix M-3 during initial stages

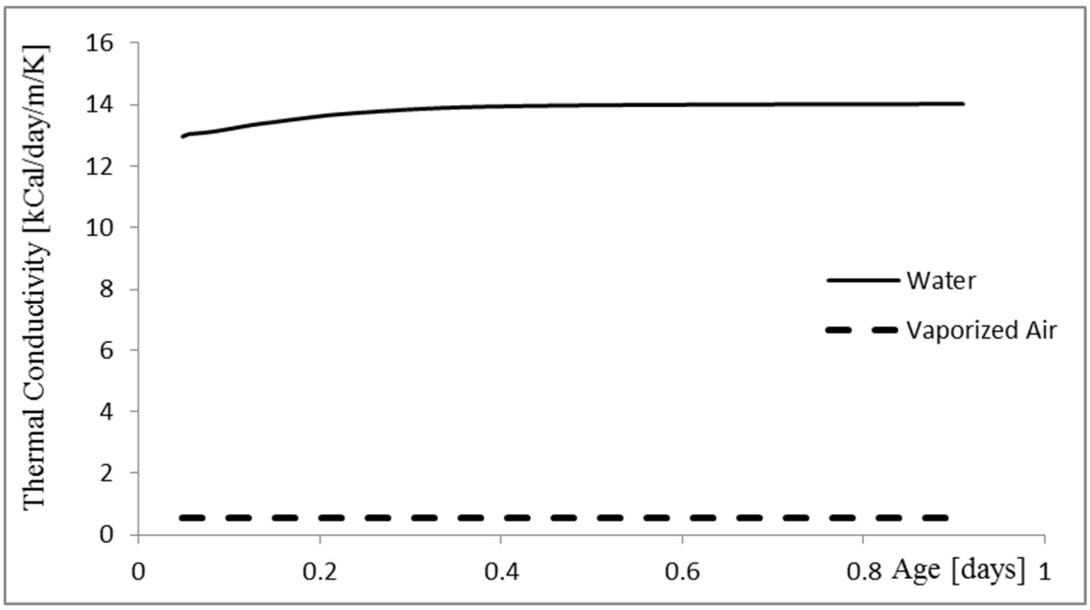

Figure I-7: Variation of thermal conductivity of water and vaporized air in pores of cement paste of mix M-1 during initial stages

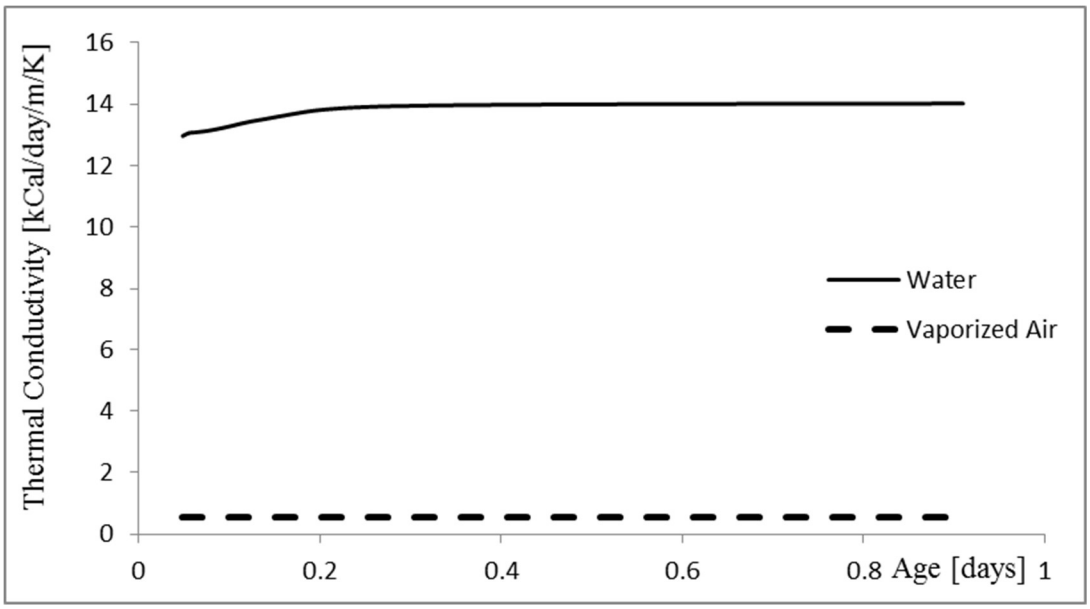

Figure I-8: Variation of thermal conductivity of water and vaporized air in pores of cement paste of mix M-3 during initial stages

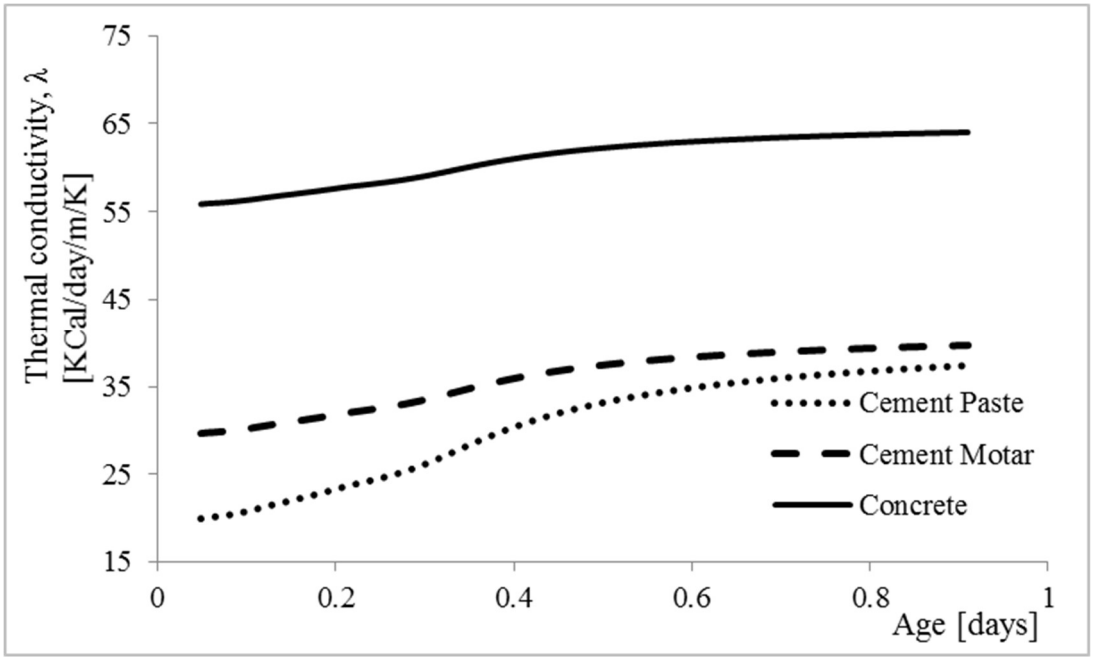

Figure I-9: Variation of Thermal Conductivity of Cement Paste, Mortar, and Concrete for mix M-1

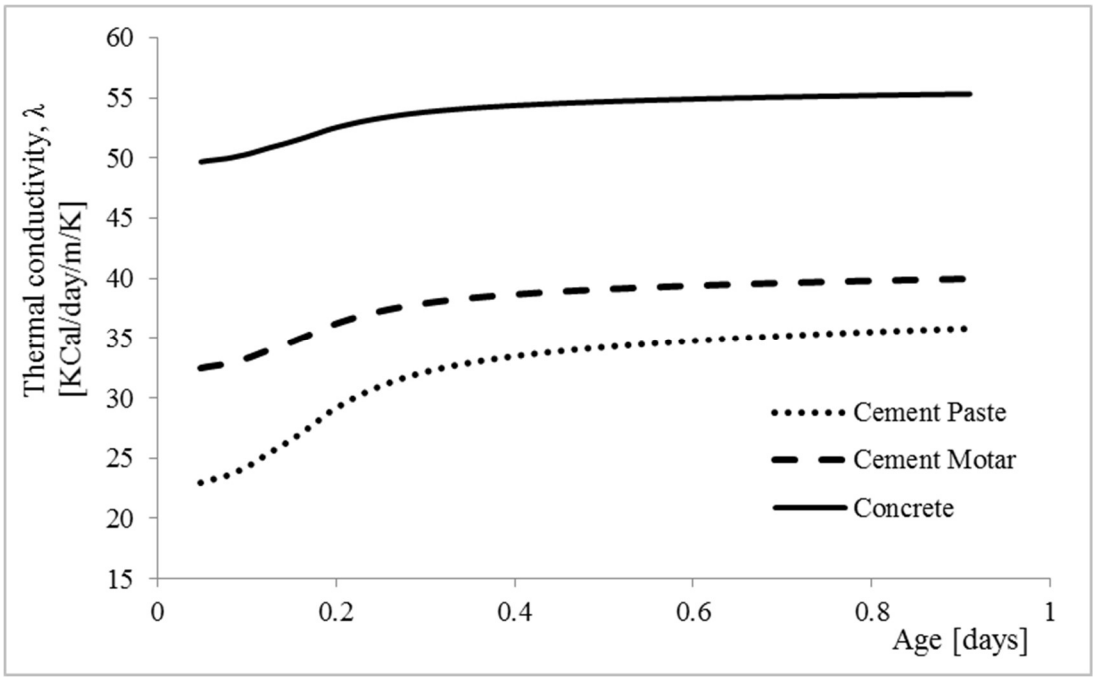

Figure I-10: Variation of Thermal Conductivity of Cement Paste, Mortar, and Concrete for mix M-3